

Simple magnetic nanoparticles as catalysts for hydrogenation, condensation and coupling reactions

A thesis submitted to McGill University
in partial fulfillment of the requirements of the degree of
Doctor of Philosophy

by
Reuben Hudson

Department of Chemistry
McGill University
Montreal, Quebec, Canada

August 2013

© Reuben Hudson, 2013

Abstract

Processes for chemical conversions often either involve one of two divergent catalyst types. Heterogeneous catalysts (bulk material) represent a simple system, which can easily be removed from the reaction mixture after use. Homogeneous catalysts (soluble species) on the other hand, are often much more difficult to separate, but generally provide excellent improved catalytic performance in part because of their equal homogeneous distribution within the reaction media. Moreover, they allow for more tuneability through the use of various ligands. The emerging use of nanoparticle catalysts effectively bridges the gap between homogeneous and heterogeneous catalysis. Often, the smaller the particles become, the more they offer catalytic properties similar to homogeneous catalyst systems. Unfortunately, the reduction in size also makes separation increasingly difficult—again, similar to homogeneous systems. To address the issue of separation, the field of magnetic nanoparticle catalysis emerged. By simple application of an external magnet, magnetic nanoparticle catalysts can be recovered and easily reused. Most examples of magnetic nanoparticle catalysis employ the particle only as a vehicle for magnetic recovery, rather than the catalyst itself. Complex strategies of this kind include coating with a polymer or silica, to which a metal-binding ligand can be anchored. By such a system, one could envision anchoring of nearly any pseudo-homogeneous metal, enabling a broad catalytic scope.

The focus of this work is instead on the use of simple magnetic nanoparticles where the particles themselves act not only as the means for magnetic recovery, but also as catalysts. This thesis covers three general types of simple magnetic nanoparticle catalysts. First, this work demonstrated that reduced iron nanoparticles with a shell of iron oxide can efficiently catalyze the hydrogenation of unsaturated hydrocarbons. This scheme can also be adapted to a flow system by growing the nanoparticles in the presence of amphiphilic polymers. Second, in order to address the limited catalytic offering of iron, the scope of reactions can be expanded by decorating these same iron/iron oxide nanoparticles with a more

catalytically active metal. Copper- and ruthenium- decorated nanoparticles have been synthesized and used for the azide-alkyne click reaction and transfer hydrogenation, respectively. Third, work presented in this thesis shows that other metals can also be incorporated directly into the magnetic nanoparticle lattice. For example, CuFe_2O_4 nanoparticles have been used to catalyze the Biginelli condensation and cross-dehydrogenative coupling reactions. By the use of these three general types of bare particles, we have expanded the scope of simple magnetic nanoparticle catalyzed reactions.

Résumé

Les procédés chimiques impliquent souvent des catalyseurs de l'un des deux types suivants. Les catalyseurs hétérogènes (matériaux) constituent un système simple, qui peut généralement être aisément retiré du mélange réactionnel après usage. D'autre part, les catalyseurs homogènes (espèces solubles) sont souvent beaucoup plus difficiles à séparer ; en revanche, ils offrent en général une excellente performance catalytique étant donnée leur répartition homogène dans le milieu réactionnel. De plus, ces derniers peuvent être facilement modifiés par l'usage de divers ligands pour ainsi améliorer leur performance. L'utilisation croissante de nanoparticules en catalyse offre une alternative entre la catalyse homogène et hétérogène. De façon générale, plus leur taille est petite, plus les particules possèdent des propriétés catalytiques similaires à celles des systèmes homogènes. Malheureusement, la réduction de leur taille rend d'autant plus difficile leur séparation, comme dans le cas des systèmes homogènes. Pour résoudre ce problème de séparation, le domaine de la catalyse à base de nanoparticules magnétiques a vu le jour. Grâce à l'utilisation d'un aimant externe, les catalyseurs de nanoparticules magnétiques peuvent être récupérés et réutilisés facilement. Dans la plupart des exemples de catalyse faisant usage de nanoparticules magnétiques, les particules sont uniquement utilisées comme ancre pour la récupération magnétique, et non comme catalyseurs. Les stratégies complexes de ce type comprennent l'enrobage des nanoparticules avec un polymère ou bien avec de la silice, auquel un ligand de coordination peut être ancré. Par un tel système, on peut envisager l'ancrage de presque n'importe quel métal pseudo-homogène, ce qui permet un large éventail catalytique.

L'objectif de ce travail est plutôt axé sur l'utilisation de nanoparticules magnétiques simples où les particules agissent non seulement comme moyen de récupération magnétique, mais également en tant que catalyseurs. Cette thèse porte sur trois types généraux de catalyseurs simples de nanoparticules magnétiques. Tout d'abord, il est démontré que des nanoparticules de fer réduit, dotés d'une coquille

d'oxyde de fer, peuvent catalyser efficacement l'hydrogénation d'hydrocarbures insaturés. Cette réaction peut également être adaptée à un système "in flow", en préparant les nanoparticules en présence de polymères amphiphiles.

Deuxièmement, considérant le potentiel catalytique limité du fer, la portée de ces réactions peut être étendue par la décoration de ces mêmes nanoparticules de fer / oxyde de fer à l'aide d'un second métal possédant un potentiel catalytique plus élevé. Des nanoparticules décorées de cuivre et de ruthénium ont été synthétisées et utilisées pour effectuer des réactions de couplage azoture-alcyne (click) et d'hydrogénation de transfert, respectivement. Troisièmement, il est démontré que d'autres métaux peuvent également directement être incorporés dans un réseau de nanoparticules magnétiques. Par exemple, des nanoparticules de CuFe_2O_4 peuvent être utilisées pour catalyser des réactions de condensation de Biginelli ainsi que des réactions de couplage inter-déshydrogénation. Par l'utilisation de ces trois types généraux de particules nues, nous avons élargi la portée des réactions catalysées par des nanoparticules magnétiques simples.

To all my friends and family who have encouraged me along the way.

“Look to this day! For it is life, the very life of life.
In its brief course lay all the verities and realities of your existence:
the bliss of growth, the glory of action, the splendor of beauty.
For yesterday is but a dream, and tomorrow only a vision,
but today, well-lived, makes every yesterday a dream of happiness,
and every tomorrow a vision of hope.
Look well, therefore, to this day!”

-Kalidas

Acknowledgements

First and foremost I would like to thank professors Audrey Moores and Chao-Jun Li for their expert guidance and knowledge in research, as well as a great perspective on teaching, industry, collaboration and life beyond graduate school. I would not have been able to develop into a critically thinking, independent scientist without being able to turn to them in the course of maturing as a researcher. Additionally, they provided me with an invaluable experience by sending me to attend and present at numerous conferences and allowing me to twice travel to Japan for research collaborations during the course of my Ph.D.

I would like to thank the Center for Green Chemistry and Catalysis for their financial support to me, as well as the following agencies, which provided financial support to the Moores and Li groups during the course of my Ph.D.: The Canada Foundation for Innovation (CFI), The Fonds de Recherche sur le Nature et les Technologies (FQRNT), the Canada Research Chairs (CRC), Natural Sciences and Engineering Council of Canada (NSERC), the Green Chemistry - NSERC Collaborative Research and Training Experience (CREATE) Program, and McGill University.

I am indebted to all those in the McGill Chemistry department who helped my research by loaning chemicals, explaining laboratory techniques, serving as a sounding board for ideas, correcting my missteps, or pointing me in the right direction. I am grateful to many of those same people for sharing a good time on the softball field, hockey rink, or out on the town. To Kylie for serving as inspiration in the lab and helping me get my feet on the ground, to Sam for her enthusiasm, to Monika for making me think, to Madhu helping me on the GC and with cooking, to Antoine L. for a willingness to help out, to Karl for always smiling and chatting, to Antoine R. for keeping things interesting, to Ciprian for guidance and help, to Mary for rolling up your sleeves and trying anything, to Monique for your patience, to Mitra for a new perspective, to Annie as a pillar of wisdom, to Nick and Simon for insightful comments, to Shingo for showing me what work ethic truly means, to Zeng for including me as an author in a paper for which I would have been thrilled

to be only mentioned in the acknowledgements, to Rodrigo and Daniel for help with my proposal, thank you. A special thanks also to the folks behind the scenes who keep the place running: Claude, Mario, Normand, and Chantal.

I am thankful to everyone at the Chewonki Foundation for instilling in me an appreciation for the natural world and desire to do everything I can to preserve it. Without Chewonki, I would never have chosen to study Green Chemistry at McGill.

Thanks to all who have contributed to my development as a teacher. It all starts on the water with Ryan Linehan. At McGill, Youla Tsantrizos, David Harpp, Ariel Fenster, Nic Moitessier, Audrey Moores and Laura Pavelka helped me develop in the classroom.

Thanks to all my friends and family for the love and support over the years. Mom, Dad and Charlie have always been there for me. Kit has driven me to finish as early as possible so we can finally live together. Thanks to everyone else for sharing a laugh, being there to talk, giving advice, going boating or skiing, playing games, and keeping me smiling.

The completion of my thesis was made possible with the help, support, guidance, training, love and friendship of the wonderful folks I've been blessed to know in my 27 years.

Contribution of Authors

This thesis is composed of 8 manuscripts written primarily by the author and most co-written by Audrey Moores and Chao-Jun Li, who acted as research supervisors. Each citation is listed below, followed by a detailed explanation of each author's contributions.

Reuben Hudson, Yuting Feng, Rajender Varma and Audrey Moores. Bare magnetic nanoparticles: synthesis and application in catalysis (invited review). *Green Chem.* Manuscript in preparation.

The author wrote the manuscript. Yuting Feng gathered references and contributed to the section on mixed metal oxides. Audrey Moores designed and edited the manuscript. Rajender Varma will review and edit the manuscript prior to submission.

Reuben Hudson, Antoine Rivière, Ciprian M. Cirtiu, Kylie L. Luska and Audrey H. Moores. Iron-iron oxide core-shell nanoparticles are active and magnetically recyclable olefin and alkyne hydrogenation catalysts in protic and aqueous media. *Chem. Commun.*, 2012, 48, 3360-3362.

The author collected all data and wrote the manuscript. Antoine Rivière and Ciprian M. Cirtiu demonstrated the proof of concept experiments that spawned this project. Kylie L. Luska helped the author obtain TEM images. Audrey Moores designed the experiments and edited the manuscript. Chao-Jun Li also reviewed and edited the manuscript, although does not appear as an author.

Reuben Hudson, Go Hamasaka, Takao Osaka, Yoichi Y. A. Yamada, Yasuhiro Uozumi, Chao-Jun Li, and Audrey Moores. Highly efficient iron(0) nanoparticle-catalyzed hydrogenation in water in flow. *Green Chem.*, 2013, 15, 2141-2148

The author collected all data for the manuscript and served as the primary author. Go Hamasaka helped the author obtain TEM images. Takao Osaka and Yoichi M. A. Yamada trained the author in the experimental techniques for data collection. Yasuhiro Uozumi, Chao-Jun Li and Audrey Moores designed the experiments and edited the manuscript.

Reuben Hudson, Vanessa Chazelle, Chao-Jun Li, and Audrey Moores. Magnetic Ru@Fe nanoparticles as transfer hydrogenation catalysts. Manuscript in preparation.

The author trained Vanessa Chazelle for all laboratory techniques involved in the paper, and both Vanessa Chazelle and the author shared equally in the collection of data. The author wrote the manuscript, which was edited by both Chao-Jun Li and Audrey Moores, both of whom shared with the author the task of experimental design.

Reuben Hudson, Chao-Jun Li and Audrey Moores. Magnetic copper–iron nanoparticles as simple heterogeneous catalysts for the azide–alkyne click reaction in water. *Green Chem.*, 2012, 14, 622-624.

The author collected all data and wrote the manuscript. Chao-Jun Li and Audrey Moores designed the experiments and edited the manuscript.

Reuben Hudson. Copper Ferrite (CuFe_2O_4) Nanoparticles. *Synlett*. 2013; 24(10): 1309-1310

The author wrote the manuscript. Audrey Moores reviewed and edited it, although does not appear as a co-author.

Reuben Hudson, Shingo Ishikawa, Chao-Jun Li and Audrey Moores. Magnetically Recoverable CuFe₂O₄ Nanoparticles as Highly Active Catalysts for Csp³-Csp and Csp³-Csp³ Oxidative Cross-Dehydrogenative Coupling. *Synlett*. 2013; 24(13): 1637-1642

The author collected all data and wrote the manuscript. Shingo Ishikawa synthesized starting materials and offered advice. Chao-Jun Li and Audrey Moores designed the experiments and edited the manuscript.

Reuben Hudson, Julian Silverman, Chao-Jun Li and Audrey Moores. Copper ferrite nanoparticle catalyzed Biginelli condensation: proof of concept for a novel class of magnetically recoverable catalyst. *Proceedings of the 3rd International Conference on Nanotechnology*. 7-9 August 2012. Paper No. 318

The author trained Julian Silverman for all laboratory techniques used in the collection of data. The author and Julian Silverman shared equally in the collection of data. Julian Silverman performed analysis of compounds, the author performed materials analysis. The author wrote the manuscript, which was edited by Chao-Jun Li and Audrey Moores, both whom designed the experiments.

Table of Contents

| | |
|--|-----------|
| Abstract | iii |
| Résumé | v |
| Acknowledgements..... | ix |
| Contribution of Authors | xi |
| List of Figures | xvii |
| List of Schemes | xvii |
| List of Tables | xviii |
| List of Abbreviations | xx |
| List of Symbols | xxii |
| 1 Introduction | 1 |
| 1.1 Bare Magnetic Nanoparticles for Catalysis | 2 |
| 1.1.1 Abstract..... | 2 |
| 1.1.2 Introduction | 2 |
| 1.1.3 Iron oxide nanoparticles as catalysts..... | 4 |
| 1.1.3.1 Synthesis..... | 4 |
| 1.1.3.2 Catalytic applications | 6 |
| 1.1.4 Iron/transition metal mixed oxide nanoparticles as catalysts | 8 |
| 1.1.4.1 Synthesis..... | 8 |
| 1.1.4.2 Catalytic applications of mixed metal ferrite nanoparticles..... | 8 |
| 1.1.5 Reduced iron nanoparticles as catalysts | 13 |
| 1.1.5.1 Synthesis:..... | 14 |
| 1.1.5.2 Catalytic Applications | 16 |
| 1.1.5.2.1 Hydrogenation: | 16 |
| 1.1.5.2.2 Ammonia-Borane Dehydrogenation..... | 18 |
| 1.1.5.2.3 Grignard-type reactions | 18 |
| 1.1.5.2.4 Reduction of Environmental Contaminants | 19 |
| 1.1.5.3 Other magnetic reduced metal nanoparticles..... | 19 |
| 1.1.6 Reduced iron nanoparticles as seeds for other transition metal nanocatalysts... | 20 |
| 1.1.6.1 Synthesis..... | 20 |
| 1.1.6.2 Catalytic applications | 21 |
| 1.1.7 Conclusions..... | 22 |
| 1.1.8 Acknowledgements..... | 22 |
| 1.1.9 References..... | 22 |
| 2 Reduced Iron Nanoparticles for Hydrogenation Reactions | 29 |
| 2.1 Iron-iron oxide core-shell nanoparticles are active and magnetically recyclable olefin and alkyne hydrogenation catalysts in protic and aqueous media | 30 |
| 2.1.1 Abstract..... | 30 |
| 2.1.2 Introduction | 30 |
| 2.1.3 Results and Discussion | 32 |
| 2.1.4 Conclusions..... | 36 |
| 2.1.5 Acknowledgements..... | 36 |
| 2.1.6 References..... | 37 |
| 2.1.7 Appendix..... | 39 |
| 2.1.7.1 Blank catalytic runs | 39 |
| 2.1.7.2 Experimental section: | 39 |
| 2.1.7.2.1 Chemicals..... | 39 |
| 2.1.7.2.2 Analytical Methods | 40 |
| 2.1.7.2.3 Synthesis of Fe CSNPs | 40 |
| 2.1.7.2.4 Typical catalytic run..... | 40 |

| | |
|--|-----------|
| 2.1.7.2.5 TEM Preparation..... | 41 |
| Estimated Fe:FeO ratio from TEM data..... | 43 |
| 2.2 Highly Efficient Iron(0) Nanoparticle-Catalyzed Hydrogenation in Water in Flow | 46 |
| 2.2.1 Introduction | 46 |
| 2.2.2 Results and Discussion | 49 |
| 2.2.2.1 Synthesis and characterization of polymer resin stabilized Fe(0) NPs..... | 49 |
| 2.2.2.2 Catalytic tests..... | 52 |
| 2.2.3 Conclusion..... | 61 |
| 2.2.4 Experimental Section | 62 |
| 2.2.4.1 Chemicals..... | 62 |
| 2.2.4.2 Instruments | 62 |
| 2.2.4.3 Synthesis of FeNP@PS-LK by thermal decomposition: | 62 |
| 2.2.4.4 Synthesis of FeNP@PS-(PEG)-NH ₂ by black tea reduction: | 63 |
| 2.2.4.5 Characterization of PS-LK supported Fe nanoparticles: | 63 |
| 2.2.4.6 PS-LK supported Fe nanoparticles for flow hydrogenation: | 64 |
| 2.2.4.7 PS-LK supported Fe nanoparticles for batch hydrogenation:..... | 64 |
| 2.2.5 Acknowledgements..... | 64 |
| 2.2.6 References..... | 65 |
| 2.2.7 Appendix..... | 69 |
| 3 Reduced Iron Nanoparticles Decorated with a more Catalytically Active Metal..... | 71 |
| 3.1 Magnetic copper-iron nanoparticles as simple heterogeneous catalysts for the azide-alkyne click reaction in water..... | 72 |
| 3.1.1 Abstract..... | 72 |
| 3.1.2 Introduction | 72 |
| 3.1.3 Results and Discussion | 73 |
| 3.1.4 Conclusions..... | 76 |
| 3.1.5 Experimental Section | 77 |
| 3.1.6 Acknowledgements..... | 78 |
| 3.1.7 References..... | 78 |
| 3.1.8 Appendix..... | 81 |
| 3.2 Magnetic Ru@Fe nanoparticles as transfer hydrogenation catalysts | 82 |
| 3.2.1 Abstract..... | 82 |
| 3.2.2 Introduction | 82 |
| 3.2.3 Results and Discussion | 84 |
| 3.2.3.1 Synthesis of Ru@Fe nanoparticles..... | 84 |
| 3.2.3.2 Characterization of Ru@Fe nanoparticles | 85 |
| 3.2.3.3 Ru@Fe nanoparticles for transfer hydrogenation..... | 85 |
| 3.2.4 Conclusions..... | 88 |
| 3.2.5 Acknowledgements..... | 88 |
| 3.2.6 References..... | 88 |
| 3.2.7 Appendix..... | 92 |
| 3.2.7.1 Experimental details | 92 |
| 3.2.7.1.1 Reagents:..... | 92 |
| 3.2.7.1.2 Instruments | 93 |
| 4 CuFe₂O₄ Nanoparticles for Catalysis..... | 95 |
| 4.1 General Introduction: Copper Ferrite (CuFe ₂ O ₄) Nanoparticles For Catalysis... | 96 |
| 4.1.1 Introduction | 96 |
| 4.1.1.1 Azide-alkyne 'click' reaction | 96 |

| | |
|--|------------|
| 4.1.1.2 C-C cross coupling | 97 |
| 4.1.1.3 C-N cross coupling..... | 97 |
| 4.1.1.4 C-O cross coupling..... | 98 |
| 4.1.1.5 C-S cross coupling..... | 98 |
| 4.1.1.6 C-Se cross coupling | 98 |
| 4.1.1.7 Sugar deacylation..... | 99 |
| 4.1.1.8 A3 coupling..... | 99 |
| 4.1.1.9 Biginelli condensation | 100 |
| 4.1.1.10 Synthesis of dihydropyridines | 100 |
| 4.1.1.11 Tetrazole synthesis | 101 |
| 4.1.1.12 Asymmetric hydrosilation..... | 101 |
| 4.1.1.13 Aza-Michael addition..... | 101 |
| 4.1.2 References..... | 102 |
| 4.2 Magnetically Recoverable CuFe₂O₄ Nanoparticles as Highly Active Catalysts for Csp³-Csp and Csp³-Csp³ Oxidative Cross-Dehydrogenative-Coupling..... | 104 |
| 4.2.1 Abstract..... | 104 |
| 4.2.2 Introduction | 104 |
| 4.2.3 Results and Discussion | 107 |
| 4.2.4 Conclusions..... | 111 |
| 4.2.5 Experimental Proceedure..... | 112 |
| 4.2.6 Acknowledgements..... | 112 |
| 4.2.7 References..... | 112 |
| 4.2.8 Appendix..... | 116 |
| 4.3 Copper-Iron-Oxide Nanoparticles as Magnetically Recoverable Catalysts for the Biginelli Condensation..... | 117 |
| 4.3.1 Abstract..... | 117 |
| 4.3.2 Introduction | 117 |
| 4.3.3 Results and Discussion | 120 |
| 4.3.3.1 Catalytic Tests | 120 |
| 4.3.3.2 Evaluation of the Heterogeneous Nature of the Reaction | 121 |
| 4.3.3.3 Reaction Scope | 123 |
| 4.3.4 Experimental Section | 125 |
| 4.3.4.1 Materials and Equipments..... | 125 |
| 4.3.4.2 Biginelli Condensation Catalytic Tests | 125 |
| 4.3.5 Conclusions..... | 126 |
| 4.3.6 Acknowledgements..... | 126 |
| 4.3.7 References..... | 126 |
| 4.3.8 Appendix..... | 129 |
| 4.3.8.1 Appendix References..... | 130 |
| 5 Conclusions and Future Work | 131 |
| 5.1 Conclusions..... | 131 |
| 5.2 Future Work | 132 |
| 5.3 References | 134 |

List of Figures

| | |
|--|-----|
| Figure 1.1: Synthesis of Iron oxide nanoparticles..... | 6 |
| Figure. 1.2 Synthesis of Reduced Iron Nanoparticles..... | 16 |
| Figure 2.1.1. TEM pictures of Fe CSNPs a) before catalysis and b) after 10 cycles.... | 34 |
| Figure 2.1.2. High resolution TEM pictures of Fe CSNPs..... | 41 |
| Figure 2.1.3. TEM picture of Fe CSNPs after 5 cycles..... | 42 |
| Figure 2.1.4. TEM picture of commercial FeCSNPs..... | 42 |
| Figure 2.1.5. XPS of Fe CSNPs..... | 43 |
| Figure 2.1.6. High resolution XPS for Fe2p..... | 44 |
| Figure 2.1.7. XRD analysis of Fe CSNPs | 45 |
| Figure 2.2.1. Schematic of hydrogenation reactions undertaken with polymer supported iron nanoparticles, under flow conditions (PS = polystyrene) | 48 |
| Figure 2.2.2 TEM images of images of A) and B) FeNP@PS-PEG-NH ₂ (thermal decomposition); C) FeNP@PS-PEG-NH ₂ (tea reduction); D) FeNP@PS-PEG-Br (thermal decomposition); E) FeNP@PS-PEG-COOH (thermal decomposition); F) FeNP@PS-NH ₂ (thermal decomposition) | 51 |
| Figure 2.2.3. High resolution TEM image of a single Fe(0) NP exhibiting lattice fringes in FeNP@PS-PEG-NH ₂ | 51 |
| Figure 2.2.4. Scale up and long-term catalyst performance for the hydrogenation of 5 grams of cinnamyl acetate over 5.7 hours (TON= 434) | 61 |
| Figure 3.1.1. XPS Analysis of Cu@Fe NPs | 81 |
| Figure 3.1.2. TEM image of Cu@FeNPs | 81 |
| Figure 3.2.1. TEM images of core shell iron-iron oxide nanoparticles and ruthenium plated iron-iron oxide nanoparticles below schematic representations. | 92 |
| Figure 4.2.1. Various types of magnetically recoverable nanoparticle catalysts. | 105 |
| Figure 4.2.2. Photographs of A: reaction mixture with active stirring; B: CuFe ₂ O ₄ nanoparticles adsorbed to the stir bar and attracted to external magnet. | 109 |
| Figure 4.2.3. Recycling of CuFe ₂ O ₄ nanoparticles (0.02 mmol) for the coupling of nitromethane (0.5 mL) with 2-phenyl-1,2,3,4-tetrahydroisoquinoline (0.2 mmol) with 1atm O ₂ at 100°C for 24 hours..... | 110 |
| Figure 4.2.4. TEM images of CuFe ₂ O ₄ nanoparticles before catalysis and after 10 cycles | 116 |
| Figure 4.3.1. CuFe ₂ O ₄ NP dispersed in solution (left) and adsorbed to a magnetic stir bar (right)..... | 121 |
| Fig. 4.3.3. CuFe ₂ O ₄ NPs (a) before catalysis and (b) after 7 cycles..... | 124 |
| Figure 4.3.4. XRD Analysis of a commercial sample of CuFe ₂ O ₄ nanoparticles. | 129 |
| Figure 4.3.5. XPS analysis of a commercial sample of CuFe ₂ O ₄ nanoparticles..... | 130 |

List of Schemes

| | |
|--|---|
| Scheme 1.1. Strategies for bare magnetic nanoparticle catalysis | 4 |
| Scheme 1.2. Oxidizing potential of iron oxide nanoparticles..... | 7 |
| Scheme 1.3. A ³ -type reactions catalyzed by iron oxide nanoparticles..... | 7 |
| Scheme 1.4. Cross-coupling reactions catalyzed by CuFe ₂ O ₄ nanoparticles | 9 |

| | |
|---|-----|
| Scheme 1.5. CuFe ₂ O ₄ nanoparticle catalyzed reactions with alkynes | 9 |
| Scheme 1.6. CuFe ₂ O ₄ nanoparticle catalyzed condensation reactions..... | 10 |
| Scheme 1.7. CuFe ₂ O ₄ nanoparticle catalyzed sugar deacylation | 10 |
| Scheme 1.8. CuFe ₂ O ₄ nanoparticle catalyzed hydrosilation..... | 11 |
| Scheme 1.9. CoFe ₂ O ₄ nanoparticle catalyzed oxidation reactions..... | 12 |
| Scheme 1.10. CoFe ₂ O ₄ nanoparticle catalyzed Knoevenagel reaction..... | 12 |
| Scheme 1.11. Co ₃ O ₄ nanoparticle catalyzed oxidation reactions | 13 |
| Scheme 1.12. Reduced iron nanoparticle catalyzed reactions | 14 |
| Scheme 1.13. Coordination, seeding and growth for the synthesis of M@FeNPs | 20 |
| Scheme 1.14. Catalytic application of M@FeNPs..... | 21 |
| Scheme 2.1.1. Hydrogenation of olefin catalyzed by Fe CSNPs..... | 31 |
| Scheme 2.2.1. Synthesis of FeNP@PS-PEG-FG by thermal decomposition of Fe(CO) ₅ | 49 |
| Scheme 2.2.2. Synthesis of FeNP@PS-PEG-NH ₂ by black tea reduction of FeSO ₄ | 49 |
| Scheme 2.2.3. Proposed mechanism for olefin hydrogenation catalyzed by iron nanoparticles | 69 |
| Scheme 3.1.1. Cu@FeNP catalyzed azide-alkyne 'click' reaction | 73 |
| Scheme 3.2.1. Synthesis of Ru@FeNPs | 85 |
| Scheme 4.1.1. Synthesis of CuFe ₂ O ₄ NPs by co-precipitation ⁹ | 96 |
| Scheme 4.1.2. CuFe ₂ O ₄ catalyzed azide-alkyne 'click' reaction..... | 97 |
| Scheme 4.1.3. CuFe ₂ O ₄ catalyzed C-C cross coupling..... | 97 |
| Scheme 4.1.4. CuFe ₂ O ₄ catalyzed C-N cross coupling. | 97 |
| Scheme 4.1.5. CuFe ₂ O ₄ catalyzed C-O cross coupling. | 98 |
| Scheme 4.1.6. CuFe ₂ O ₄ catalyzed C-S cross coupling. | 98 |
| Scheme 4.1.7. CuFe ₂ O ₄ catalyzed C-Se cross coupling..... | 99 |
| Scheme 4.1.8. CuFe ₂ O ₄ catalyzed sugar deacylation. | 99 |
| Scheme 4.1.9. CuFe ₂ O ₄ catalyzed A ³ coupling..... | 100 |
| Scheme 4.1.10. CuFe ₂ O ₄ catalyzed Biginelli condensation. | 100 |
| Scheme 4.1.11. CuFe ₂ O ₄ catalyzed synthesis of dihydropyridines..... | 100 |
| Scheme 4.1.12. CuFe ₂ O ₄ catalyzed tetrazole synthesis. | 101 |
| Scheme 4.1.13. CuFe ₂ O ₄ catalyzed asymmetric hydrosilation. | 101 |
| Scheme 4.1.14. CuFe ₂ O ₄ catalyzed aza-Michael addition | 102 |
| Scheme 4.2.1 Oxidative CDC with Fe ₃ O ₄ and CuFe ₂ O ₄ nanoparticles..... | 106 |
| Scheme 4.2.2. Proposed mechanism for CuFe ₂ O ₄ nanoparticle catalyzed Csp ³ -Csp Cross-Dehydrogenative-Coupling..... | 111 |
| Scheme 4.3.1 Examples of magnetically recoverable nanoparticles catalysts..... | 118 |
| Scheme 4.3.2. 3,4-dihydropyrimidine-2-ones (DHPMs) synthesis by Biginelli Condensation | 119 |

List of Tables

| | |
|--|----|
| Table 2.1.1. Fe CSNP catalyzed olefin hydrogenation..... | 33 |
| Table 2.1.2. Recycling reactions for the hydrogenation of styrene to ethyl benzene | 36 |
| Table 2.1.3. Comparison of Fe CSNP catalyzed olefin hydrogenation with H ₂ , Ar, or no additional gas..... | 39 |

| | |
|---|-----|
| Table 2.1.4. ICP-MS analysis of Fe CSNPs | 44 |
| Table 2.2.1. Ethylbenzene yield in batch and flow as a function of polymer-immobilized Fe NP composition..... | 53 |
| Table 2.2.2. Screening of hydrogenation conditions ^a | 55 |
| Table 2.2.3. Functional group tolerance and selectivity ^a | 57 |
| Table 2.2.4. Catalytic selectivity of the polymer-immobilized Fe NPs | 58 |
| Table 2.2.5. Reactivity of various types of alkenes ^a | 59 |
| Table 2.2.6. Activity of styrene derivatives..... | 60 |
| Table 3.1.1. Performance of a series of Cu and Fe based catalysts for the AAC ^a | 73 |
| Table 3.1.2 Cu@Fe NP Catalyzed Azide-Alkyne Cycloaddition. ^a | 75 |
| Table 3 Recycling of Cu@FeNPs Catalyst for AAC. ^a | 76 |
| Table 3.2.1. Transfer hydrogenation conditions screening. ^a | 86 |
| Table 3.2.2. Transfer hydrogenation substrate scope. ^a | 87 |
| Table 3.2.3. Catalyst recycling for acetophenone transfer hydrogenation. ^a | 88 |
| Table 4.2.1. Comparison of Csp ³ -Csp ³ and Csp ³ -Csp CDC reaction catalyzed by Fe ₃ O ₄ and CuFe ₂ O ₄ nanoparticles. ^a | 107 |
| Table 4.3.1 Catalytic Tests | 120 |
| Table 4.3.2. Biginelli condensation reaction scope..... | 124 |

List of Abbreviations

| | |
|---------------------------------|---|
| AAC | Azide-alkyne 'click' reaction |
| A ³ | Azide-Alkyne-Amine |
| bcc | body centered cubic |
| BINAP | 2,2'-bis(diphenylphosphino)-1,1'-binaphthyl |
| B ₂ pin ₂ | Bis(pinacolato)diboron |
| CDC | Cross dehydrogenative coupling |
| C-Fe CSNPs | Commercial iron core-shell nanoparticles |
| CSNP | Core-shell iron nanoparticle |
| Cu@FeNP | Copper decorated iron nanoparticle |
| DDQ | 2,3-Dichloro-5,6-dicyano-1,4-benzoquinone |
| DHPMs | 3,4-dihydropyrimidine-2-ones |
| DMF | Dimethylformamide |
| Et | Ethyl |
| eV | Electron volt |
| fcc | face centered cubic |
| FeNP | Iron nanoparticle |
| FID | Flame ionization detector |
| FDA | Food and drug administration |
| FG | Functional group |
| GC | Gas chromatography |
| HPLC | High pressure liquid chromatography |
| ICP | Inductively coupled plasma |
| JCPDS | Joint Committee on Powder Diffraction Standards |
| LK | Linker |
| LUMO | Lowest unoccupied molecular orbital |
| M | Molar mass |
| Me | Methyl |
| mp | melting point |
| MS | Mass spectrometry |

| | |
|---------|---------------------------------------|
| M@FeNP | Metal decorated iron nanoparticle |
| NMR | Nuclear Magnetic Resonance |
| NZVI | Nano zero valent iron |
| OES | Optical emission spectroscopy |
| Pd@FeNP | Palladium decorated iron nanoparticle |
| PEG | Polyethylene glycol |
| Ph | Phenyl |
| ppb | parts per billion |
| ppm | parts per million |
| PS | Polystyrene |
| NP | Nanoparticles |
| r.t. | Room temperature |
| Ru@FeNP | Ruthenium decorated iron nanoparticle |
| T | Temperature |
| TBAF | Tetrabutylammonium fluoride |
| TBHP | Tert-butyl hydroperoxide |
| TEM | Transmission electron spectroscopy |
| THF | Tetrahydrofuran |
| TOF | Turn over frequency |
| TON | Turn over number |
| UV | Ultraviolet |
| W | Watt |
| XPS | X-ray photoelectron spectroscopy |
| XRD | X-ray diffraction |

List of Symbols

| | |
|-----|-------------------|
| °C | Degrees Celcius |
| Å | Angstroms |
| ⊗ | Cation vacancy |
| © | Copyright |
| μ | Micro |
| Ω | Ohm |
| % | Per cent |
| [O] | Oxidant (generic) |

1 Introduction

This chapter provides an introduction to the use of bare magnetic nanoparticles for catalysis. It is based on an invited review to the journal *Green Chemistry*, which will be submitted soon.

Reuben Hudson, Yuting Feng, Rajender Varma and Audrey Moores. Bare magnetic nanoparticles: synthesis and application in catalysis (invited review). *Green Chem.* Manuscript in preparation.

1.1 Bare Magnetic Nanoparticles for Catalysis

1.1.1 Abstract

The field of magnetic nanoparticle catalysis has developed quickly over the past 10 years because it provides an easy, economical and environmentally benign mode for catalyst recovery. Most strategies employ the nanoparticles only as a vehicle for recovery and not as the catalyst directly. Herein, we review the synthesis and application of only those systems where the nanoparticle serves as both the means for magnetic recovery and the catalyst itself. Examples of such bare nanoparticles include iron oxide (Fe_2O_3 and Fe_3O_4), metal ferrite (MFe_2O_4), zero-valent iron, cobalt or nickel, and decorated nanoparticles. Herein we follow the development of this field to date and suggest where future contributions may provide the most impact to academia and industry.

1.1.2 Introduction

Catalysis enables aspects of Green Chemistry by affording less polluting processes, and opening synthetic pathways between novel resources and currently needed products.¹⁻³ Recent discoveries in the field have been intimately associated with knowledge at a very fundamental level, for instance in the catalytic activities of metal complexes of rhodium, palladium, iron, and heteroelement-containing molecules.⁴⁻⁷ However, catalyst recovery is a condition of its applicability at the industrial scale. This is a principal reason the majority of industrial catalysts are heterogeneous.⁸ In this context, metal-containing nanoparticles (NPs) are attractive candidates as dispersible and recoverable catalysts as they can combine high activity, selectivity and tunability, with improved recyclability possibilities.⁹ With purification and separation often ranking as some of the most energy and resource intensive steps in chemical processes, academia and industry alike have been searching for heterogeneous catalysts to minimize purification and separation

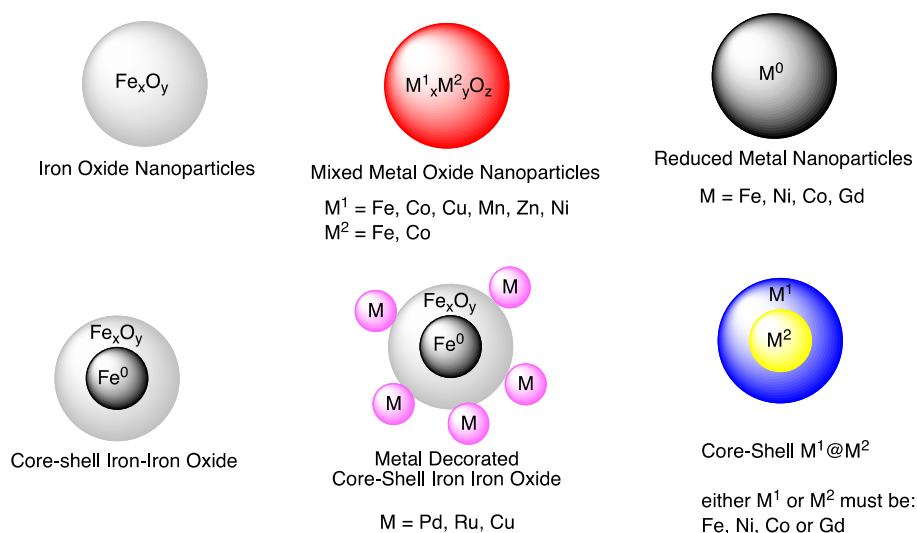
waste on this front.^{2,3} Heterogeneous catalysts, although easier to recover than their homogeneous counterparts, more often than not offer inferior catalytic properties.

For the past 10-15 years nanoparticles (NPs) have been touted as bridging the gaps in reactivity and recoverability between homogeneous and heterogeneous catalysts by combining the catalytic properties of the former with the ease of recovery of the latter.¹⁰⁻¹² Many nanoparticles offer size dependent catalytic properties, and in any case, the surface area to volume ratio increases with decreasing size, meaning more active sites per weight of material.¹² The smaller the particle, the more it emulates a homogeneous catalyst as far catalytic properties, but unfortunately, it also becomes more like a homogeneous catalyst with regards to the difficulty of separation.

In the last 8 years, the concept of magnetically recoverable nanoparticles has quickly developed to further simplify the recovery process.^{13, 14} Various strategies exist for magnetic nanocatalysis, the majority of which use the nanoparticle simply as a vehicle for recovery, to which a protective coating, then a metal binding ligand is anchored—at the cost of much synthetic effort. By such a method, one could envision anchoring of nearly any homogeneous catalyst to a magnetic particle, so this method has a very broad scope of potential reactions. The focus of this review is instead on the simpler but often less popular approach of using bare magnetic nanoparticles for catalysis. In these cases, the catalytic activity relies on the surface of the magnetic particle itself, in a heterogeneous fashion. Although the scope of the catalytic reactions that can be explored seems limited by the number of magnetic materials that can be used, many design features including the NPs size, the use of ligands or additives, or the use of hybrid structures have contributed to the development of the rich chemistry of magnetic NPs over the past few years. This thesis is being written at a time of rapid expansion of the field of catalysis using bare magnetic nanoparticles.

Iron oxide nanoparticles (Fe_2O_3 and Fe_3O_4) have been used for several oxidative and coupling reactions.^{15, 16} By substituting a second metal into the lattice (MFe_2O_4), the catalytic scope can be expanded, while the remaining iron continues to enable magnetic recovery.¹⁷ Zero-valent iron particles offer their own distinct

reactivity, which several groups have taken advantage of to catalyse reductive reactions.¹⁸ This new reactivity bears with it a new challenge: protecting against oxidative catalyst deactivation. Once again, catalytic offering of iron can be expanded by the use of several recently developed strategies for incorporation of other catalytically active metals, including: decorated^{19, 20} or core shell^{21, 22} structures (scheme 1.1).



Scheme 1.1. Strategies for bare magnetic nanoparticle catalysis

1.1.3 Iron oxide nanoparticles as catalysts

Iron oxide nanoparticles represent one of the simplest types of magnetically recoverable catalysts. Such nanoparticles already contain oxidized iron, which means that handlers should have few fears of oxidative catalyst deactivation (a common problem with iron), so the particles can be exposed to air, used in water or other protic solvents.

1.1.3.1 Synthesis

Bottom-up approaches for iron oxide nanoparticle synthesis include co-precipitation, microemulsion techniques and thermal decomposition. Iron (II) and (III) salts can be co-precipitated out of an aqueous solution by addition of base for the formation of Fe_3O_4 nanoparticles.^{24, 25} To gain more control over nanoparticle size and morphology, a microemulsion technique can be adopted wherein separate oil-water microemulsions containing the different salts can be combined.²⁶ Given their dynamic nature, the micelles will continually coalesce and break apart,²⁷ ultimately forming microreactors containing mixtures of the two metal salts.¹⁴ Micelle size can be tuned by controlling oil-water ratios, providing more control over the nanoparticle synthesis environment. Rather than forming nanoparticles by chemically separating iron cations from their counteranions, the same can be achieved by thermal decomposition.^{28, 29} Decomposing metal acetoacetonates or other organometallic precursors in high boiling solvents effectively destroys the ligand and forms the desired oxides. Inclusion of appropriate surfactants or stabilizers limits the growth of these solids to the nanometer regime.

Top-down or lateral approaches for iron oxide nanoparticle syntheses rely on transforming existing solid phase materials. Grinding of bulk iron oxide produces particles in the nanometer regime, depending on grinding time and frequency.²³ Such processes often yield irregular and polydispersed particles. For more control of particle morphology, pre-existing, well-defined, reduced iron particles can be oxidized in a controlled environment to provide the desired iron oxide nanoparticles with a high degree of precision (Figure 1.1).³¹

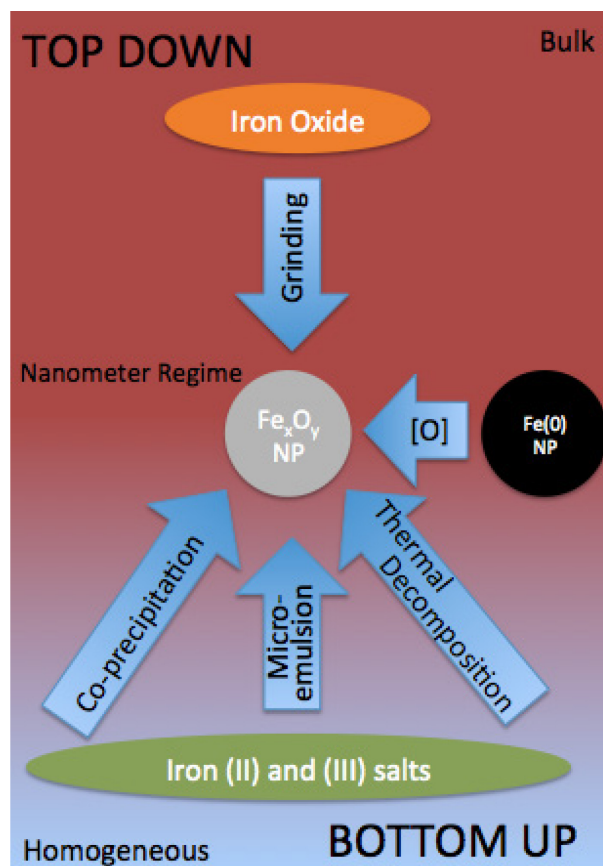
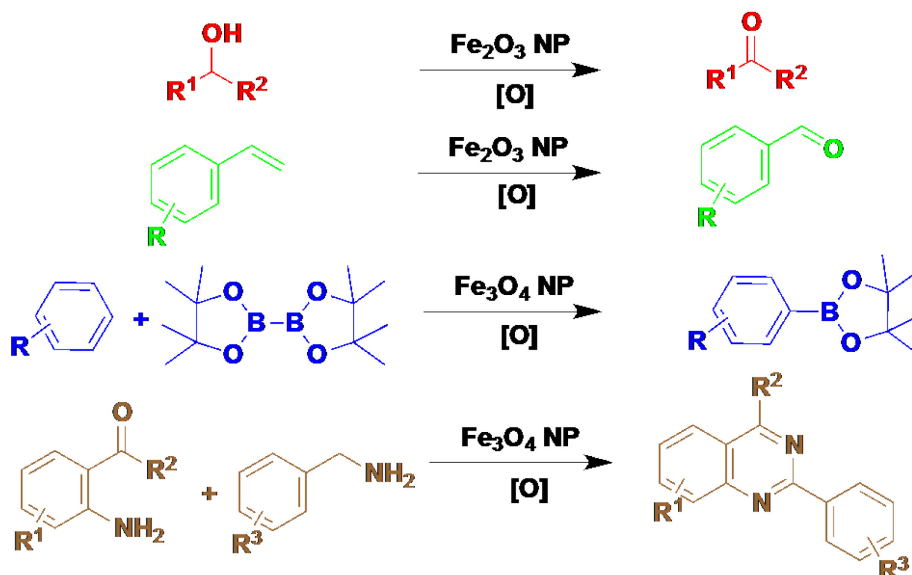


Figure 1.1: Synthesis of Iron oxide nanoparticles.

1.1.3.2 Catalytic applications

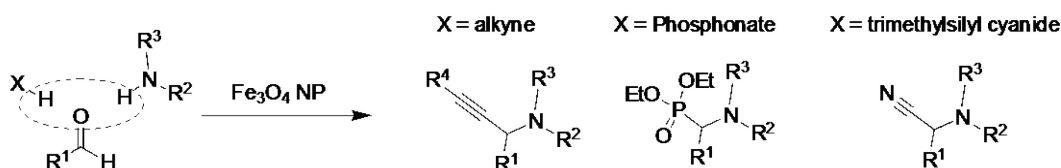
The oxidized state of Fe_3O_4 and Fe_2O_3 nanoparticles imparts a potential for oxidative reactions (scheme 1.2). The Beller group first exploited this potential by catalyzing O_2 or hydrogen peroxide oxidation of olefins and alcohols with Fe_2O_3 nanoparticles.³² This reactivity toward styrene specifically was later tuned in greater depth.³³ Additionally, the Wang group³⁴ catalysed the direct borylation of arenes by Fe_2O_3 nanoparticle catalysis with bis(pinacolato)diboron (B_2pin_2) and various mild oxidants. The Burri group likewise exhibited the strength of iron oxide nanoparticles for oxidative reactions by catalysing the formation of 2-phenylquinazoline derivatives by reaction of benzyl amine with 2-aminoaryl ketones.³⁵ Our group further demonstrated this oxidative potential by catalyzing the

oxidative cross dehydrogenative coupling of two sp^3 hybridized C-H bonds with Fe_2O_3 and Fe_3O_4 .³⁶



Scheme 1.2. Oxidizing potential of iron oxide nanoparticles

Another class of reactions involving C-H activation that can be catalysed by Fe_3O_4 nanoparticles is the one-pot three-component coupling of aldehyde, alkyne, and amine (A^3 coupling, scheme 1.3). In 2010, we³⁷ and the group of Reddy³⁸ independently reported the use of Fe_3O_4 nanoparticles to catalyse this transformation. Several variations have also been reported. In 2011, Reddy replaced the alkyne component with a phosphonate for the synthesis of α -aminophosphonates.³⁹ Likewise, Mojtahedi et al. did use the alkyne but instead used trimethylsilyl cyanide for the synthesis of α -aminonitriles.⁴⁰ The group of Gao instead replaced the alkyne with isatoic anhydride for the synthesis of various 2,3-dihydroquinazolin-4(1H)-ones.⁴¹ In a similar substitution, Ghasemzadeh et al.⁴² replaced the alkyne with dimedone for the synthesis of 1,8-dioxo-decahydroacridines.



Scheme 1.3. A^3 -type reactions catalyzed by iron oxide nanoparticles

Fe₃O₄ nanoparticles can also catalyse the Sonagashira-Hagihara reaction.⁴³

1.1.4 Iron/transition metal mixed oxide nanoparticles as catalysts

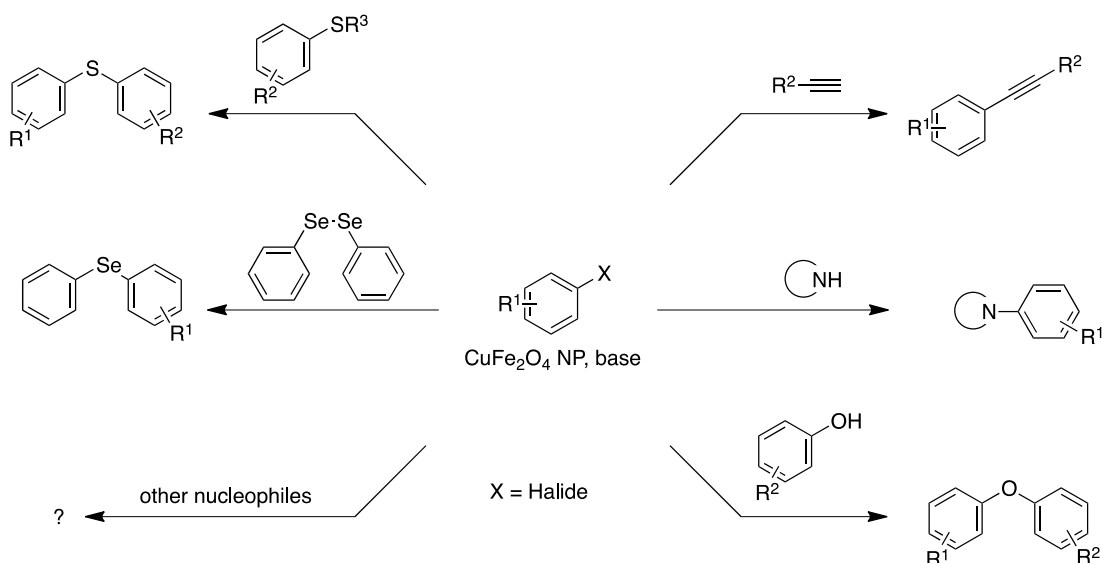
The catalysis thus far demonstrated with iron oxide nanoparticles represents an impressive feat for a generally inactive catalytic metal. However, the narrow catalytic scope of iron limits further use to only a handful of reaction types. To overcome this limitation, researchers have taken advantage of some spinel structures' ability to incorporate a second metal within the lattice. Stable bi-metallic spinels include Cu-, Zn-, Mn, Ni and Co ferrite (MFe₂O₄). In many cases the second metal opens new catalytic avenues, while the remaining iron continues to provide a means for magnetic recovery.

1.1.4.1 Synthesis

In general, the synthesis of mixed metal ferrite nanoparticles mirrors that of monometallic iron ferrite nanoparticles discussed previously. Common methods again include co-precipitation, thermal decomposition, microemulsion techniques and mechanical milling.¹⁴

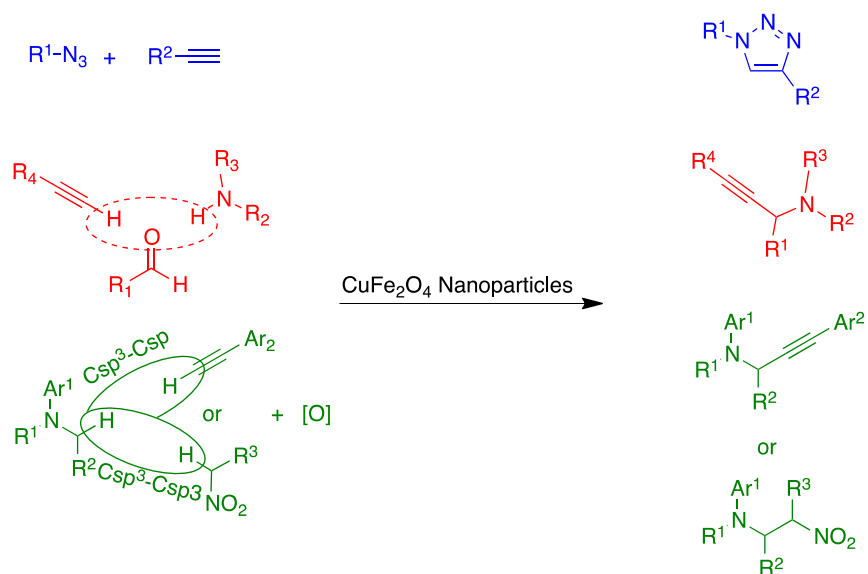
1.1.4.2 Catalytic applications of mixed metal ferrite nanoparticles

The incorporation of copper into the ferrite lattice represents the most developed branch of the mixed metal ferrites for catalysis. Copper ferrite nanoparticles can catalyze the coupling of aryl halides with C-H,⁴⁴ N-H,⁴⁵ O-H,⁴⁶ S-H,⁴⁷ or Se-Se⁴⁸ bonds under basic conditions to activate the nucleophilic coupling partner (scheme 1.4). It is only a matter of time before researchers explore more coupling partners.



Scheme 1.4. Cross-coupling reactions catalyzed by CuFe_2O_4 nanoparticles

In addition to the previously mentioned Csp-H coupling to aryl halides, the ability of copper to activate alkyne species helps with the azide-alkyne click reaction,^{49, 50} cross dehydrogenative coupling⁵¹ and A^3 coupling (scheme 1.5).⁵²



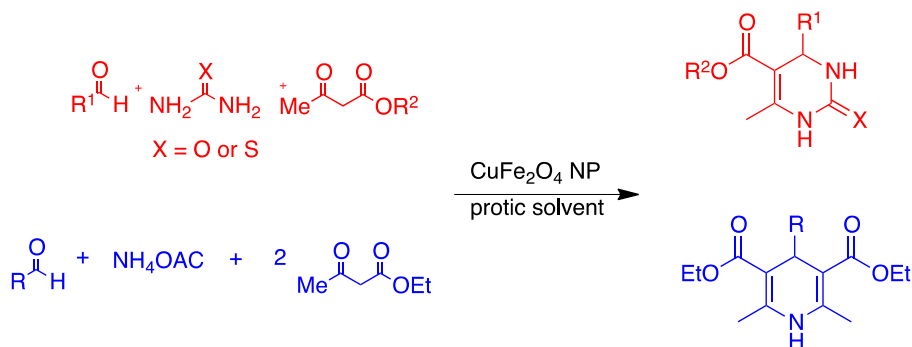
Scheme 1.5. CuFe_2O_4 nanoparticle catalyzed reactions with alkynes

Under the traditional homogeneous Cu(I) conditions, the click reaction can proceed at room temperature, however, since copper ferrite can offer only Cu(II)

within the lattice, the reaction requires either elevated temperatures⁵⁰ or the use of a ligand such as 2,2-bipyridine.⁴⁹

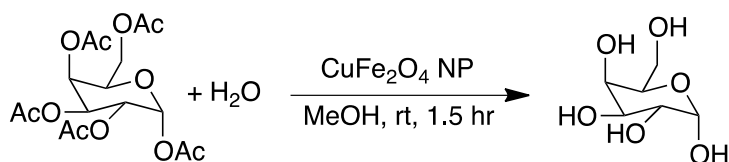
A³ coupling³⁷ and cross dehydrogenative coupling³⁶ represent two reactions that are also capable with Fe₃O₄, but where substituting copper within the ferrite lattice offers improvements. The use of CuFe₂O₄ instead of Fe₃O₄ for A³ coupling enables the use of milder conditions,⁵² while their use for cross-dehydrogenative coupling opens new catalytic avenues. For example, Fe₃O₄ can catalyze Csp³-Csp³ coupling, but not Csp³-Csp coupling (which CuFe₂O₄ can).⁵¹

CuFe₂O₄ nanoparticles are also active for the catalysis of the Biginelli⁵³ and similar condensation reactions,⁵⁴ usually requiring elevated temperatures (scheme 1.6).



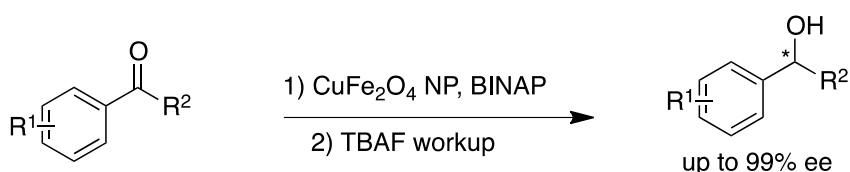
Scheme 1.6. CuFe₂O₄ nanoparticle catalyzed condensation reactions

Deprotection of acylated sugars can also be achieved with CuFe₂O₄ nanoparticles under mild conditions, even selectively at the anomeric position (scheme 1.7).⁵⁵



Scheme 1.7. CuFe₂O₄ nanoparticle catalyzed sugar deacylation

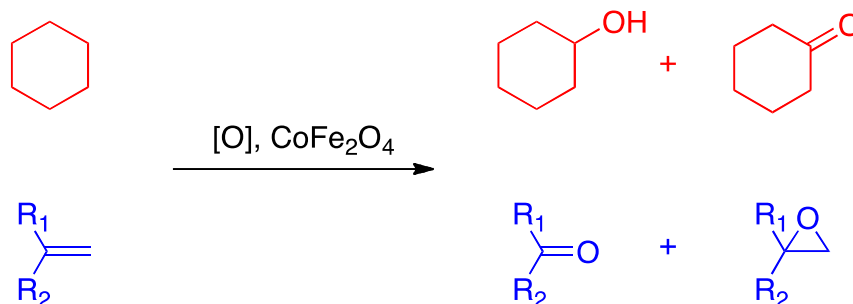
One of the draws for the use of CuFe_2O_4 nanoparticles lays in the simplicity of the system; no ligand is required to bridge the magnetic particle with the metal species actually involved in catalysis. Rather, the catalytic metal involved in catalysis is incorporated in the ferrite lattice itself. This, however, does not rule out the use of ligands to improve catalysis. In some cases, ligands have been used to reduce the temperature required for a given reaction.⁴⁷ In other cases, chiral ligands have been used for asymmetric catalysis. Such is the case with BINAP ligands imparting chiral information in the CuFe_2O_4 nanoparticle catalyzed hydrosilation of prochiral ketones, affording the corresponding alcohols (scheme 1.8).⁵⁶



Scheme 1.8. CuFe_2O_4 nanoparticle catalyzed hydrosilation.

Substituting cobalt into the ferrite lattice carries two major advantages over the use of iron alone. First, similar to the addition of copper, cobalt opens new catalytic avenues. Second, the cobalt ferrite lattice offers a higher degree of thermal and chemical stability, enabling the use of more extreme conditions.

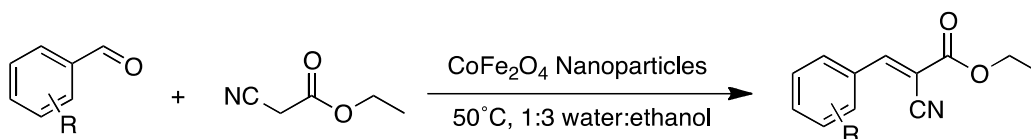
Oxidation reactions (scheme 1.9) demonstrate this increased stability. Fe_3O_4 nanoparticles can catalyze mild oxidation reactions, but cobalt ferrite nanoparticles can tolerate harsher conditions. For example, in excess of 15 bar O_2 and 140°C , CoFe_2O_4 nanoparticles can catalyze the aerobic oxidation of cyclohexane to cyclohexanol and cyclohexanone.⁵⁷ Similarly, CoFe_2O_4 nanoparticles can catalyze the oxidation of alkenes to ketones or epoxides with tert-butyl hydroperoxide at 70°C .⁵⁸



Scheme 1.9. $CoFe_2O_4$ nanoparticle catalyzed oxidation reactions

Further demonstrating the stability of $CoFe_2O_4$ nanoparticles, Manova et al.⁵⁹ subjected them to temperatures between 225°C and 325°C in order to catalyze the decomposition of methanol into CO and H_2 .

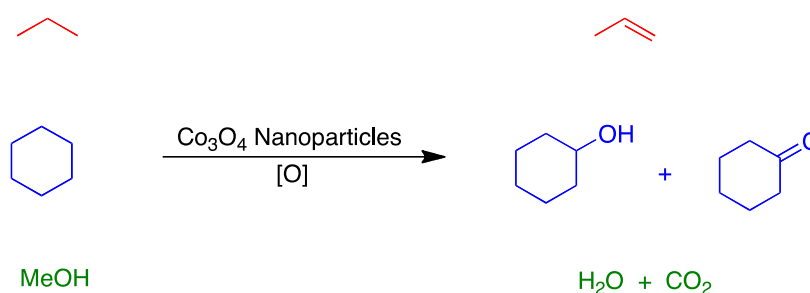
Showcasing cobalt's unique catalytic contribution within the ferrite lattice (rather than simply the increased stability) Senapati et al.⁶⁰ used $CoFe_2O_4$ nanoparticles to catalyze the Knoevenagel reaction (scheme 1.10) between various aldehydes and ethyl cyanoacetate. The reaction proceeded under mild conditions (50°C for 25 minutes), with an environmentally benign solvent mixture—1:3 water to ethanol.



Scheme 1.10. $CoFe_2O_4$ nanoparticle catalyzed Knoevenagel reaction

The tuning of catalytic properties with other metals in the ferrite lattice is not limited to stoichiometric constructions. Rather, Menini et al. doped ferrite structures with substoichiometric cobalt and manganese (approximate structure: $M_{0.5}Fe_{2.4} \otimes_{0.1}O_4$, where $M = Co$ or Mn and \otimes = cation vacancy) for the aerobic oxidation of various monoterpenic alkenes. The catalysts operated under mild conditions: neat, 1 atm O_2 , 60°C and provided a 40% conversion with 75-95% selectivity.⁶¹

On the other end of the doping spectrum, cobalt can entirely replace iron within the ferrite lattice, providing Co_3O_4 nanoparticles. Though no iron remains, cobalt is still magnetic, which enables the same easy mechanisms for catalyst recovery. Such particles have been used to catalyze ammonium perchlorate decomposition.⁶² Similar to iron oxide nanoparticles, these Co_3O_4 nanoparticles provide an oxidizing potential, which has been exploited for methanol oxidation,⁶³ cyclohexane oxidation⁶⁴ to cyclohexanol or cyclohexanone and alkane to alkene oxidation (scheme 1.11).⁶⁶



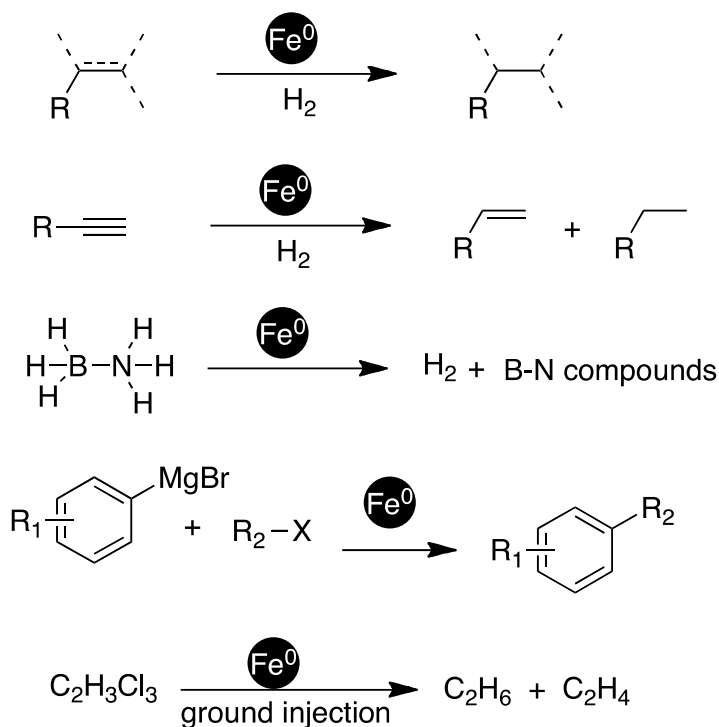
Scheme 1.11. Co_3O_4 nanoparticle catalyzed oxidation reactions

The inclusion of other metals into the ferrite lattice helps to open new catalytic avenues. The wealth of reactions catalyzed by copper ferrite nanoparticles demonstrates this increased reactivity while cobalt and manganese substituted ferrites are making strides as well. It likely won't be long until researchers uncover novel reactivity for other substituted ferrites such as NiFe_2O_4 or ZnFe_2O_4 .

1.1.5 Reduced iron nanoparticles as catalysts

The electron-rich nature of zero-valent nanoparticles often enables a unique functionality impossible with their oxidized counterparts. On the other hand, the intrinsic roots of their unique functionality, an inherent reducing power, harbor their own distinct challenges toward oxidizing conditions.

Reactions requiring such a reductive catalyst include: hydrogenation⁶⁶⁻⁶⁸ and transfer hydrogenation⁷⁰ of unsaturated hydrocarbons and carbonyls for fine chemical synthesis, dehydrogenation of ammonia borane for release of stored hydrogen fuel,⁷¹⁻⁷³ Grignard-type reactions as well as phosphate,⁷⁴ nitrate⁷⁵ and trichloroethane⁷⁶ reduction for environmental remediation (scheme 1.12).



Scheme 1.12. Reduced iron nanoparticle catalyzed reactions

1.1.5.1 Synthesis:

As is the case with most nanoparticles, reduced iron nanoparticles can be synthesized by either a top down or bottom-up approach. Industry often prefers simple, top-down approaches because they are often less expensive and easily scalable. Mechanical grinding of bulk iron represents one such industrially relevant process currently used on a large scale. The resultant nanoparticles, though inexpensive, are also highly polydisperse with regards to size and shape.⁷⁵

Bottom-up approaches offer more control over particle size and shape, so these syntheses are often used when monodispersity is of greater concern than cost.

Reduction of FeII or FeIII salts by various Grignard reagents, for example, generates highly monodisperse nanoparticles in the 1-5 nanometer regime, this synthesis is limited to strict anoxic conditions and aprotic solvents because of the Grignard reagent sensitivity.^{66, 67} Use instead of sodium borohydride as the reducing agent enables iron-nanoparticle synthesis in protic media, including even alcohols and water.⁶⁸ However, the presence of water or alcohol in this route inevitably leads to the formation of an oxide layer surrounding the zero-valent iron core.

Unfortunately, this reduction with sodium borohydride offers relatively polydisperse nanoparticles in the size range of 30-50 nm. In search of more environmentally benign reductants, the Varma group took advantage of the natural anti-oxidants (polyphenols) in tea extract to reduce FeNO_3 .^{77, 78} Similar to the sodium borohydride reduction, this synthesis could also be carried out in water and afforded particles in the 40-50 nanometer regime.

Bottom-up approaches are not limited to iron salt precursors. Indeed, several strategies have been developed for decomposition of Fe(0) precursors, which provide well defined, monodisperse nanoparticles. Fe(CO)_5 can be effectively decomposed into nanoparticles in the presence of appropriate ligands or stabilizing agents by either high temperature,⁷⁹ ultrasound,⁸⁰ or UV.⁸¹ The nanoparticles generated by this method are extremely monodisperse with tunable sizes between 5 and 20 nanometers, depending on the temperature and reaction conditions. Because examples of zero-valent iron nanoparticles for catalysis vary so differently in their size, polydispersity and degree of surface oxidation, we focus on how these aspects affect reactivity.

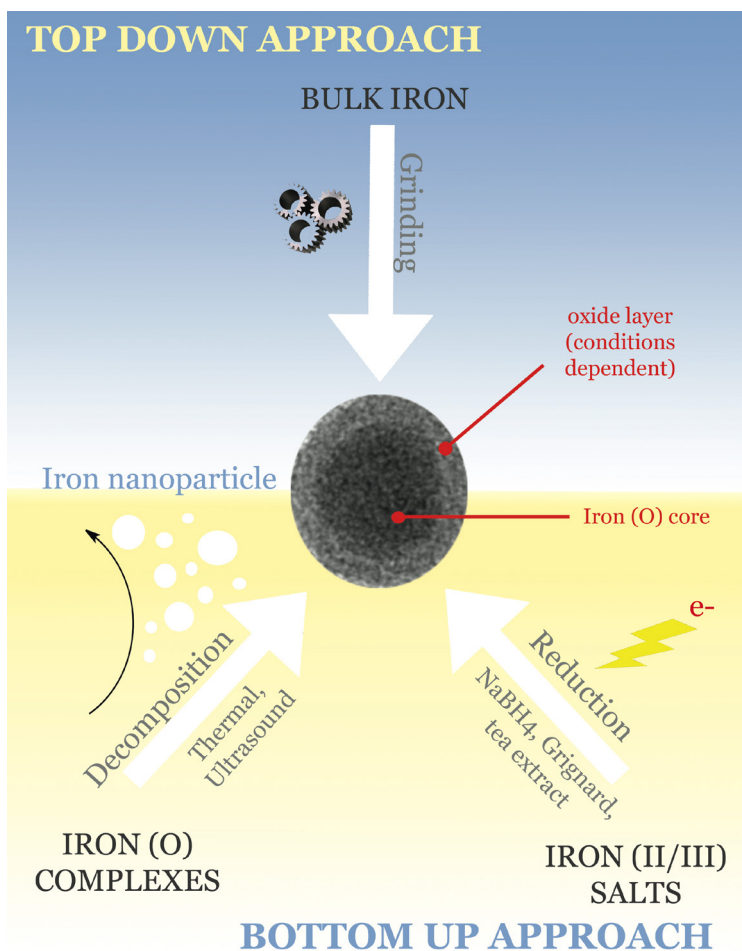


Figure. 1.2 Synthesis of Reduced Iron Nanoparticles.

1.1.5.2 Catalytic Applications

1.1.5.2.1 Hydrogenation:

Precious and toxic transition metals such as platinum, palladium and nickel (toxic, not precious) dominate the field of hydrogenation catalysts. Although iron represents a cheaper, less toxic alternative, it is generally considered a less active catalyst and as a result has achieved only limited use for hydrogenation applications. The group of De Vries, however, unlocked the hidden reductive potential of zero-valent iron at the nanoscale.⁶⁷

Iron nanoparticles (1-5 nm) generated by the reduction of Fe(II) or Fe(III) salts with an excess of Grignard reagent (EtMgCl, PhMgBr, MeMgCl, etc...) were used for the hydrogenation of alkenes and alkynes under hydrogen pressure in THF. Quantitative hydrogenation of norbornene, a strained, cyclic olefin was observed after half an hour at room temperature and 1 bar H₂. Less strained, linear olefins required 15 hours for completion. Alkynes could be hydrogenated under similar conditions, with selectivity for alkene or alkane product depending on reaction time.^{66, 67}

This novel system suffered from two major drawbacks. The nanoparticles' small size renders them non-magnetic. Second, the particles readily oxidized, thereby losing catalytic activity. Indeed, the reaction requires strict oxygen-free conditions, and even the presence of only 1% water in the solvent completely deactivated the catalyst.⁶⁷ The group of Breit overcame the first challenge of recoverability by further heterogenizing the system. They seeded iron on chemically derived graphene sheets, where particles then grew by ultrasound-induced degradation of Fe(CO)₅. These supported nanoparticles were then used for similar hydrogenation reactions with the added benefit of being magnetically recoverable.⁸⁰ In hopes of further improving recoverability, while also addressing the challenge of oxidative deactivation, we used larger core-shell iron-iron oxide nanoparticles.⁶⁹ Their 30-50 nm size rendered them magnetically recoverable, while the oxide shell apparently slowed further oxidation of the zero-valent core. Indeed, the catalyst survived exposure to air and demonstrated activity even in 1:1 water:ethanol mixtures.

In most cases of iron nanoparticle-catalyzed hydrogenation, reduction of alkenes and alkynes is more favorable compared to carbonyls or imines. Indeed, even in the rare occasion that slight conversion of carbonyl compounds has been observed, there is overwhelming selectivity for the alkene. For example, Andanson et al.⁸² with iron nanoparticles in ionic liquid were able to hydrogenate cyclohexenone with 82% selectivity for cyclohexanone over cyclohexanol (18%). Our attempt to hydrogenate cyclohexenone (100% conversion) with iron nanoparticles in a flow system gave 100% selectivity for cyclohexanone, i.e. 0%

conversion of the carbonyl.⁶⁸ We further found that aromatic imines were active for hydrogenation, as were aromatic aldehydes. Carboxylic acids, nitriles, aliphatic imines and aliphatic aldehydes demonstrated no activity. The exception to this observed selectivity of nonpolar C-C multiple bonds over more polar analogues is provided by the Morris⁷⁰ group using iron nanoparticles for asymmetric transfer hydrogenation of ketones, which of course operates on a different mechanism from the previous examples.

1.1.5.2.2 Ammonia-Borane Dehydrogenation

Some schemes for reactions catalyzed by zero-valent iron shield from oxidation the Fe surface either by using inert conditions,^{66, 67} protective polymer or oxide⁶⁹ layers. Another option is to use reaction conditions as reducing as those that generated the nanoparticles in the first place. This unique method for preventing oxidation has been demonstrated with the hydrolytic dehydrogenation of ammonia borane. Given its high hydrogen content (19.6 % by weight) this reaction is useful from the perspective of a potential hydrogen energy economy. In 2007, the group of Xu⁷¹ used a traditional NaBH_4 reduction of FeSO_4 to generate iron nanoparticles. These nanoparticles either generated beforehand, or in situ catalyzed the hydrolytic dehydrogenation of ammonia borane. With excess NaBH_4 still in solution, and NH_3BH_3 as the reactant, the nanoparticles faced little threat of oxidation even when the reaction was carried out in water and in the presence of air. Indeed, the nanoparticles could be used up to 20 times with no appreciable decrease in yield. In an effort to further make the catalyst system more robust, Dinc et al.⁷² wrapped the particles in polyethylene glycol and used them up to 10 times for catalysis, albeit with diminishing yields.

1.1.5.2.3 Grignard-type reactions

Another reaction that benefits from the inherent highly reducing conditions to avoid oxidation is the coupling of alkyl halides with aryl-Grignard reagents.⁸³ Indeed, the presence of these Grignard reagents may help to re-reduce any surface iron that may otherwise become oxidized, although the authors took the extra step of further stabilizing the nanoparticles with either 1,6-bis(diphenylphosphino)hexane or polyethylene glycol. Despite these steps to limit the oxidative deactivation of the iron nanoparticle catalyst, the reaction must still be run under inert conditions given the sensitivity not only of the catalyst but of the Grignard reagent as well.

1.1.5.2.4 Reduction of Environmental Contaminants

Zero valent iron nanoparticles can dechlorinate organic solvents, detoxify pesticides, transform fertilizers and immobilize heavy metals. Because environmental remediation is outside the scope of this journal, it will not be covered in depth here, so for detailed discussions of iron for environmental remediation, refer elsewhere.^{18, 74} The salient point to our broader discussion is that when the nanoparticles serve as a source of electrons to stoichiometrically reduce environmental contaminants, oxidation no longer must be entirely avoided, but instead serves a necessary role in their function.

1.1.5.3 Other magnetic reduced metal nanoparticles

Iron represents one of the quintessential magnetic materials because it is cheap, earth abundant and generally non-toxic, however, there are several other magnetic metals not to be forgotten, from which magnetically recoverable nanoparticle catalysts can be made. For example, reduced cobalt⁸⁴ or nickel^{85, 86} nanoparticles can be used for room temperature ammonia borane dehydrogenation. Such particles are also active for hydrogenation reactions as well.^{22, 87} These examples can already be performed by iron, so the most impactful future projects

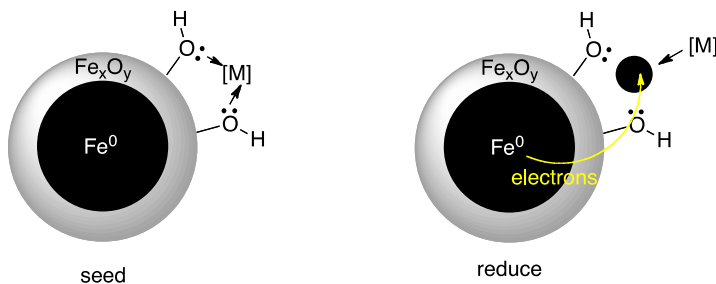
into this field may see reduced cobalt, nickel or gadolinium nanoparticles used to catalyze reactions outside the established scope of iron. For example, Shen et al. effectively used Ni nanoparticles to catalyze the thermal decomposition of ammonium perchlorate.⁸⁸

1.1.6 Reduced iron nanoparticles as seeds for other transition metal nanocatalysts

Simple iron particles offer one of the least complicated means for bare magnetic nanoparticle catalysis. However, just as many groups have used substituted ferrite nanoparticles to overcome the limited catalytic scope of mono-metallic oxidized iron particles, a similar movement has begun for the development of bi-metallic reduced particles (M@FeNP).

1.1.6.1 Synthesis

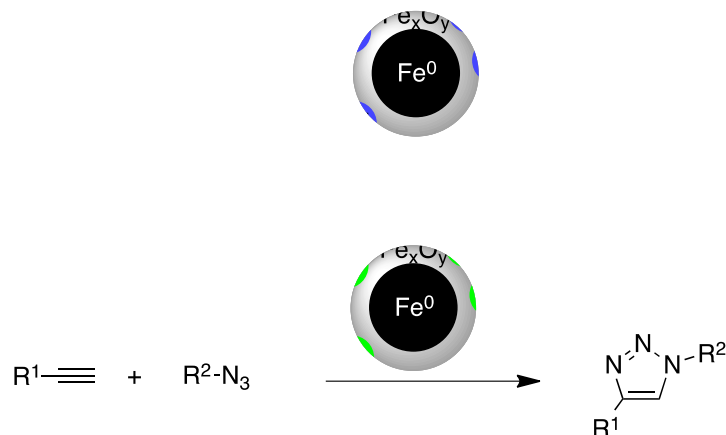
The synthesis of such particles relies on galvanic reduction of an introduced metal salt by the reduced iron core (scheme 1.13). Veinot¹⁹ postulated that the iron oxide shell first coordinates the metal center, which serves as a seed for a new particle to grow. Examples of metal particles successfully plated to iron-iron oxide core-shell nanoparticles include palladium,¹⁹ copper⁸⁹ and ruthenium.⁹⁰ Our efforts to synthesize the gold analogue afforded gold particles (presumably by reduction by the iron) but they did not stay attached to the iron particle (potentially because of significant lattice mis-match).



Scheme 1.13. Coordination, seeding and growth for the synthesis of M@FeNPs

1.1.6.2 Catalytic applications

The Pd@FeNP generated by Venoit were useful for Suzuki-Miyaura coupling.¹⁹ Our own Cu@FeNP and Ru@FeNP were active for the Huigsen 1,3-dipolar cycloaddition,⁸⁹ and for selective transfer hydrogenation of ketones over nitro compounds,⁹⁰ respectively (scheme 1.14).



Scheme 1.14. Catalytic application of M@FeNPs

Successful future endeavors into this type of bi-metallic nanoparticle catalysis must be mindful of the second metals' compatibility with iron on several fronts. First, the redox potential of the second metal salt must be high enough to be reduced by Fe(0). Second, the lattice of the second metal must be similar enough to the iron oxide shell in order for the second particle to remain attached in the long term. In a similar way that MFe₂O₄ nanoparticles expanded the scope of reactions that could be catalyzed by simple Fe₃O₄ nanoparticles, these M@FeNP successfully expand the catalytic scope of reduced iron particles. However, this field is significantly less developed and requires continuing work to determine suitable metals.

1.1.7 Conclusions

After the establishment of the broader field of magnetic nanocatalysis, a simpler scheme began to develop later where bare particles act both as catalysts and provide the means for magnetic recovery. Iron oxide particles provide an oxidative potential, while zero-valent particles impart a reductive potential. In either case, the incorporation of a second metal serves to expand the modest catalytic offering of iron alone. In the past few years many examples have been demonstrated, though the field is now developed enough to the point where meaningful future contributions will likely showcase the necessity for magnetic recoverability more than simply the novelty. This necessity could manifest as the need for multiple modes of catalyst recovery in one system or in cases where removal of metal species is both exceedingly difficult but also entirely necessary, such as macromolecule synthesis or biologically relevant systems.

1.1.8 Acknowledgements

We thank Natural Science and Engineering Research Council of Canada (NSERC), the Canada Foundation for Innovation (CFI), the Canada Research Chairs (CRC), the Fonds de Recherche sur la Nature et les Technologies (FQRNT), the Centre for Green Chemistry and Catalysis (CGCC), the Green Chemistry - NSERC Collaborative Research and Training Experience (CREATE) Program, and McGill University for financial support. Thanks to Vanessa Chazelle for artistic inputs.

1.1.9 References

1. J. Garcia-Martinez and E. Serrano-Torregrosa *The Chemical Element: Chemistry's Contribution to Our Global Future*; Wiley, VCH: Weinheim, Germany, 2011.
2. P. T. Anastas and M. M. Kirchhoff, *Acc. Chem. Res.*, 2002, 35, 686-694.

3. P. T. Anastas, L. B. Bartlett, M. M. Kirchhoff and T. C. Williamson, *Catal. Today*, 2000, 55, 11-22.
4. L.-C. Campeau, D.J. Schipper, K. Fagnou. *J. Am. Chem. Soc.* 2008, 130, 3266.
5. P.A. Chase, T. Jurca, D.W. Stephan. *Chem. Comm.* 2008, 1701.
6. H. H. Rao, C. J. Li, , *Angew. Chem.-Int. Edit.* 2011, 50, 8936.
- 7 C. Sui-Seng, F. Freutel, A. J. Lough, R. H. Morris. *Angew. Chem.-Int. Edit.* 2008, 47, 940.
8. D. J. Cole-Hamilton, R. Tooze. *Catalyst Separation, Recovery and Recycling*; Springer: Dordrecht, The Netherlands, 2006; Vol. 30.
9. D. Astruc. *Nanoparticles and Catalysis*; Wiley-VCH: Weinheim, 2008.
10. V. Polshettiwar and R. S. Varma, *Green Chem.*, 2010, 12, 743-754.
11. A. M. Molenbroek, S. Helveg, H. Topsoe and B. S. Clausen, *Top. Catal.*, 2009, 52, 1303-1311.
12. D. Astruc, F. Lu and J. Ruiz Aranzaes, *Angew. Chem., Int. Ed.*, 2005, 44, 7852-7872.
13. V. Polshettiwar, R. Luque, A. Fihri, H. Zhu, M. Bouhrara and J.-M. Bassett, *Chem. Rev.*, 2011, 111, 3036-3075.
14. A. H. Lu, E. L. Salabas and F. Schüth, *Angew. Chem., Int. Ed.*, 2007, 46, 1222-1244.
15. S. Enthaler, K. Junge and M. Beller, *Angew. Chem.-Int. Ed.*, 2008, 47, 3317-3321.
16. C. Bolm, J. Legros, J. Le Paih and L. Zani, *Chem. Rev.*, 2004, 104, 6217-6254.
17. R. Hudson, *Synlett*, 2013, 1309-1310.
18. W. X. Zhang, *J. Nanopart. Res.*, 2003, 5, 323-332.
19. S. Zhou, M. Johnson and J. G. C. Veinot, *Chem. Commun.*, 2010, 46, 2411-2413.
20. R. Hudson, C. J. Li and A. Moores, *Green Chem.*, 2012, 14, 622-624.
21. G. Chen, S. Desinan, R. Nechache, R. Rosei, F. Rosei and D. Ma, *Chem. Commun.*, 2011, 47, 6308-6310.
22. R. Xu, T. Xie, Y. Zhao and Y. Li, *Nanotechnology*, 2007, 18, 055602.
23. N. T. S. Phan, C. S. Gill, J. V. Nguyen, Z. J. Zhang and C. W. Jones, *Angew. Chem. Int. Ed.*, 2006, 45, 2209-2212.

24. J. Lee, T. Isobe and M. Senna, *Colloids Surf. A*, 1996, 109, 121-127.
25. A. Bee, R. Massart and S. Neveu, *J. Magn. Magn. Mater.*, 1995, 149, 6-9.
26. C. Liu, B. Zou, A. J. Rondinone and Z. J. Zhang, *J. Phys. Chem. B.*, 2000, 104, 1141-1145.
27. A. K. Gupta and M. Gupta, *Biomaterials*, 2005, 26, 3995-4021.
28. F. X. Redl, C. T. Black, G. C. Papaefthymiou, R. L. Sandstrom, M. Yin, H. Zeng, C. B. Murray and S. P. O'Brien, *J. Am. Chem. Soc.*, 2004, 126, 14583-14599.
29. S. Sun, H. Zeng, D. B. Robinson, S. Raoux, P. M. Rice, S. X. Wang and G. Li, *J. Am. Chem. Soc.*, 2004, 126, 273-279.
30. S. Bid, A. Banerjee, S. Kumar, S. Pradhan, U. De and D. Banerjee, *J. Alloy Comd.*, 2001, 326, 292-297.
31. T. Hyeon, S. S. Lee, J. Park, Y. Chung and H. B. Na, *J. Am. Chem. Soc.*, 2001, 123, 12798-12801.
32. F. Shi, M. K. Tse, M.-M. Pohl, A. Brückner, S. Zhang and M. Beller, *Angew. Chem. Int. Ed.*, 2007, 46, 8866-8868.
33. F. Rajabi, N. Karimi, M. R. Saidi, A. Primo, R. S. Varma and R. Luque, *Adv. Synth. Catal.*, 2012, 354, 1707-1711.
34. G. Yan, Y. Jiang, C. Kuang, S. Wang, H. Liu, Y. Zhang and J. Wang, *Chem. Commun.*, 2010, 46, 3170-3172.
35. N. Anand, K. H. P. Reddy, T. Satyanarayana, K. S. R. Rao and D. R. Burri, *Catal. Sci. Technol.*, 2012, 2, 570-574.
36. T. Zeng, G. Song, A. Moores and C. Li, *Synlett*, 2010, 13, 2002-2008.
37. T. Q. Zeng, W.-W. Chen, C. M. Cirtiu, A. Moores, G. H. Song and C. J. Li, *Green Chem.*, 2010, 12, 570-573.
38. B. Sreedhar, A. S. Kumar and P. S. Reddy, *Tetrahedron Lett.*, 2010, 51, 1891-1895.
39. B. V. S. Reddy, A. S. Krishna, A. V. Ganesh and G. G. K. S. N. Kumar, *Tetrahedron Lett.*, 2011, 52, 1359-1362.
40. M. M. Mojtahedi, M. S. Abaee and T. Alishiri, *Tetrahedron Lett.*, 2009, 50, 2322-2325.

41. E. Solano, L. Perez-Mirabet, F. Martinez-Julian, R. Guzmán, J. Arbiol, T. Puig, X. Obradors, R. Yañez, A. Pomar, S. Ricart and J. Ros, *J. Nanopart. Res.*, 2012, 14, 1-15.
42. M. A. Ghasemzadeh, J. Safaei-Ghomi and H. Molaei, *Comptes Rendus Chimie*, 2012, 15, 969-974.
43. H. Firouzabadi, N. Iranpoor, M. Gholinejad and J. Hoseini, *Adv. Synth. Catal.*, 2011, 353, 125-132.
44. N. Panda, A. K. Jena and S. Mohapatra, *Chem. Lett.*, 2011, 40, 956-958.
45. N. Panda, A. K. Jena, S. Mohapatra and S. R. Rout, *Tetrahedron Lett.*, 2011, 52, 1924-1927.
46. R. Z. Zhang, J. M. Liu, S. F. Wang, J. Z. Niu, C. G. Xia and W. Sun, *ChemCatChem*, 2011, 3, 146-149.
47. K. Swapna, S. N. Murthy, M. T. Jyothi and Y. V. D. Nageswar, *Org. Biomol. Chem.*, 2011, 9, 5989-5996.
48. K. Swapna, S. N. Murthy and Y. V. D. Nageswar, *Eur. J. Org. Chem.*, 2011, 1940-1946.
49. S. Ishikawa, R. Hudson, A. Moores and C.-J. Li, *Heterocycles*, 2012, 86, 1970.
50. B. Kumar, K. H. V. Reddy, B. Madhav, K. Ramesh and Y. V. D. Nageswar, *Tetrahedron Lett.*, 2012, 53, 4595-4599.
51. R. Hudson, S. Ishikawa, C. J. Li and A. Moores, *Synlett*, 2013, DOI: 10.1055/s-0033-1339278.
52. M. L. Kantam, J. Yadav, S. Laha and S. Jha, *Synlett*, 2009, 1791-1794.
53. R. Hudson, J. Silverman, C. J. Li and A. Moores, *Proceedings of the 3rd International Conference on Nanotechnology*, 2012, Paper No. 318.
54. I. V. K. Viswanath and Y. L. N. Murthy, *Chem. Sci. Trans.*, 2012, 2, 227-233.
55. J. E. Tasca, A. Ponzinibbio, G. Diaz, R. D. Bravo, A. Lavat and M. G. Gonzalez, *Top. Catal.*, 2010, 53, 1087-1090.
56. M. L. Kantam, J. Yadav, S. Laha, P. Srinivas, B. Sreedhar and F. Figueras, *J. Org. Chem.*, 2009, 74, 4608-4611.
57. J. Tong, L. Bo, Z. Li, Z. Lei and C. Xia, *J. Mol. Catal. A: Chem.*, 2009, 307, 58-63.
58. M. Kooti and M. Afshari, *Scientia Iranica*, 2012.

59. E. Manova, B. Kunev, D. Paneva, I. Mitov, L. Petrov, C. Estournès, C. D'Orléan, J.-L. Rehspringer and M. Kurmoo, *Chem. Mater.*, 2004, 16, 5689-5696.
60. K. K. Senapati, C. Borgohain and P. Phukan, *J. Mol. Catal. A: Chem.*, 2011, 339, 24-31.
61. L. Menini, M. C. Pereira, L. A. Parreira, J. D. Fabris and E. V. Gusevskaya, *J. Catal.*, 2008, 254, 355-364.
62. L.-N. Jin, Q. Liu and W.-Y. Sun, *CrystEngComm*, 2012, 14, 7721-7726.
63. R. Jing, A. Shan, R. Wang and C. Chen, *CrystEngComm*, 2013, 15, 3587-3592.
64. F. Cao, D. Wang, R. Deng, J. Tang, S. Song, Y. Lei, S. Wang, S. Su, X. Yang and H. Zhang, *CrystEngComm*, 2011, 13, 2123-2129.
65. T. E. Davies, T. Garcia, B. Solsona and S. H. Taylor, *Chem. Commun.*, 2006, 3417-3419.
66. C. Rangheard, C. De Julian Fernandez, P. H. Phua, J. Hoorn, L. Lefort and J. G. De Vries, *Dalton Trans.*, 2010, 39, 8464-8471.
67. P. H. Phua, L. Lefort, J. A. F. Boogers, M. Tristany and J. G. de Vries, *Chem. Commun.*, 2009, 3747-3749.
68. R. Hudson, G. Hamasaka, T. Osako, Y. M. A. Yamada, C.-J. Li, Y. Uozumi and A. Moores, *Green Chem.*, 2013.
69. R. Hudson, A. Riviere, C. M. Cirtiu, K. L. Luska and A. Moores, *Chem. Commun.*, 2012, 48, 3360-3362.
70. J. F. Sonnenberg, N. Coombs, P. A. Dube and R. H. Morris, *J. Am. Chem. Soc.*, 2012, 134, 5893-5899.
71. J.-M. Yan, X.-B. Zhang, S. Han, H. Shioyama and Q. Xu, *Angew. Chem. Int. Ed.*, 2008, 47, 2287-2289.
72. M. Dinç, Ö. Metin and S. Özkar, *Catal. Today*, 2012, 183, 10-16.
73. J. F. Sonnenberg and R. H. Morris, *ACS Catalysis*, 2013, 3, 1092-1102.
74. T. Almeelbi and A. Bezbaruah, *J. Nanopart. Res.*, 2012, 14.
75. Y. H. Hwang, D. G. Kim and H. S. Shin, *J. Hazard. Mater.*, 2011, 185, 1513-1521.
76. Y. Q. Liu, S. A. Majetich, R. D. Tilton, D. S. Sholl and G. V. Lowry, *Environ. Sci. Tech.*, 2005, 39, 1338-1345.

77. G. E. Hoag, J. B. Collins, J. L. Holcomb, J. R. Hoag, M. N. Nadagouda and R. S. Varma, *J. Mater. Chem.*, 2009, 19, 8671-8677.
78. M. N. Nadagouda, A. B. Castle, R. C. Murdock, S. M. Hussain and R. S. Varma, *Green Chem.*, 2010, 12, 114-122.
79. S. Peng, C. Wang, J. Xie and S. Sun, *J. Am. Chem. Soc.*, 2006, 128, 10676-10677.
80. M. Stein, J. Wieland, P. Steurer, F. Toelle, R. Muelhaupt and B. Breit, *Adv. Synth. Catal.*, 2011, 353, 523-527.
81. G. B. Khomutov, R. V. Gaynutdinov, S. P. Gubin, A. Y. Obydenov, E. S. Soldatov, A. L. Tolstikhina and A. S. Trifonov, *MRS Proceedings*, Cambridge Univ Press, 2000.
82. J.-M. Andanson, S. Marx and A. Baiker, *Catal. Sci. Tech.*, 2012, 2, 1403-1409.
83. R. B. Bedford, M. Betham, D. W. Bruce, S. A. Davis, R. M. Frost and M. Hird, *Chem. Commun.*, 2006, 1398-1400.
84. M. Rakap and S. Özkar, *Int. J. Hydrogen Energy*, 2010, 35, 3341-3346.
85. Ö. Metin, V. Mazumder, S. Özkar and S. Sun, *J. Am. Chem. Soc.*, 2010, 132, 1468-1469.
86. J.-M. Yan, X.-B. Zhang, S. Han, H. Shioyama and Q. Xu, *Inorg. Chem.*, 2009, 48, 7389-7393.
87. Y. Hu, Y. Yu, Z. Hou, H. Yang, B. Feng, H. Li, Y. Qiao, X. Wang, L. Hua, Z. Pan and X. Zhao, *Chem. Asian J.*, 2010, 5, 1178-1184.
88. X.-J. Shen, J.-P. Yang, Y. Liu, Y.-S. Luo and S.-Y. Fu, *New J. Chem.*, 2011, 35, 1403-1409.
89. R. Hudson, C.-J. Li and A. Moores, *Green Chem.*, 2012, 14, 622-624.
90. R. Hudson, V. Chazelle, C. J. Li and A. Moores, *Green Chem.*, 2013, Manuscript in preparation.

2 Reduced Iron Nanoparticles for Hydrogenation Reactions

Core-shell iron-iron oxide nanoparticles were synthesized by a sodium borohydride reduction of iron sulfate in a mixture of water and methanol. These particles were active for the catalysis of various unsaturated hydrocarbons with ethanol as the solvent. The particles could be easily recovered and recycled. This chemistry could be adapted to a flow system by generating the nanoparticles in the presence of an amphiphilic polymer. The polymer-supported particles could then be packed into a flow column and similarly be used for the hydrogenation of various unsaturated compounds.

This chapter is based upon two published articles, whose citations appear below, which are both reprinted with permission from the Royal Society of Chemistry and all co-authors.

Reuben Hudson, Antoine Rivière, Ciprian M. Cirtiu, Kylie L. Luska and Audrey H. Moores. Iron-iron oxide core-shell nanoparticles are active and magnetically recyclable olefin and alkyne hydrogenation catalysts in protic and aqueous media. *Chem. Commun.*, 2012, 48, 3360-3362.

Reuben Hudson, Go Hamasaka, Takao Osaka, Yoichi Y. A. Yamada, Yasuhiro Uozumi, Chao-Jun Li, and Audrey Moores. Highly efficient iron(0) nanoparticle-catalyzed hydrogenation in water in flow. *Green Chem.*, 2013, 15, 2141-2148

2.1 Iron-iron oxide core-shell nanoparticles are active and magnetically recyclable olefin and alkyne hydrogenation catalysts in protic and aqueous media

2.1.1 Abstract

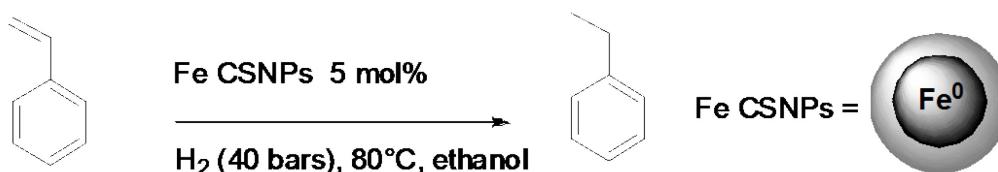
We report for the first time the use of iron-iron oxide core-shell nanoparticles for the hydrogenation of olefins and alkynes under mild conditions in ethanol and in an aqueous medium. This catalyst proves robust towards the presence of oxidants, such as oxygen and water, is magnetically recoverable and shows selectivity towards the less activated double bonds.

2.1.2 Introduction

Hydrogenation is a ubiquitous reaction that is used in all fields of chemistry, from petrochemistry to drug synthesis.¹ Transition metals, such as Pd, Pt, Ru, Rh or Ni, both homogenous and heterogeneous, are catalysts of choice for this reaction. However, in an effort to develop a more sustainable approach,^{2,3} their cost, toxicity and potential depletion has fuelled the development of alternative hydrogenation catalysts. Very recently, several catalysts⁴⁻⁶ have been designed to avoid the use of precious metals, among which iron is a very attractive option. Iron is non-toxic, naturally abundant, cheap and potentially amenable to magnetic recovery.⁷ Iron complexes were shown to be active catalysts⁸ for the hydrogenation of olefins,⁹ carbonyl bonds^{10,11} and the selective hydrogenation of alkynes to alkenes.^{12,13} Such complexes can also hydrogenate carbonates¹⁴ and dehydrogenate formic acid.¹⁵ Besides these developments in homogenous catalysis, iron in the form of suspendable nanoparticles has been investigated as a catalyst.^{16,17} The de Vries group evinced that ligand-free iron nanoparticles (Fe NPs) are active catalysts for the hydrogenation of alkenes and alkynes under very mild conditions.^{4,18} These particles proved very active, however, they could not be separated from the reaction medium magnetically because of their small size. Breit and co-workers overcame

this limitation by stabilizing Fe NPs made by decomposition of $\text{Fe}(\text{CO})_5$ onto graphene sheets. Although the resulting particles were active hydrogenation catalysts,¹⁹ they were prone to oxidation in the presence of either oxygen or water. Growth of the oxide shell in the presence of an oxidant was suggested to be an absolute limitation to catalysis in terms of reactivity.

Herein, we present the use of simple and stabilizer-free iron-iron oxide core-shell nanoparticles (Fe CSNPs) for the hydrogenation of alkenes and alkynes (scheme 2.1.1). These nanoparticles represent the first iron-based catalyst in ethanol, and in water-ethanol mixtures. These nanoparticles are either synthesized in an aqueous medium, or available in large quantity commercially, and suspended in water.



Scheme 2.1.1. Hydrogenation of olefin catalyzed by Fe CSNPs

These nanoparticles are recoverable magnetically and recyclable up to 10 times. Our results indicate that a thin shell of iron oxide surrounding the zero-valent core can provide protection of nanoparticles against excessive oxidation without obstructing hydrogenation reactivity, in protic and aqueous environments.

Fe CSNPs were produced by the reduction of FeSO_4 in a water/methanol mixture using NaBH_4 .^{20, 21} Such particles have been investigated as stoichiometric reductants for water remediation²²⁻²⁵ and also studied as magnetic seeds for Pd C-C couplings catalysts.²⁶ We were thus intrigued to see if these particles could also be active as hydrogenation catalysts. These Fe CSNPs featured an average core diameter of 44 ± 8.3 nm and a shell thickness of 6 ± 2 nm, which is comparable to what has been reported in the literature (Fig.1).^{25, 27} Alternatively, we used commercial iron core-shell nanoparticles (C-Fe CSNPs) which also presented iron oxide sheets at their surface.


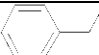

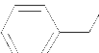

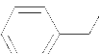

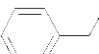
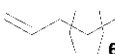

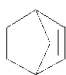
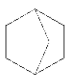
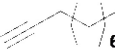


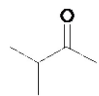
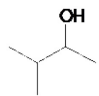
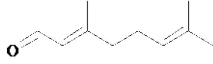

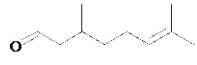
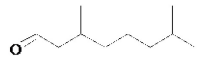
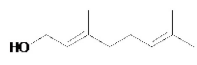
2.1.3 Results and Discussion

Fe CSNPs proved to be an active hydrogenation catalyst for a range of substrates in ethanol, under 40 bar H_2 at 80°C in 24h (table 2.1.1). Terminal alkenes were easily converted. Styrene provided ethyl benzene quantitatively (entry 1), while decene afforded decane with a conversion of 91% (entry 5). Norbornene, a strained disubstituted cis-alkene (entry 6), was converted in 96%. These Fe CSNPs were also active for alkyne hydrogenation, in which a conversion of 88% was achieved for 1-decyne. The major product of 1-decyne hydrogenation was decane (82%), (entry 7) and is in agreement with the reactivity observed for decene. Conversions of C=O bonds (entry 8, 9) and aromatic C=C bonds (entry 1) were not observed. Hydrogenation of citral (entry 9) highlighted the selectivity of this catalyst for C=C bonds as no conversion of the aldehyde was observed. Citral also features two trisubstituted C=C double bonds. 55% of citral was hydrogenated at, at least, one of these positions. Surprisingly, the less activated, less polar bond proved more reactive, at a ratio 2.9:1. Fe CSNPs could be magnetically recovered and recycled up to 10 times with only a slight decrease in yield observed after 8 cycles (table 2.2.2). This ease of recovery provides for a more industrially relevant system, compared to other Fe NP-based hydrogenation catalysts which could either not be separated magnetically,¹⁸ or had to employ functionalized graphene sheets to do so.¹⁹

A limitation of the use of pure FeNPs for hydrogenation resides in their sensitivity toward oxidation by either O_2 or H_2O . Even the presence of 1% water completely deactivates these catalysts (it is possible that complete deactivation could occur without complete oxidation).^{18,19} We found that 1% water had no effect on the hydrogenation activity of Fe CSNPs (table 2.2.1, entry 2). We were pleased to see that performing the reaction directly in a 50:50 water:ethanol mixture only reduced conversion to 62% (table 2.2.1, entry 3). Performing the reaction in water as a solvent did not quench reactivity completely but led to irregular results. On the other hand, O_2 exposure was not detrimental either. Between each recycling test, the catalyst was exposed to O_2 for a few minutes, as our set up did not allow for an inert

atmosphere to be completely maintained. This did not seem to adversely impact on the conversion, at least for the first 8 recycling tests.

Table 2.1.1. Fe CSNP catalyzed olefin hydrogenation

| Entry ^a | Substrate | Product | Conversion (%) |
|--------------------|---|--|----------------|
| 1 |  |  | 100 |
| 2 ^b |  |  | 100 |
| 3 ^c |  |  | 62 |
| 4 ^d |  |  | 44 |
| 5 |  |  | 91 |
| 6 |  |  | 96 |
| 7 |  |  (82%)  (6%) | 88 |
| 8 |  |  | 0 |
| 9 |  |  (40%)  (12%)  (3%)  (0%) | 55 |

^a Reaction conditions: substrate (1 mmol), Fe CSNPs (5 mol%, relative to total iron), EtOH (17mL), 80°C, H₂ (40 bars), 24 hour. ^b EtOH:H₂O as solvent 99:1 ^c EtOH:H₂O as solvent 50:50 ^d CFe CSNP as catalyst

We also tested the activity of C-Fe CSNPs, commercially synthesized iron nanoparticles from Nanoiron© (table 2.1.1, entry 4). We were pleased to see that despite a lower activity, still 44% of the styrene could be converted in ethanol, under the same conditions. Since these particles are produced in large scale, in water, this opens an opportunity to apply this reaction in an industrial setting.

In order to better understand the nature of the catalyst, we performed an XPS and XRD analysis of these Fe CSNPs. These analyses revealed the presence of iron zero and some iron oxides, mostly FeO, which is consistent with the TEM observations. We also performed a TEM study before and after catalysis. After 5 reaction cycles, we saw no change in particle size, shape or shell thickness. After 10 cycles, however, the oxide shell thickness grew and oxide build up was visible. We also witnessed the appearance of sheets of what was determined to be crystalline FeO by EDAX, beside the Fe CSNPs. These two observations correlate with a decrease in activity and can be explained by the exposure to oxygen over time, between recycling runs.

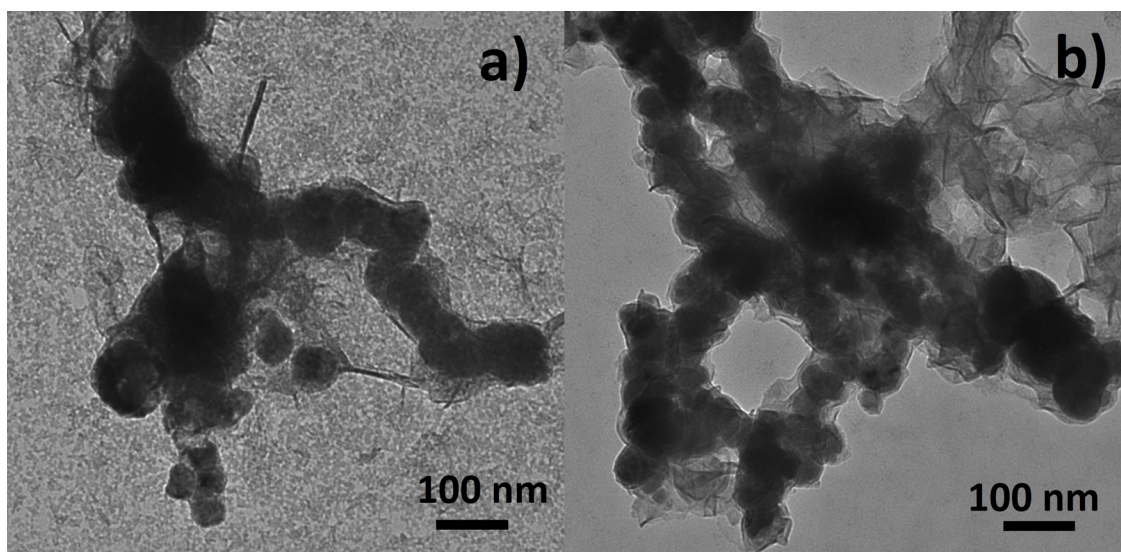


Figure 2.1.1. TEM pictures of Fe CSNPs a) before catalysis and b) after 10 cycles

We also investigated the heterogeneous nature of the catalyzed reaction. Upon magnetic removal of the nanoparticles, the reaction supernatant was exposed to styrene under the exact same conditions and no conversion of styrene was observed. ICP-MS analysis of this same supernatant indicated the presence of 35 μM

of dissolved iron. As a blank test, we used an equivalent amount of soluble FeSO₄ as catalyst and observed no hydrogenation of styrene. Tests in absence of H₂ led to no conversion.

Overall, Fe CSNPs feature a scope that is similar to that of the pure Fe NPs described before,^{18, 27} namely a good activity for olefin and alkyne hydrogenation and no activity towards C=O double bonds. This suggests a mechanism in which Fe(0) surface acts as the catalyst, indicating that the nanoparticle iron oxide shell is sufficiently porous to allow substrate access to the surface of the Fe(0) core. While the porosity of the Fe CSNPs is under investigation, porosity in iron oxide shells caused by a Kirkendall effect, as an oxide shell is formed onto a reduced core, has been reported.²⁸ Indeed, the formation of the oxide shell around both Fe CSNPs and C-Fe CSNPs results directly from the presence of water during their synthesis. This contrasts with the previously reported examples of Fe NPs, relying on either reduction of iron salt in THF by Grignard reagents,¹⁸ or Fe(CO)₅ decomposition.¹⁹ Fe CSNPs were less active than Fe NPs, but their oxide shell does provide protection to allow reaction in an aqueous environment and under ligand-free conditions. Water, as a main poison to a pure Fe(0) surface, may interact strongly with this shell and migrate more slowly than the lipophilic substrates. The selectivity of the hydrogenation of citral (table 2.1.1, entry 9) is of interest. Of the two available C=C double bonds, the isolated double bond was converted more quickly than the traditionally more active conjugated C=C bond.^{29, 30} This, perhaps, could be due to an orienting affect of the iron oxide shell—directing the less polar double bond to the zero valent core, thus leaving the more polar aldehyde (along with its conjugated partner) to interact with the oxide shell and polar solvent environment.

Table 2.1.2. Recycling reactions for the hydrogenation of styrene to ethyl benzene

| Cycle number ^a | Conversion (%) |
|---------------------------|----------------|
| 1-8 | 100 |
| 9 | 94 |
| 10 | 89 |

^a Reaction conditions: substrate (1 mmol), Fe CSNP (5 mol%, relative to total iron), EtOH (17mL), 80°C, H₂ (40 bars), 24 hour. Magnetic recovery in air was applied between cycles

2.1.4 Conclusions

We have described the first water-stable catalytic hydrogenation system based on iron nanoparticles. Specifically, we have identified iron-iron oxide core-shell nanoparticles as robust, magnetically recoverable catalysts for hydrogenation of olefins and alkynes, in ethanol and aqueous ethanol. The system is active towards many substrates and strictly selective towards alkenes and alkynes over carbonyl and aromatic groups. These results suggest that the presence of an oxide shell is not an obstacle to activity and does provide protection towards oxidation by oxygen and water. Commercially prepared particles were also active, opening an opportunity to apply this reaction under more realistic conditions.

2.1.5 Acknowledgements

We thank the Natural Science and Engineering Research Council of Canada (NSERC), the Canada Foundation for Innovation (CFI), the Canada Research Chairs (CRC), the Fonds de Recherche sur la Nature et les Technologies (FQRNT), the Center for Green Chemistry and Catalysis (CGCC) and McGill University for their financial support. Ecole Polytechnique (France) financially supported AR.

Nanoiron© is thanked for providing C-Fe CSNPs to test. We are grateful K. Wilkinson and M. Hadioui for their help with ICP-MS, and to F. Qi, A. Lacasse and T. Friscic for XRD. CJ Li, N. Braid, T. Friscic and Y. Feng are acknowledged for fruitful discussions.

2.1.6 References

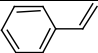
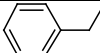
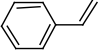
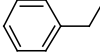
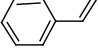
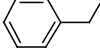
1. J. G. de Vries and C. J. Elsevier, *Handbook of Homogeneous Hydrogenation*, Wiley-VCH, Weinheim, 2007.
2. P. T. Anastas and M. M. Kirchhoff, *Acc. Chem. Res.*, 2002, 35, 686-694.
3. P. T. Anastas, M. M. Kirchhoff and T. C. Williamson, *Appl. Catal., A*, 2001, 221, 3-13.
4. P. A. Chase, T. Jurca and D. W. Stephan, *Chem. Comm.*, 2008, 1701-1703.
5. P. A. Chase and D. W. Stephan, *Angew. Chem.-Int. Ed.*, 2008, 47, 7433-7437.
6. B. Dudle, K. Rajesh, O. Blacque and H. Berke, *J. Am. Chem. Soc.*, 2011, 133, 8168-8178.
7. S. Enthaler, K. Junge and M. Beller, *Angew. Chem.-Int. Ed.*, 2008, 47, 3317-3321.
8. R. H. Morris, *Chem. Soc. Rev.*, 2009, 38, 2282-2291.
9. S. C. Bart, E. Lobkovsky and P. J. Chirik, *J. Am. Chem. Soc.*, 2004, 126, 13794-13807.
10. A. Mikhailine, A. J. Lough and R. H. Morris, *J. Am. Chem. Soc.*, 2009, 131, 1394-1395.
11. C. Sui-Seng, F. Freutel, A. J. Lough and R. H. Morris, *Angew. Chem.-Int. Ed.*, 2008, 47, 940-943.
12. S. Enthaler, M. Haberberger and E. Irran, *Chem. Asian J.*, 2011, 6, 1613-1623.
13. M. Haberberger, E. Irran and S. Enthaler, *Eur. J. Inorg. Chem.*, 2011, 2797-2802.
14. C. Federsel, A. Boddien, R. Jackstell, R. Jennerjahn, P. J. Dyson, R. Scopelliti, G. Laurenczy and M. Beller, *Angew. Chem. Int. Ed.*, 2010, 49, 9777-9780.
15. A. Boddien, D. Mellmann, F. Gaertner, R. Jackstell, H. Junge, P. J. Dyson, G. Laurenczy, R. Ludwig and M. Beller, *Science*, 2011, 333, 1733-1736.

16. V. Polshettiwar and R. S. Varma, *Green Chem.*, 2010, 12, 743-754.
17. R. B. Bedford, M. Betham, D. W. Bruce, S. A. Davis, R. M. Frost and M. Hird, *Chem. Comm.*, 2006, 1398-1400.
18. P.-H. Phua, L. Lefort, J. A. F. Boogers, M. Tristany and J. G. de Vries, *Chem Comm.*, 2009, 3747-3749.
19. M. Stein, J. Wieland, P. Steurer, F. Toelle, R. Muelhaupt and B. Breit, *Adv. Synth. Catal.*, 2011, 353, 523-527.
20. C. M. Cirtiu, T. Raychoudhury, S. Ghoshal and A. Moores, *Colloids Surf., A*, 2011, doi:10.1016/j.colsurfa.2011.1009.1011.
21. Y. Q. Liu, H. Choi, D. Dionysiou and G. V. Lowry, *Chem. Mater.*, 2005, 17, 5315-5322.
22. G. E. Hoag, J. B. Collins, J. L. Holcomb, J. R. Hoag, M. N. Nadagouda and R. S. Varma, *J. Mater. Chem.*, 2009, 19, 8671-8677.
23. Y. Q. Liu, S. A. Majetich, R. D. Tilton, D. S. Sholl and G. V. Lowry, *Environ. Sci. Tech.*, 2005, 39, 1338-1345.
24. J. T. Nurmi, P. G. Tratnyek, V. Sarathy, D. R. Baer, J. E. Amonette, K. Pecher, C. M. Wang, J. C. Linehan, D. W. Matson, R. L. Penn and M. D. Driessen, *Environ. Sci. Tech.*, 2005, 39, 1221-1230.
25. W.-X. Zhang, *J. Nanopart. Res.*, 2003, 5, 323-332.
26. S. Zhou, M. Johnson and J. G. C. Veinot, *Chem. Comm.*, 2010, 46, 2411-2413.
27. B. Schrick, B. W. Hydutsky, J. L. Blough and T. E. Mallouk, *Chem. Mater.*, 2004, 16, 2187-2193.
28. S. Peng and S. Sun, *Angew. Chem. Int. Ed.*, 2007, 46, 4155-4158.
29. G. Guo, F. Qin, D. Yang, C. Wang, H. Xu and S. Yang, *Chem. Mater.*, 2008, 20, 2291-2297.
30. M. Steffan, F. Klasovsk, J. Arras, C. Roth, J. Radnik, H. Hofmeister and P. Claus, *Adv. Synth. Catal.*, 2008, 350, 1337-1348.
31. J. Vanwonderghem, S. Morup, C. J. W. Koch, S. W. Charles and S. Wells, *Nature*, 1986, 322, 622-623.

2.1.7 Appendix

2.1.7.1 Blank catalytic runs

Table 2.1.3. Comparison of Fe CSNP catalyzed olefin hydrogenation with H₂, Ar, or no additional gas

| Entry | Gas | Substrate | Product | Conversion (%) |
|----------------|-----------------------|---|---|----------------|
| 1 | 40 bar H ₂ |  |  | 100 |
| 2 ^b | None |  |  | 0 |
| 3 ^c | 40 bar Ar |  |  | 0 |

^a Reaction conditions: substrate (1 mmol), Fe CSNPs (5 mol%), EtOH (17mL), 80°C, 24 hour.

Hydrogenation of styrene proceeds quantitatively in the presence of 40 bar H₂ (entry 1), though not in the absence of an external gas (entry 2) or in the presence of the same pressure of Ar (entry 3). The dependence of hydrogenation on H₂ refutes the possibility of EtOH as a transfer hydrogenation agent in this system. Blank test with no catalyst under H₂ pressure (40 bars) resulted in no conversion.

2.1.7.2 Experimental section:

2.1.7.2.1 Chemicals

NaBH₄ (99.99%) was purchased from and FeSO₄·7H₂O from AlfaAesar, 99+%. High-purity water (18.2 MΩ•cm from a Nanopure Diamond unit, Barnstead) was used to prepare the solutions. Methanol (HPLC grade) was purchased from Fischer Scientific and used with no further purification. Ethanol (anhydrous) was purchased from GreenField Ethanol and used only after being passed through an Innovative

Reduced Iron Nanoparticles for Hydrogenation Reactions

Technologies Pure Solve solvent purification system. All the hydrogenation substrates tested were purchased from Aldrich and used as received. All Solvents were deoxygenated prior to reaction by bubbling nitrogen gas for 1 hour. Unless specified otherwise, all reactions were carried out in an inert atmosphere in either a glovebox or using the Schlenk technique.

2.1.7.2.2 Analytical Methods

High-pressure experiments were performed employing a Parr Instruments 5000 Series Multiple Reactor System equipped with 45 mL reaction vessels. TEM images of bare-NZVI nanoparticles were taken with a Philips CM200 instrument operated at 200 kV. High resolution TEM images presented in the appendix were taken with a FEI Tecnai G2 F20 instrument. X-ray photoelectron spectrometry (XPS) was performed on a VG ESCALAB 3 MKII spectrometer (VG, Thermo Electron Corporation, UK) equipped with an MgK α source. X-ray diffraction (XRD) was achieved on a Bruker AXS D8 Discover using Cu K α radiation at 40kV & 40 mA.

2.1.7.2.3 Synthesis of Fe CSNPs

This synthesis is adapted from ref 20 of the article. 8.4 g of FeSO₄·7H₂O was dissolved in a 480 mL methanol/water solution (30% methanol, v/v). An aqueous solution NaBH₄ (2.4 g in 60 mL) was added with stirring at a constant rate of 3 mL/min using a syringe pump. Once all of the NaBH₄ solution was added, the mixture was stirred for an additional 30 min. Magnetic collection followed by solvent removal and three ethanol washes (200 mL each) yielded an ethanol dispersion of Fe CSNPs used directly in catalysis.

2.1.7.2.4 Typical catalytic run

In a general reaction procedure, Fe CSNPs or C-Fe CSNPs (5 mol%- assuming all the sample is composed of iron) were loaded in the high pressure reactor liner, as

a suspension, followed by application of an external magnet to pull the nanoparticles out of suspension. Then the excess solvent could be removed. 1 mmol of substrate and 0.5 mmol dodecane as an internal standard were then loaded. with 17 mL of EtOH and a magnetic stirbar. After pressurizing with H₂ and raising the reactor to the appropriate temperature, the reaction proceeded for 24 hour. After the reaction, the reactor was open to air for a few minutes, the catalysts was recovered magnetically, washed three times with 10-15 mL EtOH and reused on another catalytic run as is. The conversion was monitored by GC-FID.

2.1.7.2.5 TEM Preparation.

TEM samples were prepared by adding a drop of a dilute ethanol solution of nanoparticles onto a carbon film over 400 mesh copper grid. After the solvent evaporated, the grid was stored under vacuum until brought to the TEM for analysis.

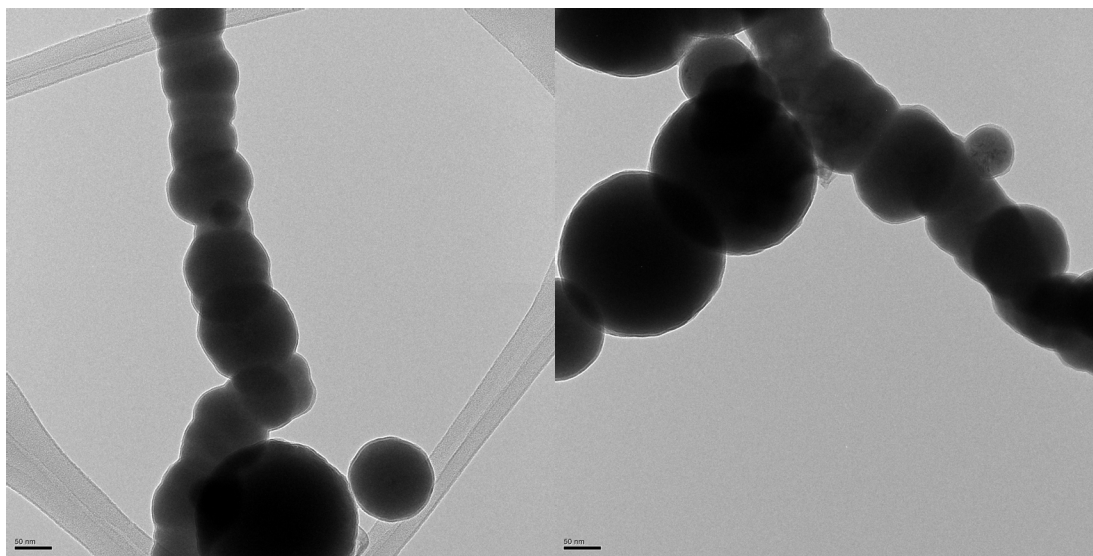


Figure 2.1.2. High resolution TEM pictures of Fe CSNPs

The scale bar represents 50 nm.

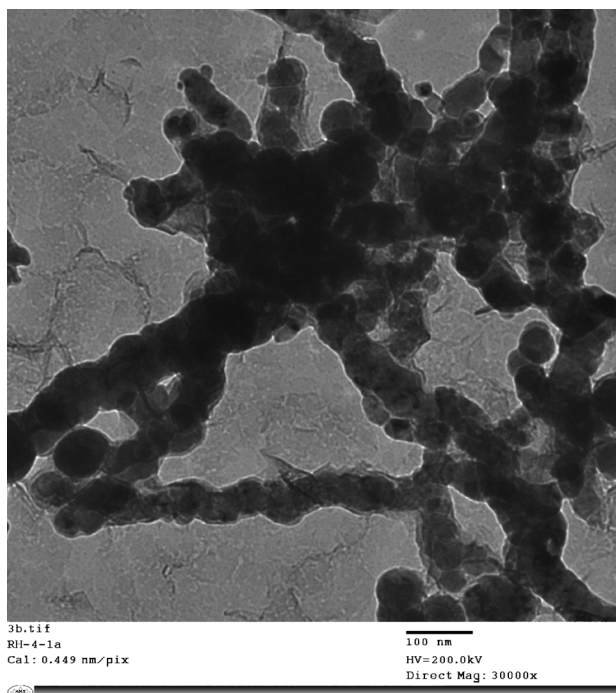


Figure 2.1.3. TEM picture of Fe CSNPs after 5 cycles

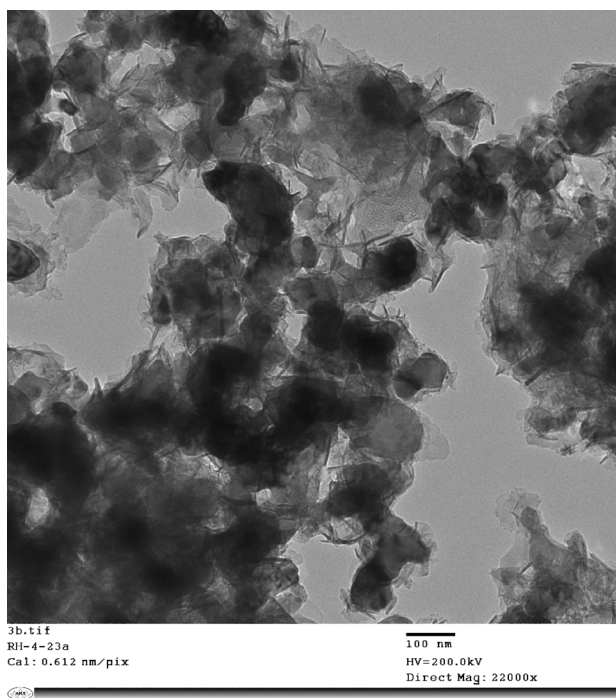


Figure 2.1.4. TEM picture of commercial FeCSNPs

Estimated Fe:FeO ratio from TEM data

The average nanoparticle (44 nm core, 6 nm shell) should have 3.5×10^{-19} g Fe and 1.2×10^{-19} g FeO (for a molar ratio of 3.75:1 Fe:FeO).

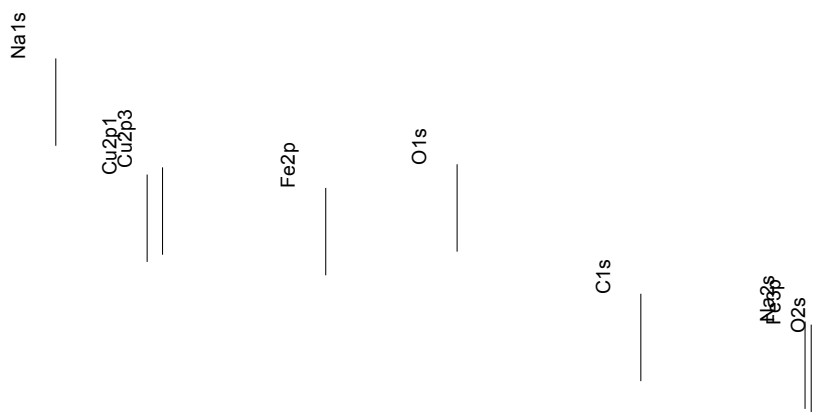


Figure 2.1.5. XPS of Fe CSNPs

Full spectrum (note that the presence of copper is caused by the type of holder used during analysis)

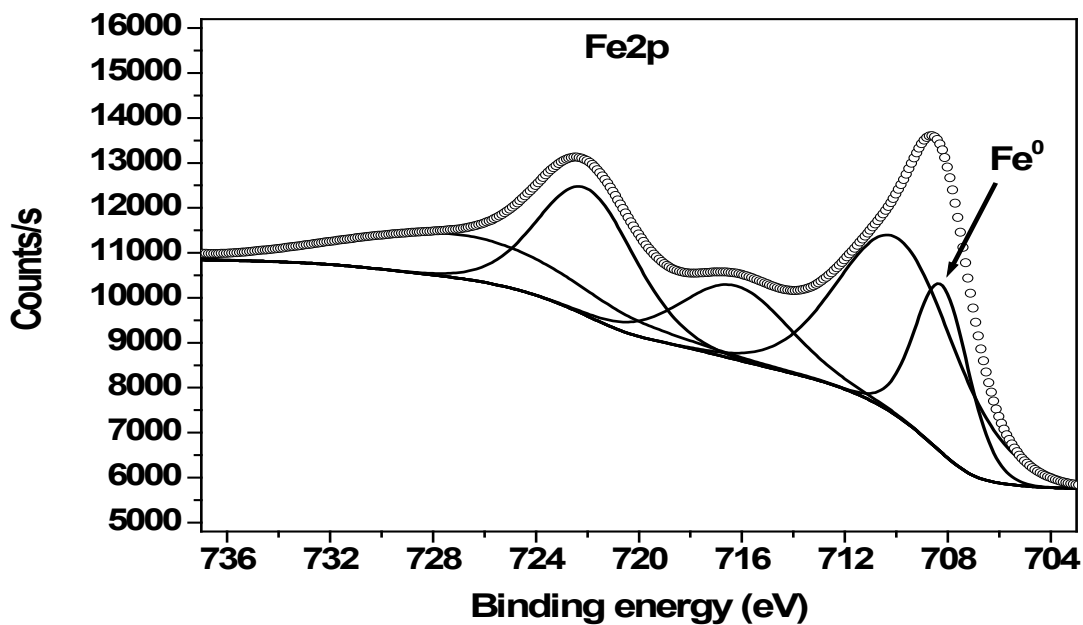


Figure 2.1.6. High resolution XPS for Fe2p

Table 2.1.4. ICP-MS analysis of Fe CSNPs

| Element | Quantity detected | Quantity detected / Quantity of iron detected |
|---------|-------------------|--|
| Fe | 6867184.97 | 1 |
| B | 226309.718 | 3.30 % |
| Co | 55.1642745 | 8 ppm |
| Cu | 175.839891 | 25 ppm |
| Ru | 0.06552416 | 9 ppb |
| Rh | 0.03524121 | 5 ppb |
| Pd | 0.05011601 | 7 ppb |

Performed by digesting 100 mg of Fe CSNPs in 10mL aqueous nitric acid.

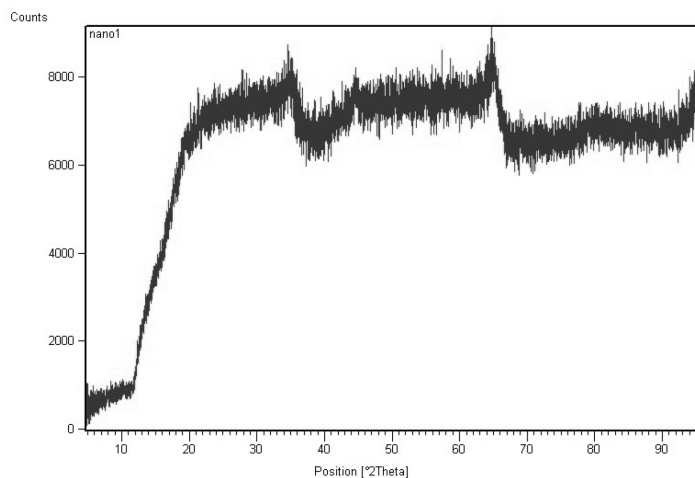


Figure 2.1.7. XRD analysis of Fe CSNPs

The signal was very noisy due to iron interferences. The peak around $36^\circ 2\theta$ can be associated with FeO.

2.2 Highly Efficient Iron(0) Nanoparticle-Catalyzed Hydrogenation in Water in Flow

Highly efficient catalytic hydrogenations are achieved by using amphiphilic polymer-stabilized Fe(0) nanoparticle (Fe NP) catalysts in ethanol or water in a flow reactor. Alkenes, alkynes, aromatic imines and aldehydes were hydrogenated nearly quantitatively in most cases. Aliphatic amines and aldehydes, ketone, ester, arene, nitro, and aryl halide functionalities are not affected, which provides an interesting chemoselectivity. The Fe(0) NPs used in this system are stabilized and protected by an amphiphilic polymer resin, providing a unique system that combines long-term stability and high activity. The NPs were characterized by TEM of microtomed resin, which established that iron remains in the zero-valent form despite exposure to water and oxygen. The amphiphilic resin-supported Fe(0) nanoparticles in water in flow provide a novel, robust, cheap and environmentally benign catalyst system for chemoselective hydrogenations.

2.2.1 Introduction

Hydrogenation, known to chemists for decades, remains one of the most studied reactions. Its industrial applications span petrochemical conversion to pharmaceuticals synthesis; plenty of catalysts exists for this transformation. However, hydrogenation reactions heavily rely on the chemistry of group 9 and 10 metals.¹ These elements are very expensive and their price is highly volatile on the stock market.² Regulatory organizations, such as the FDA, limit residual levels in pharmaceutical products to ppm or less levels because of their inherent toxicity. In response to these economic, regulatory and environmental concerns, efforts have been made to improve recovery and limit leaching,³ or to seek metal-free solutions.⁴ Iron has also been at the centre of renewed interest in both homogeneous and heterogeneous hydrogenation.^{6,7} Iron complexes can catalyse the hydrogenation of alkenes,^{8,9} carbonyls,^{6,10,11} imines,¹¹ carbonates¹² in addition to the selective hydrogenation of alkynes to alkenes,^{13,14} but such systems have limited

recoverability. In contrast, heterogeneous catalysts are more amenable to recycling,¹⁵ and several groups turned to iron-based nanoparticles (NPs).¹⁶⁻¹⁹ The de Vries group used soluble Fe NPs for hydrogenation of alkenes and alkynes,^{7, 20} while the Breit group functionalized graphene sheets with Fe NPs²¹ to further aid recoverability and recycling. In these two systems, an accessible Fe(0) surface is responsible for the catalytic activity.²² These two systems, however, exhibit great sensitivity to traces of either oxygen or water, thus limiting use in practical applications.

Over the past two decades, the use of water has gained considerable momentum as a solvent for organic reactions.²³ It enables novel reactivity,^{24, 25} speeds reactions by the hydrophobic²⁶ and 'on water' effects.²⁷ Ohde et al.²⁸ hydrogenated olefins with palladium nanoparticles in water-supercritical CO₂ microemulsions. More recently, Xiao et al. achieved asymmetric transfer hydrogenation 'on water'.^{29, 30} Amphiphilic polymers have also been used as supports for metal complexes and nanoparticles.³¹⁻³³ They are able to extract organic substrates from the aqueous phase resulting in higher concentrations near the catalyst, speeding the reaction. These systems demonstrate efficiency in hydrogenation,^{34, 35 36} oxidation,^{37, 38} cross coupling³⁹ and hydrodechlorination^{31, 40, 41} reactions in water. The field of heterogeneous catalysis in water has been extensively reviewed.⁴²

We recently demonstrated that core-shell iron/iron oxide nanoparticles are effective hydrogenation catalysts in protic media.⁴³ Exposure to oxygen and/or the presence of up to 1% of water does not affect catalytic activity, thanks to the protective effect of the iron oxide shell. However, neither pure nor water-rich mixtures could be used as a medium due to rapid catalyst deactivation. Additionally the presence of the oxide shell, although protective, limited access to the active surface and forced the use of more drastic conditions and longer reaction times.

Building upon those initial results, we investigated supporting catalytically active Fe NPs on an amphiphilic polymer resin (Figure 2.2.1). This combination provides the opportunity to use the catalyst in a flow system.⁴⁴ Flow systems are widely used to alleviate waste, work-up effort and scale-up problems.^{45, 46}

Reduced Iron Nanoparticles for Hydrogenation Reactions

Hydrogenation, in fact, has been one of the most researched reactions in flow systems because they allow to greatly reduce the volume to pressurize, improving both gas consumption and safety.⁴⁷⁻⁴⁹

We herein report catalytic and selective hydrogenation of alkenes and alkynes, as well as aromatic imines and ketones, involving three green chemistry themes—flow chemistry, water as a benign solvent, and the use of cheap, non-toxic and biologically-essential heterogeneous iron (Figure 2.2.1). By adapting known syntheses of reduced iron particles to the presence of a stabilizing polymer, we report the discovery of novel polymer supported iron nanoparticles that are uniquely robust toward oxidation, and yet active for hydrogenation catalysis. Quite remarkably, the polymer resin increased drastically the longevity of the nanoparticles, resulting in catalytic activity in ethanol and water:ethanol mixtures of up to 9:1. Interestingly, this method is very selective and specifically preserves aryl halide functionalities, a known limitation of palladium-based systems. In a demonstration of durability, scale-up of the system to 20 grams of substrate (styrene) can easily be achieved by increasing reaction time. Because this system is robust to water, iron can now be envisaged as a realistic competitor to platinum series metals as a practical hydrogenation catalyst.

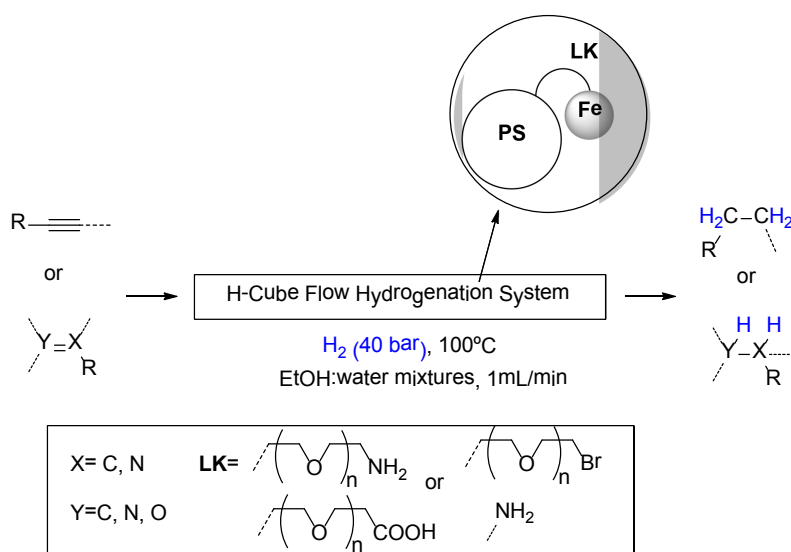
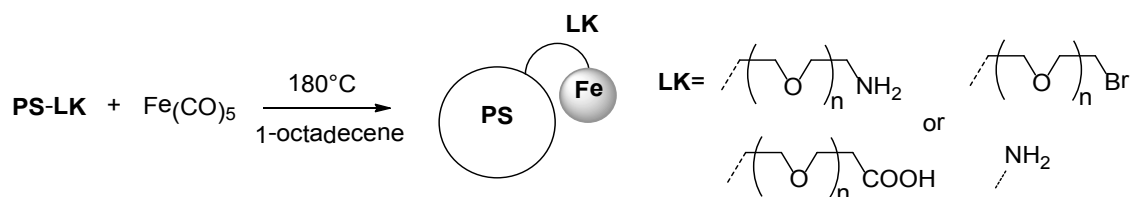
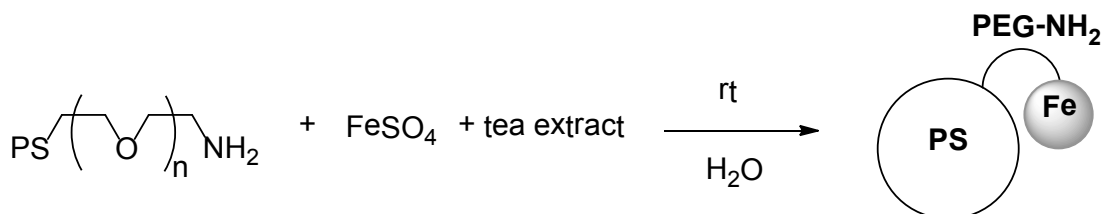


Figure 2.2.1. Schematic of hydrogenation reactions undertaken with polymer supported iron nanoparticles, under flow conditions (PS = polystyrene)



Scheme 2.2.1. Synthesis of FeNP@PS-PEG-FG by thermal decomposition of Fe(CO)₅



Scheme 2.2.2. Synthesis of FeNP@PS-PEG-NH₂ by black tea reduction of FeSO₄

2.2.2 Results and Discussion

2.2.2.1 Synthesis and characterization of polymer resin stabilized Fe(0) NPs

Amphiphilic polymer resins composed of polystyrene (PS) beads (average size 90 micron), functionalized with a variety of linkers (LK) were used to support Fe NPs (Figure 2.2.1). The PS beads serve as compact supports, whose surfaces are covered with LK-stabilized Fe NPs. These LKs are terminated with a functional group (FG = NH₂, COOH, Br) and may also contain a polyethylene glycol (PEG) spacer. The Fe NPs were synthesized in situ, in the presence of the polymer. We adapted two known methods to produce our novel catalysts: 1) the thermal decomposition^{50, 51} of Fe(CO)₅ (scheme 2.2.1) and 2) the reduction of FeSO₄ using black tea as a reducer⁵² (scheme 2.2.2). The first method was expected to afford salt

free, smaller and more reduced NPs than any other known method of Fe NPs production. The second synthesis proceeds via reduction of iron salts by tea polyphenols⁵² and was selected as a green alternative to the first synthesis. The catalysts reported herein are notably different from already published methods in two notable ways. First, rather than using oleyamine, or other stabilizers, as a stabilizing agent, we use FG terminated PEGylated spacers, which likely passivate the nanoparticle surface (*vide infra*), dissuading formation of a surface oxide layer, as generally observed.^{50, 51} Second, because the polymer is present during the time of nanoparticle seeding and growth, it affords a robust resin that can be used in a flow system.

The resulting materials were characterized by transmission electron microscopy (TEM) of microtomed slices of the materials. This method allowed visualization of the Fe NPs embedded in the linker covering the PS beads (Figure 2.2.2). PS-(PEG)-NH₂ afforded the best results. Well dispersed and monodisperse ~5 nm Fe NPs were observed in the case of thermal decomposition (Figure 2.2.2, A and B). At high resolution, regular lines evince the crystal lattice of FeNP@PS-PEG-NH₂ (Figure 2.2.3). The lines are separated by 2.45 Å, which is in good agreement with the interatomic spacing calculated to be 2.49 Å, from either bcc or fcc iron.⁵³ These are very different from spacing measured for iron oxides.^{54, 55} They demonstrate the Fe(0) nature of the nanoparticles. Fewer particles were visible when using the tea reduction method, most of them having again a size of ~5 nm (Figure 2.2.2 C). With both PS-(PEG)-Br and PS-(PEG)-COOH, the thermal decomposition afforded larger particles between 15 and 20 nm for Br and 5 and 20 nm for COOH. PS-NH₂ afforded localized clusters of particles between 5 and 10 nm. Large sections of the matrix did not contain Fe NPs. In no sample did we see any iron oxide layer at the surface of the particles, as we had observed in previous work.⁴³ This demonstrates the excellent stability of this system toward oxidation, presumably through a stabilizing effect of the polymeric support.

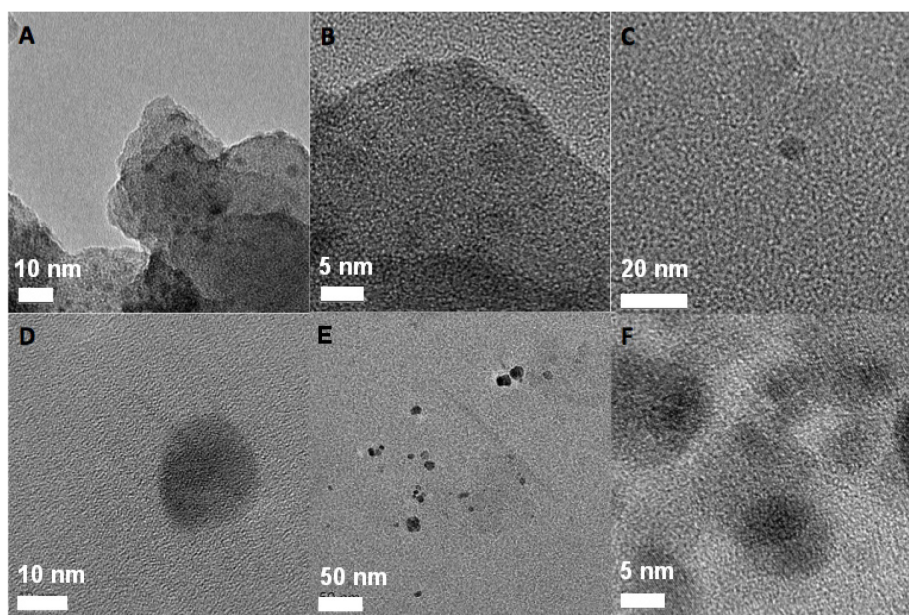


Figure 2.2.2 TEM images of images of A) and B) FeNP@PS-PEG-NH₂ (thermal decomposition); C) FeNP@PS-PEG-NH₂ (tea reduction); D) FeNP@PS-PEG-Br (thermal decomposition); E) FeNP@PS-PEG-COOH (thermal decomposition); F) FeNP@PS-NH₂ (thermal decomposition)

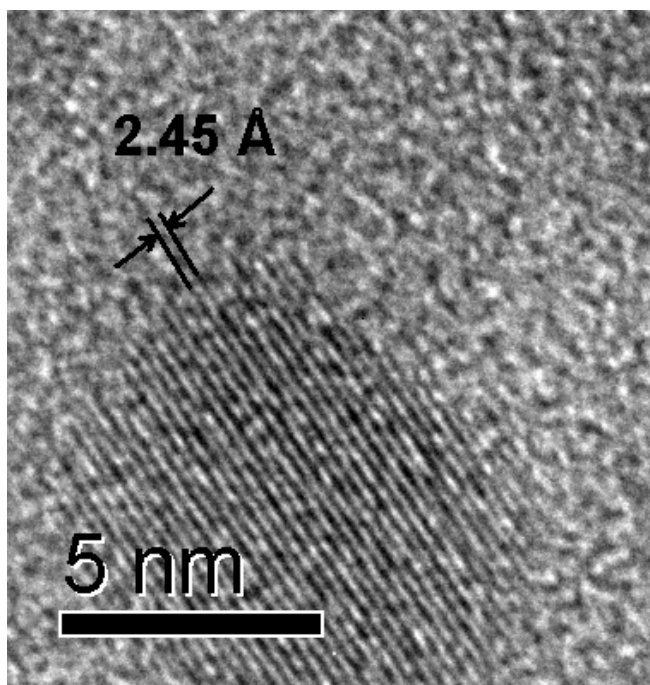


Figure 2.2.3. High resolution TEM image of a single Fe(0) NP exhibiting lattice fringes in FeNP@PS-PEG-NH₂

In addition to TEM, the materials were characterized by ICP (Table 2.2.1). The highest loading was obtained with FeNP@PS-PEG-NH₂ with 11.72 mg Fe/g (entry 1), confirming the observation made by TEM. In terms of loading, thermal decomposition was a more efficient method than tea reduction as the latter afforded material with about 5 times less iron content (entry 2). Indeed, the reaction conditions of thermal decomposition, which occurs at 180°C, were more favourable to iron diffusion, than those of tea reduction (room temperature). Additionally, the neutral nature of Fe(CO)₅ is more adapted to the PEGylated environment surrounding the PS beads than Fe²⁺ salts. A change in the terminal group, from NH₂ to COOH (entry 3) or Br (entry 4) affected loading, although all PEGylated systems could successfully immobilize Fe NPs. Amines are classical Fe NPs stabilizers, used notably in the original synthesis of Fe NPs by thermal decomposition, and are expected to be better ligands than either -Br or -COOH functionalized polymers.^{38,39} Removal of the PEG spacer while keeping the amine functionality (entry 5) had a drastic effect on loading with a 10 fold drop in Fe content, perhaps because the extra oxygen atoms help to coordinate iron, helping seed the formation of nanoparticles.

2.2.2.2 Catalytic tests

These polymer supported-Fe NPs were then assessed in both flow and batch conditions for the hydrogenation of styrene in ethanol (Table 2.2.1). The flow system consists of a peristaltic pump that forces a solution of the solvent and substrate through a cartridge packed with the catalyst, heated and pressurized with H₂ gas.

Table 2.2.1. Ethylbenzene yield in batch and flow as a function of polymer-immobilized Fe NP composition.

| Entry | Composition | Fe Loading ^a | Yield / Flow (%) ^b | Yield / Batch (%) ^c |
|-------|--|-------------------------|-------------------------------|--------------------------------|
| 1 | FeNP@PS-PEG-NH ₂ ^d | 11.72 | 100 | 44 |
| 2 | FeNP@PS-PEG-NH ₂ ^e | 2.55 | 100 | 13 |
| 3 | FeNP@PS-PEG-COOH ^d | 5.01 | 100 | 24 |
| 4 | FeNP@PS-PEG-Br ^d | 4.05 | 100 | 8 |
| 5 | FeNP@PS-NH ₂ ^d | 1.03 | 100 | 19 |
| 6 | PS-PEG-NH ₂ | 0 | 0 | 0 |
| 7 | FeNP ^f | all iron | N/A ^g | 26 |

^a mg Fe/g polymer determined by ICP

^b reaction conditions: 100°C, 40 bar, 1 mL/min through 300 mg polymer, 0.05M styrene in EtOH (residence time 53 seconds)

^c reactions conditions: 100°C, 40 bar, 0.05M Styrene in EtOH (17 mL), 6 hours.

^d Fe nanoparticles generated by thermal decomposition of Fe(CO)₅

^e Fe nanoparticles generated by black tea-extract reduction of FeSO₄

^f reaction conditions: 100°C, 40 bar, 0.05M Styrene in EtOH (17 mL), 5 mol% FeNP (generated by thermal decomposition of Fe(CO)₅ with oleyamine as a stabilizer)⁵⁰, 6 hours.

^g the catalyst could not be tested in flow without polymer support

All iron/polymer systems provided quantitative yields in the flow conditions. However, only the FeNP@PS-PEG-NH₂ generated by thermal decomposition provided even a moderate yield in batch conditions (Table 2.2.1, entry 1). Interestingly, the FeNP@PS-PEG-NH₂ produced using the tea extract method afforded a modest yield of 13% in batch conditions (entry 2), which is superior to what could be expected from simply considering the 5-fold lower loading from the thermal decomposition method. Replacement of the NH₂ functionality by COOH (entry 3) or Br (entry 4), or the removal of the PEG spacer (entry 5), afforded lower yields than FeNP@PS-PEG-NH₂, presumably because of the lower loading. The excellent performance of all these systems in flow compared to batch conditions can be explained by the very high local catalyst concentration within the flow cell. Fe

Reduced Iron Nanoparticles for Hydrogenation Reactions

NPs were critical to catalysis, PS-PEG-NH₂ alone did not lead to any measurable conversion in the conditions used (Table 2.2.1, entry 6). Nanoparticles generated without the polymer support (and instead with oleyamine as a stabilizer) could be tested in batch conditions, but not in flow, because with no support, they would not stay anchored in the flow system. Simple Fe NPs demonstrated a reasonable activity in batch conditions, as expected for small iron NPs (~12 nm)⁵⁰ protected from oxidation by air or water.^{7, 43} Consistent with these results, this reaction is expected to proceed through the classical heterogeneous hydrogenation mechanism (see appendix). Based on these preliminary results, we used FeNP@PS-PEG-NH₂ generated by thermal decomposition in the rest of the study.

Selective hydrogenation of the styrene double bond served as a model reaction for the optimization of reaction conditions (Table 2.2.2). Conditions of 40 bar H₂, 100°C and a flow rate of 2 mL/min constituted the benchmark conditions, achieving a 92% yield of ethyl benzene (Table 2.2.2, entry 1). Increasing the pressure to 60 bar pushed the yield to 95% (Table 2, entry 2). Decreasing the flow rate to 1mL/min afforded a quantitative yield, by improving residence time on the catalyst (Table 2.2.2, entry 4). The reaction still proceeded to 95% yield in 50:50 ethanol:water (Table 2.2.2, entry 12), and an 88% yield in 10:90 ethanol:water (Table 2.2.2, entry 13).⁵⁶ This constitutes a great improvement compared to our previously reported iron/iron oxide core-shell system, where a 50:50 ethanol:water mixture significantly affected hydrogenation catalysis.⁴³ The increased stability of the Fe NPs in a 90% water medium arises from the embedding of the particles in lipophilic pockets of the polymers, preventing water oxidation of their surface. Both Fe(0) NP syntheses tested - namely the thermal decomposition of Fe(CO)₅ and the greener black tea extract reduction of FeSO₄ - afforded quantitative yields under benchmark conditions (40 bar, T=100°C, 2mL/min, with PS-PEG-NH₂ resin) (Table 2.2.1). FeNP@PS-PEG-COOH, FeNP@PS-PEG-Br, FeNP@PS-NH₂ were also equally efficient under the same conditions (Table 1).

We performed ICP analysis of the digested catalysts and could not detect any other metal, not even nickel, a common contaminant of iron known to be active for hydrogenation. This result is consistent with the fact that Fe(CO)₅ purity is claimed

to be 99.999%. This demonstrates that the catalytic activity measured originates solely from iron. Additionally, ICP analysis of the product solution indicated only 0.007 ppm soluble iron strongly suggesting a heterogeneous mechanism.

Table 2.2.2. Screening of hydrogenation conditions^a

| Entry | Pressure (bar) | Temp (°C) | Flow (ml/min) | Yield (%) | TOF (h ⁻¹) |
|-----------------|-------------------|--------------|------------------|--------------|---------------------------|
| 1 | 40 | 100 | 2 | 92 | 106 |
| 2 | 60 | 100 | 2 | 95 | 109 |
| 3 | 20 | 100 | 2 | 85 | 97 |
| 4 | 40 | 100 | 1 | 100 | 57 |
| 5 | 40 | 100 | 0.5 | 94 | 26 |
| 6 | 10 | 100 | 1 | 54 | 30 |
| 9 | 40 | 80 | 1 | 95 | 54 |
| 10 | 40 | 60 | 1 | 94 | 53 |
| 11 ^b | 40 | 100 | 1 | 100 | 57 |
| 12 ^c | 40 | 100 | 1 | 95 | 54 |
| 13 ^d | 40 | 100 | 1 | 88 | 50 |
| 14 ^e | 40 | 100 | 1 | 0 | 0 |

^aReaction conditions: styrene (0.05 M) in EtOH was circulated through 250 mg of FeNP@PS-PEG-NH₂ resin (generated by thermal decomposition of Fe(CO)₅).

^bEtOH:H₂O = 1:99 v:v

^cEtOH:H₂O = 50:50 v:v

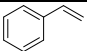
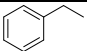
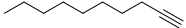
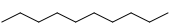
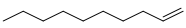
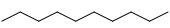

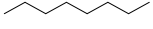
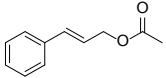
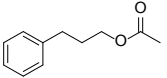
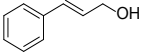
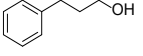
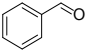
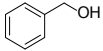
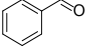
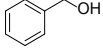
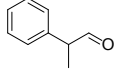
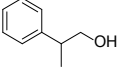
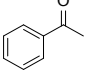
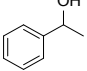
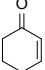
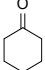
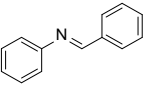
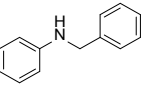
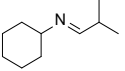
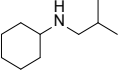
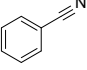
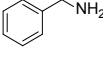
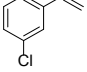
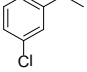
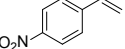
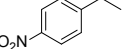
^dEtOH:H₂O = 10:90 v:v

^e No catalyst present.

With optimized conditions in hand, functional group tolerance and selectivity was explored (Table 2.2.3). The catalyst system is highly active for aromatic alkene hydrogenation (entries 1, 5, 15 and 16). The catalytic conditions are moderately efficient toward aliphatic alkenes (entry 3) and alkynes, both internal (entry 4) and terminal (entry 2). The system demonstrates selectivity for C-C double and triple bonds over ketones (Table 2.2.3, entries 6 and 11), esters (entry 5), nitriles (entry 14), arenes (entries 1, 5, 6, 15, and 16). The system also selects against aliphatic

aldehydes (entry 9) and imines (entry 13). When activated by an aromatic ring, however, aldehydes (entries 7 and 8) and imines (entry 12) react. The greater activity demonstrated by aromatic activated substrates relative to their aliphatic analogues could be attributed to the lower LUMO of the former relative to the latter. The reductive elimination of aryl halides (entry 15) or reduction of nitro groups (entry 16) does not occur under these mild conditions—opening the doors for selective synthesis. Given the sensitivity of aryl halides and aryl nitro groups to reducing conditions with platinum series catalysts,⁵⁷ these two examples of chemoselectivity open a land of opportunities in synthesis. A summary of observed chemoselectivity is provided in table 2.2.4.

Table 2.2.3. Functional group tolerance and selectivity^a

| Entry | Substrate | Product | Yield - Selectivity (%-%) |
|----------------|---|---|---------------------------|
| 1 |  |  | 100 - 100 |
| 2 |  |  | 73 - 91 |
| 3 |  |  | 67 - 100 |
| 4 |  |  | 79 - 87 |
| 5 |  |  | 98 - 100 |
| 6 |  |  | 100 - 100 |
| 7 |  |  | 35 - 96 |
| 8 ^b |  |  | 85 - 98 |
| 9 |  |  | 0 - N/A |
| 10 |  |  | 0 - N/A |
| 11 |  |  | 100 - 100 |
| 12 |  |  | 100 - 100 |
| 13 |  |  | 0 - N/A |
| 14 |  |  | 0 - N/A |
| 15 |  |  | 99 - 100 |
| 16 |  |  | 84 - 100 |

^aReaction conditions: 0.05M substrate in EtOH, 100°C, 40 bar H₂, 1 mL/min, 300 mg FeNP@PS-PEG-NH₂ (residence time 53 seconds)

^bReaction conditions: 0.05M substrate in EtOH, 100°C, 60 bar H₂, 1 mL/min 300 mg FeNP@PS-PEG-NH₂ (residence time 53 seconds)

Various substituted, non-functionalized alkenes were assessed (Table 2.2.5). The flow speed was divided by 2 because such alkenes, when not activated by an aromatic ring, are less reactive (see Table 2.2.3, entries 1 and 3). Hydrogenation of mono-substituted alkenes (Table 2.2.5, entry 1) proceeds in good yields, cis alkenes (Table 2.2.5, entry 2) reacted slightly faster than trans alkenes (Table 2.2.5, entry 3). Geminal substitution is more problematic (Table 2.2.5, entry 4). Considering this, it is not surprising that tri-substituted alkenes (Table 2.2.5, entry 5) reacted exceptionally slowly and tetra-substituted alkenes exhibit negligible reactivity (Table 2.2.5, entry 6). Although the greater degree of substitution would electronically favor hydrogenation in these substrates over the less substituted analogue, the reverse reactivity can be attributed with the difficulty of coordinating more sterically hindered substrates to a heterogeneous surface.


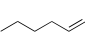
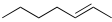
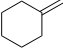
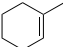
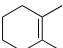
Table 2.2.4. Catalytic selectivity of the polymer-immobilized Fe NPs

| Substrate | Catalytic conversion |
|--|------------------------------------|
| Alkenes and alkynes | Yes |
| Aldehydes and imines | Yes for aromatic, No for aliphatic |
| Ketone, ester, nitro, arene, benzyl carbamate, reductive elimination of aryl halides | No |

For the sake of comparing the reactivity of various styrene derivatives, we used milder reaction conditions in order to achieve greater separation of chemical yields (Table 2.2.6). This comparison suggests that sterics affect reactivity more than electronics. For example, the difference in yield between ortho (entry 6, 35%) and meta (entry 7, 58%) chloro substituted styrene overshadows the difference in yield between electron donating (NH₂, entry 9, 50%) and electron withdrawing (NO₂, entry 10, 39%) para substituted styrene. The trend for methylstyrene further demonstrates this effect. Para methylstyrene (entry 2, 52%) and meta-methylstyrene (entry 3, 48%) both reacted faster than unsubstituted styrene (entry

1, 45%). However, ortho-methylstyrene reacts slower (entry 2, 42%). Once in the ortho position, the negative steric effect of the methyl group outweighs the positive electron-donating effect. It is therefore not surprising that the example with the largest ortho substituent (Br, entry 5) exhibits the lowest overall yield (18%). For each entry in table 2.2.6, no side products were observed (and the mass balance was verified with octane as an internal standard).

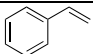
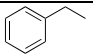
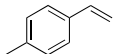
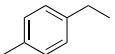
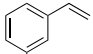
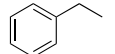
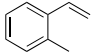
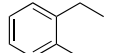
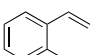
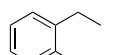
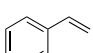
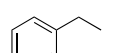
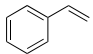
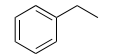
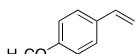
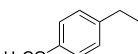
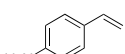
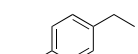
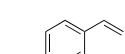
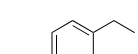
Table 2.2.5. Reactivity of various types of alkenes^a

| Entry | Substrate | Yield (%) |
|-------|--|-----------|
| 1 |  | 90 |
| 2 |  | 87 |
| 3 |  | 83 |
| 4 |  | 14 |
| 5 |  | 6 |
| 6 |  | trace |

^aReaction conditions: 40 bar H₂, 100°C, 0.5 ml/min, 0.05 M substrate in EtOH, (residence time 116 seconds)

Ease of reaction scale-up represents one of the most attractive benefits of flow chemistry. We therefore performed a scale-up test and hydrogenated five grams of cinnamyl acetate (Figure 2.2.4) in the course of 5.7 hours. This experiment demonstrated the robust nature of the catalyst in prolonged reactions. The hourly snapshots indicate that the yield incrementally decreased from 97% to 94%; this very modest yield decrease may be caused by several factors, including a slight oxidation of the Fe NPs or an excessive packing of the catalyst beads over time. This equates to a turn over number (TON) of 434. In another scale-up experiment, we fed the system with 20.7 gram of styrene over 29 hours, and obtained a total TON of 1685.

Table 2.2.6. Activity of styrene derivatives

| Entry | Substrate | Product | Yield – Selectivity (%- %) |
|-------|---|---|----------------------------|
| 1 |  |  | 45 - >99 |
| 2 |  |  | 52 - >99 |
| 3 |  |  | 48 - >99 |
| 4 |  |  | 42 - >99 |
| 5 |  |  | 18 - >99 |
| 6 |  |  | 35 - >99 |
| 7 |  |  | 58 - >99 |
| 8 |  |  | 54 - >99 |
| 9 |  |  | 50 - >99 |
| 10 |  |  | 39 - >99 |

^aReaction conditions: 0.05M substrate in EtOH, 80°C, 20 bar H₂, 3 mL/min, 300 mg FeNP@PS-PEG-NH₂, (residence time 18 seconds)

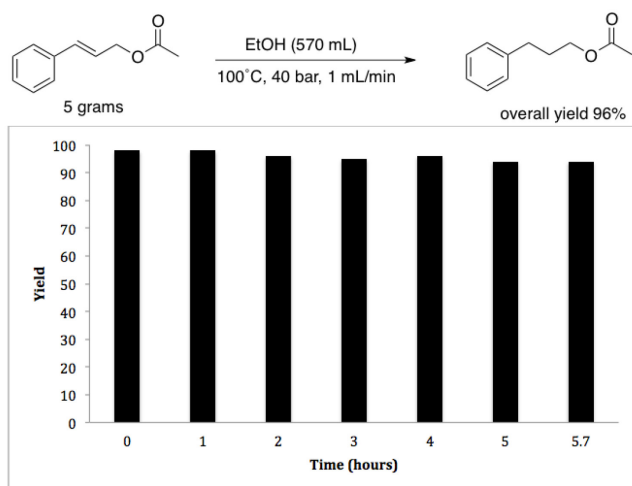


Figure 2.2.4. Scale up and long-term catalyst performance for the hydrogenation of 5 grams of cinnamyl acetate over 5.7 hours (TON= 434)

2.2.3 Conclusion

In conclusion, we describe a novel synthesis of polymer supported Fe NPs, which display excellent reactivity for the selective hydrogenation of alkenes, alkynes, aromatic imines and aldehydes in a flow system. The catalyst is robust in the presence of water, surpassing hydrogenation reaction yields for aqueous mixtures of all other iron nanoparticle systems reported to date.^{7, 43} Very interesting selectivity was achieved and complete protection of the sensitive aryl halides during hydrogenation is an important progress provided by the novel catalysts presented herein. This catalytic flow system functions well at the multi gram scale. This work reports for the first time the convergence of three green chemistry conditions: flow hydrogenation with H₂, use of water and ethanol as benign solvents and the use of heterogeneous iron as a catalyst. More importantly, it opens the possibility of using iron as a replacement to platinum series metals for hydrogenation reaction under realistic, industrial conditions. Current efforts in our labs are focused on achieving a better understanding of the stability of this system towards oxidation and of the mechanism of the reaction.

2.2.4 Experimental Section

2.2.4.1 Chemicals

Styrene (99.0% w/ ~0.003% p-t-butylcatechol stabilizer) and p-methoxystyrene (99% w/ 200 ppm p-t-butylcatechol stabilizer) were purchased from Wako Chemicals. Cinnamyl alcohol (98.0%), trans-2-heptene (99%), cis-2-heptene (97%), Fe(CO)₅ (99.999%) and 1-octadecene (90%) were purchased from Aldrich. 2-phenylpropionaldehyde (98%), cinnamyl acetate (99%), 4-methylstyrene (99%), benzylideneaniline (98%), and benzylcarbamate (97%) were purchased from TCI. Ethanol (99.5%) was purchased from Kanto Chemical Co. Tentagel S COOH, Tentagel S Br and Tentagel S NH₂ were purchased from RAPP Polymere (Germany). Aminomethylated polystyrene was purchased from Nova Biochem (Germany). High purity water was obtained by the use of a Milli-Q- Millipore with 0.22µm filter, Q-guard1 and an ultrapure organex cartridge.

2.2.4.2 Instruments

An Agilent Technologies 6850 series II Network GC System, fitted with a flame ionization detector (GC FID) was used for the determination of yields. The GC MS was an Agilent 5973 Network Mass Selective Detector. High pressure hydrogenation flow reactor catalytic tests were performed on an H-Cube (Thales Nanotechnologies). The transmission electron microscope (TEM) used for imaging was a JEM-2010F (HR7). Microtome slices were prepared using a Leica EMFCS. The inductively coupled plasma (ICP) measurements were recorded on a Leeman labs, inc. Profile Plus high dispersion ICP.

2.2.4.3 Synthesis of FeNP@PS-LK by thermal decomposition:

Linker-terminated polystyrene/(polyethylene glycol) beads (Tentagel from RAPP Polymere or aminomethylated polystyrene from Nova, 1 gram) and 1-octadecene (60 mL, 90% Aldrich) were combined with a magnetic stir bar in a 200 mL round bottom Shlenk flask. The mixture was purged with N₂ at 120°C for 30 minutes. The temperature was then raised to 180°C, at which point Fe(CO)₅ (2.1 mL, 99.99%, aldrich) was quickly injected. The reaction was stirred for 30 minutes at 180°C under a blanket of N₂, then allowed to cool to room temperature. The resulting polymer-supported iron nanoparticles (FeNP@PS-(PEG)-FG) were washed 3 times with hexanes (50 mL, 99% Aldrich) and dried under vacuum.

2.2.4.4 Synthesis of FeNP@PS-(PEG)-NH₂ by black tea reduction:

Red Label black tea (20g) was brewed with boiling water (1 L) and cooled to room temperature. The brewed tea was then added to a solution of amine-terminated polystyrene/polyethylene glycol beads (1 gram), FeSO₄ (3.767 g) and water (2 L) with a magnetic stir bar in a 4L glass jug. After stirring for 24 hours, the polymer was filtered and collected.

2.2.4.5 Characterization of PS-LK supported Fe nanoparticles:

To visualize the FeNP@PS-(PEG)-FG catalysts, the polymer was sliced with a Leica EMFCS microtome. The resulting slices were loaded onto carbon/Formvar grids and subjected to TEM analysis on a JEM-2010F (HR7) operated at 120 kV. The interatomic spacing was measured on Figure 3 using the measuring tool of the GIMP software over 14 lines. The lattice parameter is 2.87 Å for bcc iron and 3.515 Å for fcc,⁵³ and thus an interatomic spacing of 2.49 Å.

2.2.4.6 PS-LK supported Fe nanoparticles for flow hydrogenation:

A cartridge packed with 300 mg of PS-LK supported Fe nanoparticles was connected to an H-Cube flow hydrogenation system. Each substrate (0.05 M) in ethanol, water, or a mixture of the two was forced through the system at different rates, temperatures and hydrogen pressures. The resulting solution was characterized by GC-MS and quantified by GC-FID.

2.2.4.7 PS-LK supported Fe nanoparticles for batch hydrogenation:

High pressure batch reactions were performed in a Parr 5000 high pressure multireactor with 17 mL of 0.05M styrene in EtOH and a magnetic stirbar (1000 rpm) for 6 hours with 300 mg of polymer-supported catalyst. The reaction mixture was then filtered through a Buchner funnel and injected directly into a GC equipped with a flame ionization detector.

2.2.5 Acknowledgements

We thank the National Science and Engineering Council of Canada (NSERC), the Canada Foundation for Innovation (CFI), the Canada Research Chairs (CRC), the Fonds de Recherche sur la Nature et les Technologies (FQRNT), the Center for Green Chemistry and Catalysis (CCGC), the Green Chemistry - NSERC Collaborative Research and Training Experience (CREATE) Program, the Riken-McGill fund, McGill University, JSPS (Grand-in-Aid for Scientific Research # 20655035; Grant-in-Aid for Scientific Research on Innovative Areas #2105), and the CREST program “*Elemental Strategy*” for their financial support. Lynn Leger (Green Centre Canada), Shatha Qaqish (Green Centre Canada), Bruce Lennox and Tomislav Friscic are thanked for their useful comments.

2.2.6 References

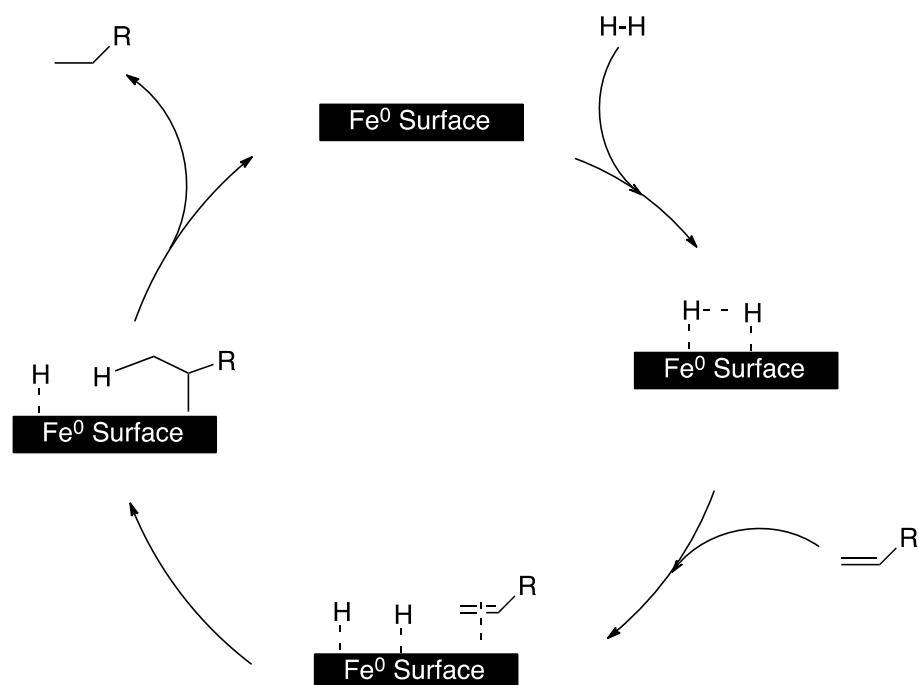
1. J. G. de Vries and C. J. Elsevier, *Handbook of Homogeneous Hydrogenation*, Wiley-VCH, Weinheim, 2007.
2. A. Behr and P. Neubert, *Applied Homogeneous Catalysis*, Wiley-VCH, Weinheim, Germany, 2012.
3. C. M. Crudden, M. Sateesh and R. Lewis, *J. Am. Chem. Soc.*, 2005, 127, 10045-10050.
4. P. A. Chase and D. W. Stephan, *Angew. Chem. Int. Ed.*, 2008, 47, 7433-7437.
5. P. A. Chase, T. Jurca and D. W. Stephan, *Chem. Commun.*, 2008, 1701-1703.
6. R. H. Morris, *Chem. Soc. Rev.*, 2009, 38, 2282-2291.
7. P.-H. Phua, L. Lefort, J. A. F. Boogers, M. Tristany and J. G. de Vries, *Chem Commun.*, 2009, 3747-3749.
8. S. C. Bart, E. J. Hawrelak, E. Lobkovsky and P. J. Chirik, *J. Organomet. Chem.*, 2005, 24, 5518-5527.
9. S. C. Bart, E. Lobkovsky and P. J. Chirik, *J. Am. Chem. Soc.*, 2004, 126, 13794-13807.
10. A. Mikhailine, A. J. Lough and R. H. Morris, *J. Am. Chem. Soc.*, 2009, 131, 1394-1395.
11. C. Sui-Seng, F. Freutel, A. J. Lough and R. H. Morris, *Angew. Chem.-Int. Ed.*, 2008, 47, 940-943.
12. C. Federsel, A. Boddien, R. Jackstell, R. Jennerjahn, P. J. Dyson, R. Scopelliti, G. Laurenczy and M. Beller, *Angew. Chem. Int. Ed.*, 2010, 49, 9777-9780.
13. S. Enthaler, M. Haberberger and E. Irran, *Chem. Asian J.*, 2011, 6, 1613-1623.
14. M. Haberberger, E. Irran and S. Enthaler, *Eur. J. Inorg. Chem.*, 2011, 2797-2802.
15. S. Shylesh, V. Schünemann and W. R. Thiel, *Angew. Chem. Int. Ed.*, 2010, 49, 3428-3459.
16. M. Armbruster, K. Kovnir, M. Friedrich, D. Teschner, G. Wowsnick, M. Hahne, P. Gille, L. Szentmiklosi, M. Feuerbacher, M. Heggen, F. Girgsdies, D. Rosenthal, R. Schlogl and Y. Grin, *Nature Mater.*, 2012, 11, 690-693.

17. D. Cantillo, M. Baghbanzadeh and C. O. Kappe, *Angew. Chem. Int. Ed.*, 2012, 51, 10190-10193.
18. J. F. Sonnenberg, N. Coombs, P. A. Dube and R. H. Morris, *J. Am. Chem. Soc.*, 2012, 134, 5893-5899.
19. J.-M. Yan, X.-B. Zhang, S. Han, H. Shioyama and Q. Xu, *Angew. Chem. Int. Ed.*, 2008, 47, 2287-2289.
20. C. Rangheard, C. de Julian Fernandez, P.-H. Phua, J. Hoorn, L. Lefort and J. G. de Vries, *Dalton Trans.*, 2010, 39, 8464-8471.
21. M. Stein, J. Wieland, P. Steurer, F. Toelle, R. Muelhaupt and B. Breit, *Adv. Synth. Catal.*, 2011, 353, 523-527.
22. A. Welther, M. Bauer, M. Mayer and A. Jacobi von Wangelin, *ChemCatChem*, 2012, 4, 1088-1093.
23. C.-J. Li and T.-H. Chan, *Comprehensive Organic Reactions in Aqueous Media*, Wiley, 2007.
24. C.-J. Li and L. Chen, *Chem. Soc. Rev.*, 2006, 35, 68-82.
25. C. J. Li, *Chem. Rev.*, 1993, 93, 2023-2035.
26. R. Breslow, *Acc. Chem. Res.*, 1991, 24, 159-164.
27. S. Narayan, J. Muldoon, M. G. Finn, V. V. Fokin, H. C. Kolb and K. B. Sharpless, *Angew. Chem. Int. Ed.*, 2005, 44, 3275-3279.
28. H. Ohde, C. M. Wai, H. Kim, J. Kim and M. Ohde, *J. Am. Chem. Soc.*, 2002, 124, 4540-4541.
29. X. Wu, X. Li, F. King and J. Xiao, 2005, 117, 3473-3477.
30. X. Wu, J. Liu, X. Li, A. Zanotti-Gerosa, F. Hancock, D. Vinci, J. Ruan and J. Xiao, *Angew. Chem. Int. Ed.*, 2006, 45, 6718-6722.
31. Y. Uozumi and Y. M. A. Yamada, *Chem. Rec.*, 2009, 9, 51-65.
32. S. M. Sarkar, Y. Uozumi and Y. M. A. Yamada, *Angew. Chem. Int. Ed.*, 2011, 123, 9609-9613.
33. Y. M. A. Yamada, S. M. Sarkar and Y. Uozumi, *J. Am. Chem. Soc.*, 2012, 134, 3190-3198.
34. M. T. Zarka, O. Nuyken and R. Weberskirch, *Chem. Eur. J.*, 2003, 9, 3228-3234.

35. Y. Arakawa, A. Chiba, N. Haraguchi and S. Itsuno, *Adv. Synth. Catal.*, 2008, 350, 2295-2304.
36. Y. Uozumi and Y. M. A. Yamada, *Chem. Rec.*, 2009, 9, 51-65.
37. Y. Uozumi and R. Nakao, *Angew. Chem. Int. Ed*, 2003, 42, 194-197.
38. Y. M. A. Yamada, T. Arakawa, H. Hocke and Y. Uozumi, *Chem. Asian J.*, 2009, 4, 1092-1098.
39. C. B. Putta and S. Ghosh, *Adv. Synth. Catal.*, 2011, 353, 1889-1896.
40. R. Nakao, H. Rhee and Y. Uozumi, *Org. Lett.*, 2004, 7, 163-165.
41. Y. M. A. Yamada, T. Watanabe, A. Ohno and Y. Uozumi, *ChemSusChem*, 2012, 5, 293-299.
42. M. Lamblin, L. Nassar-Hardy, J.-C. Hierso, E. Fouquet and F.-X. Felpin, *Adv. Synth. Catal.*, 2010, 352, 33-79.
43. R. Hudson, A. Riviere, C. M. Cirtiu, K. L. Luska and A. Moores, *Chem. Commun.*, 2012, 48, 3360-3362.
44. G. Jas and A. Kirschning, *Chem. Euro. J.*, 2003, 9, 5708-5723.
45. G. M. Whitesides, *Nature*, 2006, 442, 368-373.
46. J. Wegner, S. Ceylan and A. Kirschning, *Chem. Commun.*, 2011, 47, 4583-4592.
47. U. K. Singh and M. A. Vannice, *Appl. Catal., A*, 2001, 213, 1-24.
48. J. Kobayashi, Y. Mori, K. Okamoto, R. Akiyama, M. Ueno, T. Kitamori and S. Kobayashi, *Science*, 2004, 304, 1305-1308.
49. M. Ruta, G. Laurenczy, P. J. Dyson and L. Kiwi-Minsker, *J. Phys. Chem. C*, 2008, 112, 17814-17819.
50. S. Peng, C. Wang, J. Xie and S. Sun, *J. Am. Chem. Soc.*, 2006, 128, 10676-10677.
51. T.-J. Yoon, H. Lee, H. Shao and R. Weissleder, *Angew. Chem. Int. Ed*, 2011, 50, 4663-4666.
52. M. N. Nadagouda, A. B. Castle, R. C. Murdock, S. M. Hussain and R. S. Varma, *Green Chem.*, 2010, 12, 114-122.
53. N. Ridley and H. Stuart, *Brit. J. Appl. Phys.*, 1968, 2, 1291-1295.
54. S. Gota, E. Guiot, M. Henriot and M. Gautier-Soyer, *Surf. Sci.*, 2000, 454-456, 796-801.

- 55. A. Cabot, V. F. Puentes, E. Shevchenko, Y. Yin, L. Balcells, M. A. Marcus, S. M. Hughes and A. P. Alivisatos, *J. Am. Chem. Soc.*, 2007, 129, 10358-10360.
- 56. 100% water was not tested due to lack of solubility of the substrates used.
- 57. A. Mori, T. Mizusaki, Y. Miyakawa, E. Ohashi, T. Haga, T. Maegawa, Y. Monguchi and H. Sajiki, *Tetrahedron*, 2006, 62, 11925-11932.

2.2.7 Appendix



Scheme 2.2.3. Proposed mechanism for olefin hydrogenation catalyzed by iron nanoparticles

3 Reduced Iron Nanoparticles Decorated with a more Catalytically Active Metal

In hopes of expanding the catalytic offering of the core-shell iron-iron oxide nanoparticles described in the previous chapter, these particles were decorated with copper and ruthenium by introducing their sulfate and tri-chloride salts, respectively, to a solution of the iron particles. The resultant copper- and ruthenium- decorated iron nanoparticles could be used for the azide-alkyne ‘click’ reaction and transfer hydrogenation, respectively.

This chapter is based upon one published article and one manuscript soon to be submitted, the citations for which appear below. The Royal Society for Chemistry granted permission to reprint the published article, as did all co-authors for both manuscripts.

Reuben Hudson, Chao-Jun Li and Audrey Moores. Magnetic copper–iron nanoparticles as simple heterogeneous catalysts for the azide–alkyne click reaction in water. *Green Chem.*, 2012, 14, 622-624.

Reuben Hudson, Vanessa Chazelle, Chao-Jun Li, and Audrey Moores. Magnetic Ru@Fe nanoparticles as transfer hydrogenation catalysts. Manuscript in preparation.

3.1 Magnetic copper-iron nanoparticles as simple heterogeneous catalysts for the azide-alkyne click reaction in water

3.1.1 Abstract

The development of a novel bimetallic copper-iron nanoparticle synthesis provides a recoverable heterogeneous catalyst for the azide-alkyne “click” reaction in water. The nanoparticles catalyze the production of a diverse range of triazoles, while separation and reuse proved to be easy.

3.1.2 Introduction

The 2002 development of Cu(I) catalysed azide-alkyne cycloaddition (AAC) continues to garner much interest today.^{1, 2} This prototypical “click” reaction offers chemists a highly efficient means for connecting two potentially complex building blocks under mild conditions with high tolerance to other functional groups.^{3, 4} This reaction has thus been extensively applied to the synthesis of macromolecules^{5, 6} and the functionalization of biomolecules.⁷ The catalysed AAC reaction holds several advantages over the thermal version⁸ including regioselectivity, increased reactivity of unactivated alkynes, and high yields even at low concentrations in aqueous media.⁹

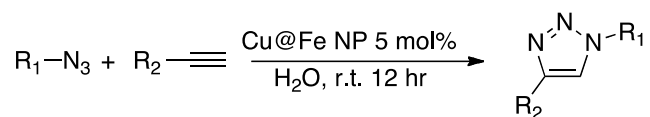
Most AAC protocols call for a homogeneous Cu(I) source – either by direct addition of a Cu(I) salt, or in situ reduction of Cu(II) by sodium ascorbate.^{2, 9, 10} In an effort to find more reusable catalysts, Cu(I) AAC catalysts have been immobilized onto polymers^{11, 12} or zeolite.¹³ Interestingly, Cu(0) on charcoal,¹⁴ Cu(0) nanoparticles,¹⁵⁻¹⁸ or microwave irradiated Cu turnings,^{19, 20} as well as CuO nanostructures,²¹ have also successfully demonstrated activity for this reaction.

Magnetically recoverable nanoparticles (NPs) represent an easy and environmentally benign means for catalyst recovery,²² providing catalytic properties intermediate between homogeneous²³ and bulk heterogeneous materials.²⁴⁻²⁶ Many schemes exist for using magnetically recoverable catalysts:

anchoring homogeneous metal complexes²⁷⁻²⁹ or organocatalysts³⁰ to a magnetic core, plating a catalytically active metal,^{31, 32} or, more simply, direct use of bare Fe(0)³³⁻³⁵ or iron oxide NPs.^{36, 37} Among the strategies recently developed to produce novel magnetic particles, core-shell iron-iron oxide nanoparticles (FeCSNPs) have been used as precursors to seed, reduce and support another metal. By this method, Pd NPs were deposited onto FeCSNPs and the resulting hybrid NPs were proven to be active and recyclable catalysts for Suzuki coupling.³⁸

3.1.3 Results and Discussion

Herein, we present the synthesis of an active and magnetically recyclable catalyst for the AAC in water (Scheme 3.1.1). This catalyst is very simple and produced from exposure to Cu(II) salts of reducing FeCSNPs seeds in a water/methanol mixture. No ligand or extra reducer is needed.



Scheme 3.1.1. Cu@FeNP catalyzed azide-alkyne ‘click’ reaction

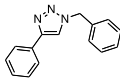
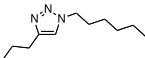
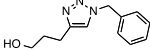
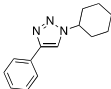
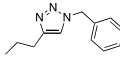
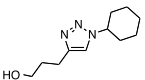
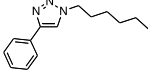
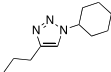
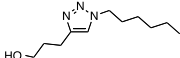
Table 3.1.1. Performance of a series of Cu and Fe based catalysts for the AAC^a

| Entry | Catalyst (loading) | Yield |
|-------|--|------------------|
| 1 | None | <5% |
| 2 | CuFe ₂ O ₄ NP (5 mol%) | <5% |
| 3 | CuFe ₂ O ₄ NP + sodium ascorbate (5 mol%) ^b | 96% ^b |
| 4 | CuI (5 mol%) | 99% |
| 5 | Cu@FeNP (5 mol%) | 93% |
| 6 | Cu@FeNP (1 mol%) | 81% |
| 7 | FeNP (5 mol%) | <5% |
| 8 | Cu@FeNP – Supernatant ^c | <5% ^c |

^a reaction conditions: 1 mmol benzyl azide, 1.2 mmol phenylacetylene, 10 mL H₂O, r.t., 12 hr. ^b Dissolution of nanoparticles observed. ^c Supernatant obtained by subjecting particles to catalytic conditions, removing them, and using supernatant as solvent for reaction.

Our initial attempts to perform AAC using magnetically recoverable NPs focused on the use of Cu ferrite (CuFe_2O_4). In 2010, Park and coworkers demonstrated that hollow structures of CuO were active catalysts for AAC.²¹ However, CuFe_2O_4 NPs proved inactive for this transformation (Table 3.1.1). In Cu ferrite, Cu is present as Cu(II) in the crystal lattice, while most AAC catalysts are based on Cu(I).^{4, 10, 39} Addition of sodium ascorbate to CuFe_2O_4 NPs afforded the expected in situ reduction of Cu(II) into Cu(I),³⁹ and enabled catalysis in yields of 96%. This activity, however, was accompanied by the complete dissolution of the CuFe_2O_4 NPs – no solid material could be recovered. These observations suggest that catalysis proceeds through a homogeneous mechanism. To alleviate this limitation, we needed to develop nanocatalysts featuring heterogenized Cu(I) species. To this end, we explored other kinds of non-functionalized, bare magnetic NPs. Following a procedure developed with Pd,³⁸ we plated FeCSNPs by galvanic reduction of CuSO_4 . FeCSNPs are obtained by NaBH_4 reduction of FeSO_4 ,⁴⁰ before being exposed to CuSO_4 . The X ray photoelectron spectroscopy (XPS) of the resultant nanoparticles indicated the presence of Cu(I) and (II)—although it is entirely possible copper oxidized before the XPS analysis, as inert conditions were not possible. These results are consistent with the reduction of Cu(II) to Cu(I) by the core of FeCSNPs.⁴¹ We did not observe evidence of Cu(0) by XPS.

Table 3.1.2 Cu@Fe NP Catalyzed Azide-Alkyne Cycloaddition.^a

| Entry | Product | Yield | Entry | Product | Yield |
|-------|---|-------|-------|---|-------|
| 1 |  | 93% | 6 |  | 78% |
| 2 |  | 89% | 7 |  | 84% |
| 3 |  | 90% | 8 |  | 67% |
| 4 |  | 88% | 9 |  | 49% |
| 5 |  | 91% | | | |

^a reaction conditions: 1 mmol azide, 1.2 mmol alkyne, 5 mol% Cu@Fe NP, 10 mL H₂O, r.t., 12 hr.

These bi-metallic nanoparticles catalyzed AAC in good yields, in most cases (Table 3.1.2). Primary and secondary aliphatic as well as the traditional benzylic azides coupled with aliphatic and aromatic alkynes to generate a range of triazoles. Generally, the more electron rich azides reacted with the highest efficiency [benzyl (entries 1, 2 and 3) > 2° alkyl (entries 4, 5 and 6) > 1° alkyl (entries 7, 8 and 9)]. Of the alkynes, phenylacetylene reacted best (entries 1, 4, and 7) while simple alkyl substituted alkynes reacted slowest (entries 3, 6 and 9). The system also proved robust toward alcohol-substituted alkynes (entries 2, 5 and 8).

Distinguishing between true heterogeneous and homogeneous catalysis - performed by a leached soluble species - is always critical when using nanoparticulate catalysts.⁴² For this reason, the reaction supernatant (in which no soluble copper could be detected by an ICP-OES with a detection limit of 0.001 ppm) was tested for catalytic activity - after the nanoparticles had been magnetically removed and the solution filtered through celite. The lack of either soluble copper in

the reaction mixture or supernatant catalytic activity coupled with the reusability of the catalyst strongly suggest a heterogeneous mechanism. In further support of a heterogeneous mechanism, the nanoparticles could be recovered and reused under stringent inert conditions up to five times with no appreciable decrease in yield (Table 3.1.3). However, when the reaction was performed on the bench top in the presence of air, the yield quickly dropped in subsequent recycling runs, most probably caused by an oxidation of Cu(I) into Cu(II).

Table 3 Recycling of Cu@FeNPs Catalyst for AAC.^a

| Run | Glovebox yield (%) | Benchtop yield (%) |
|---|--------------------|--------------------|
| 1 | 93 | 93 |
| 2 | 93 | 90 |
| 3 | 92 | 76 |
| 4 | 93 | 54 |
| 5 | 91 | <5 |
| ^a reaction conditions: 1 mmol benzyl azide, 1.2 mmol phenylacetylene, 5 mol% catalyst 10 mL H ₂ O, r.t., 12 hr. | | |

3.1.4 Conclusions

Herein, we present a bi-metallic copper-iron nanoparticle system for catalysis of the Huisgen 1,3-dipolar, azide alkyne cycloaddition in water. Interestingly, in this system, the iron(0) core serves a three-fold role. First, it provides a means for magnetic recoverability. Second, it serves as a source of electrons to reduce Cu(II) into Cu(I). Third, it acts as a support for Cu(I) species to prevent their liberation as soluble ions, enabling a heterogeneous mechanism. The synthesis of the catalyst proceeds without the use of reducer, or ligand, making this reaction very atom economical. This work represents the merger of two ubiquitous green chemistry themes: magnetic nanoparticles as easily recoverable catalysts and aqueous 'click chemistry'. Ongoing studies in our group focus on further characterizing the catalytically active Cu@FeNPs.

3.1.5 Experimental Section

All reactants were purchased from Sigma Aldrich and used as received. Organic azides were synthesized from the corresponding bromides via a previously reported procedure.²⁰ All reactions were carried out in an oxygen-free glovebox, except where noted, and all solvents were de-gassed for 20 minutes prior to use. FeCSNPs were synthesized following a procedure similar to what had been reported before.⁴⁰ In MeOH/H₂O (60 mL/140 mL), a solution of FeSO₄ (4 g in 200 mL H₂O) was reduced with aqueous NaBH₄ (0.8 g in 20 mL H₂O added with a syringe pump at 3 mL/min) at pH 6 (achieved by addition of 5 mL of 5N NaOH). Then a CuSO₄ solution (8 mg of CuSO₄ in 1 mL of H₂O at a rate of 1 mL/min) was added dropwise to the sonicating solution of FeCSNPs (28 mg in 9 mL). The resulting slurry was left to sonicate for 30 minutes after addition of CuSO₄. These nanoparticles were then washed three times with 10 mL water before being used for catalysis. A typical reaction consisted of resuspension of the nanoparticles in 10 mL water, followed by addition of azide (1 mmol) and alkyne (1.2 mmol), and a magnetic stir bar. The reaction vessel was then capped and left to stir for 12 hours. After each reaction cycle, the nanoparticles stuck to the stir bar when stirring stopped, the solution decanted off, the nanoparticles washed 3 times with acetone, then three times with water with no further purification before reuse. The reaction supernatant and washings were collected together, the solvent evaporated, and the solid product weighed and characterized by NMR spectroscopy on a Mercury 300. The XPS analysis was performed at Ecole Polytechnique Montreal on a VG ESCLAB 3 MKII with a power of 206 W. A surface of 2x3 mm was analysed at a depth of 50-100 Å. ICP-OES was performed on a Trace Scan with a baffled cyclonic spray chamber and mini cross flow nebulizer.

3.1.6 Acknowledgements

We thank the Natural Science and Engineering Research Council of Canada (NSERC), the Canada Foundation for Innovation (CFI), the Canada Research Chairs (CRC), the Fonds de Recherche sur la Nature et les Technologies (FQRNT), the Center for Green Chemistry and Catalysis (CGCC) and McGill University for their financial support. We are grateful to Suzie Poulin for the XPS analysis and Ranjan Roy for the ICP-OES analysis.

3.1.7 References

1. C. W. Tornøe, C. Christensen and M. Meldal, *J. Org. Chem.*, 2002, 67, 3057-3064.
2. V. V. Rostovtsev, L. G. Green, V. V. Fokin and K. B. Sharpless, *Angew. Chem. Int. Ed.*, 2002, 41, 2596-2599.
3. H. C. Kolb and K. B. Sharpless, *Drug Discov Today*, 2003, 8, 1128-1137.
4. V. D. Bock, H. Hiemstra and J. H. v. Maarseveen, *Eur. J. Org. Chem.*, 2006, 51-68.
5. G. Franc and A. K. Kakkar, *Chem. Soc. Rev.*, 2010, 39, 1536-1544.
6. W. H. Binder and R. Sachsenhofer, *Macromol. Rapid Commun.*, 2007, 28, 15-54.
7. P. M. E. Gramlich, C. T. Wirges, A. Manetto and T. Carell, *Angew. Chem. Int. Ed.*, 2008, 47, 8350-8358.
8. R. Huigsen, G. Szeimies and L. Möbius, *Chem. Ber.*, 1967, 100, 2494-2507.
9. V. O. Rodionov, S. I. Presolski, S. Gardinier, Y.-H. Lim and M. G. Finn, *J. Am. Chem. Soc.*, 2007, 129, 12696-12704.
10. V. O. Rodionov, S. I. Presolski, D. Díaz Díaz, V. V. Fokin and M. G. Finn, *J. Am. Chem. Soc.*, 2007, 129, 12705-12712.
11. C. Girard, E. Önen, M. Auffer, S. Beauvière, E. Samson and J. Herscovici, *Org. Lett.*, 2006, 8, 1689-1692.

12. A. Sarkar, T. Mukherjee and S. Kapoor, *J. Phys. Chem. C.*, 2008, 112, 3334-3340.
13. S. Chassaing, M. Kumarraja, A. S. S. Sido, P. Pale and J. Sommer, *Org. Lett.*, 2007, 9, 883-886.
14. B. H. Lipshutz and B. R. Taft, *Angew. Chem. Int. Ed.*, 2007, 45, 8235-8238.
15. D. Raut, K. Wankhede, V. Vaidya, S. Bhilare, N. Darwatkar, A. Deorukhkar, G. Trivedi and M. Salunkhe, *Catal. Commun.*, 2009, 10, 1240-1243.
16. G. Molteni, C. L. Bianchi, G. Marinoni, N. Santo and A. Ponti, *New J. Chem.*, 2006, 30, 1137-1139.
17. L. D. Pachón, J. H. van Maarseveen and G. Rothenberg, *Adv. Synth. Catal.*, 2005, 347, 811-815.
18. E. D. Pressly, R. J. Amir and C. J. Hawker, *J. Polym. Sci. Pol. Chem.*, 2011, 49, 814-819.
19. P. Appukkuttan, W. Dehaen, V. V. Fokin and E. Van der Eycken, *Org. Lett.*, 2004, 6, 4223-4225.
20. P. Cintas, A. Barge, S. Tagliapietra, L. Boffa and G. Cravotto, *Nat. Protocols*, 2010, 5, 607-616.
21. J. Young Kim, J. Chan Park, H. Kang, H. Song and K. Hyun Park, *Chem. Commun.* 2010, 46, 439-441.
22. T.-J. Yoon, W. Lee, Y.-S. Oh and J.-K. Lee, *New J. Chem.*, 2003, 27, 227-229.
23. D. J. Cole-Hamilton, *Science*, 2003, 299, 1702-1706.
24. S. Shylesh, V. Schünemann and W. R. Thiel, *Angew. Chem. Int. Ed.*, 2010, 49, 3428-3459.
25. D. Astruc, F. Lu and J. R. Aranzaes, *Angew. Chem., Int. Ed.*, 2005, 44, 7852-7872.
26. A.-H. Lu, E. L. Salabas and F. Schüth, *Angew. Chem. Int. Ed.*, 2007, 46, 1222-1244.
27. T. Zeng, L. Yang, R. Hudson, G. Song, A. R. Moores and C.-J. Li, *Org. Lett.*, 2010, 13, 442-445.
28. P. D. Stevens, J. Fan, H. M. R. Gardimalla, M. Yen and Y. Gao, *Org. Lett.*, 2005, 7, 2085-2088.

29. B. Baruwati, D. Guin and S. V. Manorama, *Org. Lett.*, 2007, 9, 5377-5380.
30. V. Polshettiwar, B. Baruwati and R. S. Varma, *Chem. Commun.*, 2009, 1837-1839.
31. Z. Wang, B. Shen, Z. Aihua and N. He, *Chem. Eng. J.*, 2005, 113, 27-34.
32. L. M. Rossi, F. P. Silva, L. L. R. Vono, P. K. Kiyohara, E. L. Duarte, R. Itri, R. Landers and G. Machado, *Green Chem.*, 2007, 9, 379-385.
33. C. Rangheard, C. de Julian Fernandez, P.-H. Phua, J. Hoorn, L. Lefort and J. G. de Vries, *Dalton Trans.*, 2010, 39, 8464-8471.
34. P.-H. Phua, L. Lefort, J. A. F. Boogers, M. Tristany and J. G. de Vries, *Chem. Commun.*, 2009, 3747-3749.
35. R. B. Bedford, M. Betham, D. W. Bruce, S. A. Davis, R. M. Frost and M. Hird, *Chem. Commun.*, 2006, 1398-1400.
36. T. Zeng, W.-W. Chen, C. M. Cirtiu, A. Moores, G. Song and C.-J. Li, *Green Chem.*, 2010, 12, 570-573.
37. F. Shi, M. K. Tse, M.-M. Pohl, A. Brückner, S. Zhang and M. Beller, *Angew. Chem.*, 2007, 119, 9022-9024.
38. S. Zhou, M. Johnson and J. G. C. Veinot, *Chem. Commun.*, 2010, 46, 2411-2413.
39. F. Himo, T. Lovell, R. Hilgraf, V. V. Rostovtsev, L. Noodleman, K. B. Sharpless and V. V. Fokin, *J. Am. Chem. Soc.*, 2005, 127, 210-216.
40. C. M. Cirtiu, T. Raychoudhury, S. Ghoshal and A. Moores, *Colloids Surf., A*, 2011, doi:10.1016/j.colsurfa.2011.1009.1011.
41. S. Peng, C. Lei, Y. Ren, R. E. Cook and Y. Sun, *Angew. Chem. Int. Ed.*, 2011, 50, 3158-3163.
42. I. W. Davies, L. Matty, D. L. Hughes and P. J. Reider, *J. Am. Chem. Soc.*, 2001, 123, 10139-10140.

3.1.8 Appendix

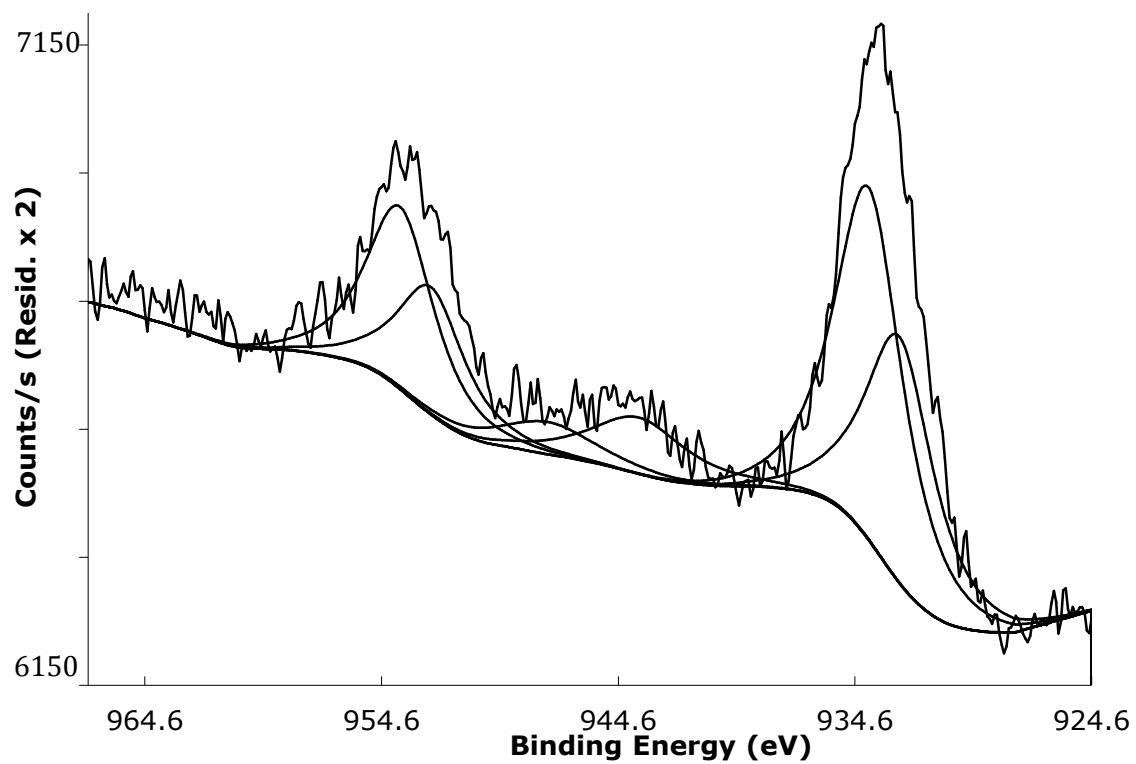


Figure 3.1.1. XPS Analysis of Cu@Fe NPs

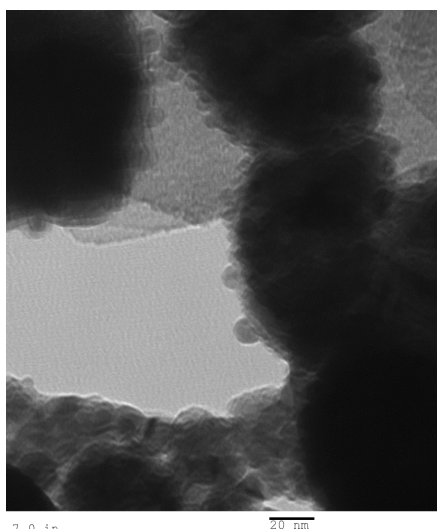


Figure 3.1.2. TEM image of Cu@FeNPs

3.2 Magnetic Ru@Fe nanoparticles as transfer hydrogenation catalysts

3.2.1 Abstract

The development of a novel bimetallic ruthenium-iron nanoparticle synthesized by galvanic reduction provides a magnetically recoverable heterogeneous catalyst for transfer hydrogenation with a pronounced selectivity for ketones over aldehydes and nitro groups. The nanoparticles are recyclable up to five times without significant decrease in activity.

3.2.2 Introduction

Over the past decade, nanoparticles (NPs) have been touted as capable of combining the catalytic activity of homogeneous catalysts with the ease of recovery of their bulk heterogeneous counterparts.¹⁻³ Magnetic NPs offer one of the easiest means of catalyst recovery and recycling—simple application of an external magnet.^{4, 5} Such a simple, environmentally benign, and economical mode of catalyst recycling could easily lend itself to practical industrial applications.

Most schemes for the use of magnetic particles offer simple recovery, but a considerably more complicated route to catalyst preparation. Indeed, the most popular schemes for the preparation of magnetic nanoparticle catalysts require coating with a polymer^{6, 7} or silica,^{8, 9} to which a metal binding ligand is then anchored. Alternatively, the Varma Group popularized a technique that forgoes the polymer or silica coating, and instead anchors the metal binding ligand¹⁰⁻¹² or organocatalyst^{13, 14} directly to the nanoparticle surface.

To further reduce the synthetic effort involved with catalyst preparation, another strategy developed wherein the surface of the magnetic particle itself is responsible for catalysis, rather than any anchored species. This bare magnetic NP approach often uses one of the following types of particles: iron oxide (Fe_3O_4 ¹⁵⁻¹⁷ or Fe_2O_3 ¹⁸), metal ferrite¹⁹⁻²⁶ ($[\text{M}]\text{Fe}_2\text{O}_4$), zero-valent iron,^{27, 28} core-shell iron-iron

oxide,²⁹ or core-shell iron-iron oxide decorated with another metal (M@FeNP).^{30, 31} Each system delivers a unique set of reactivities and inherent drawbacks.

Iron oxide nanoparticles impart an oxidizing potential, which researchers have taken advantage of to catalyse various oxidative reactions. Examples include: oxidation of olefins and alcohols,¹⁸ arene borylation,³² and cross dehydrogenative coupling.¹⁶ Additionally, iron oxide NPs can catalyse the three-component coupling of aldehyde, amine, and alkyne,¹⁷ as well as related reactions.¹⁵ Unfortunately, the modest reactivity of iron limits further use of these particles for other catalytic applications.

To remedy the limited catalytic scope of iron while at the same time retaining a similar catalyst scaffold, metal ferrite ([M]Fe₂O₄) NPs have been used as well. In this system, iron enables magnetic recovery, while the second metal within the lattice expands the catalytic scope. CuFe₂O₄³³ has been used for C-C,^{25, 34} C-O,³⁵ C-N,²⁶ C-S,³⁶ and C-Se³⁷ cross couplings as well as the azide-alkyne Huisgen 1,3 dipolar cycloaddition,³⁸ sugar deacylation,³⁹ tetrazole synthesis,⁴⁰ hydrosilation,²¹ and three-component coupling of aldehyde, alkyne and amine.²⁰ Alternatively, instead of copper, cobalt can be substituted into the ferrite lattice to enable activity for the Knoevenagel reaction,¹⁹ or aerobic oxidation of cyclohexane.²² It likely won't be long until researchers use other known ferrites such as MnFe₂O₄, ZnFe₂O₄, or NiFe₂O₄ to further demonstrate the expanded reactivity of this type of bare magnetic NP.

While iron oxide and ferrite particles often impart an oxidizing potential, some reactions require a more reduced catalyst. In this vein, zero-valent iron nanoparticles have been used to catalyze hydrogenation of olefins and alkynes with H₂,²⁷⁻²⁹ transfer hydrogenation of carbonyl compounds with isopropanol,⁴¹ dehydrogenation of ammonia borane for release of stored hydrogen fuel,^{42, 43} Grignard type reactions,⁴⁴ and reduction of environmental contaminants.⁴⁵⁻⁴⁸ Iron particles are notoriously prone to oxidation, and again the narrow catalytic scope of iron limits their potential use for other reactions. To overcome this second limitation, the group of Veinot established a technique for introducing a second metal to the surface of core-shell iron-iron oxide nanoparticles.³¹ Simply stirring a metal salt in a dispersion of these particles allows galvanic reduction of the salt and

formation of secondary particles attached to the surface. This strategy has previously been employed with palladium to enable sonogashira coupling³¹ and with copper to allow the azide-alkyne ‘click’ reaction.³⁰ Herein, we report the extension of this technique to ruthenium and the use of the resultant Ru@Fe nanoparticles for transfer hydrogenation.

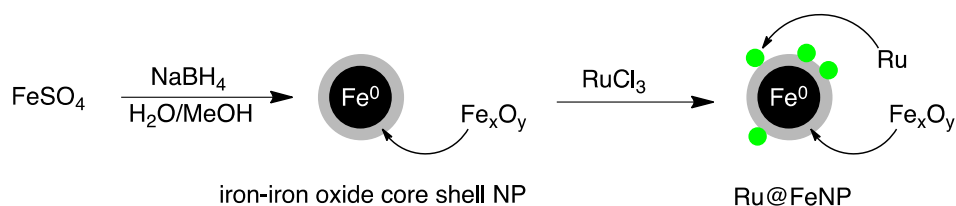
Transfer hydrogenation is an attractive alternative to hydrogenation with H₂ if the use of pressurized gases is a concern in the experimental setup. Additionally, transfer hydrogenation often offers complimentary selectivity to the traditional H₂ approach. For example, iron-nanoparticle catalysed hydrogenation with H₂ can reduce alkenes and alkynes but not carbonyl compounds.^{29, 49} On the other hand, ruthenium catalysed transfer hydrogenation can reduce carbonyls, often selectively over alkenes and alkynes.^{50, 51} Adapting transfer hydrogenation catalysts—both pseudohomogenous and purely heterogeneous—to magnetic particles is a rapidly progressing field. Two prominent demonstrations exemplify this strategy. One uses a ligand bound directly to a magnetic particle,⁵¹ and the second uses a silica coated magnetic particle as an effective ruthenium support.⁵⁰ Our contribution represents further simplification of the system by forgoing the need for a metal binding ligand or silica coating. Instead, the catalytic ruthenium particles are bound directly to the surface of the as synthesized magnetic iron/iron oxide nanoparticle—thereby shortening the synthetic route to the catalyst, eschewing the use of organic ligands, and avoiding the need for pH adjustments.

3.2.3 Results and Discussion

3.2.3.1 Synthesis of Ru@Fe nanoparticles

Core-shell iron-iron oxide nanoparticles were synthesized by a previously reported²⁹ NaBH₄ reduction of FeSO₄ in H₂O/MeOH. Subsequent addition of a RuCl₃ solution (20.1 mg of RuCl₃ in 100 mL of methanol) added dropwise to a sonicating solution of iron nanoparticles (100 mg in 100 mL methanol) afforded the

Ru@FeNPs. The particles were then magnetically recovered, and rinsed three times with 30 mL of MeOH (scheme 3.2.1).



Scheme 3.2.1. Synthesis of Ru@FeNPs

3.2.3.2 Characterization of Ru@Fe nanoparticles

Comparison of TEM images (appendix) before and after Ru plating suggest that the 30-50 nm core-shell iron-iron oxide nanoparticles become decorated with much smaller Ru particles at their surface. Digestion in HNO_3 followed by subsequent ICP-MS analysis indicated that the particles contained 2 weight percent Ru. XPS peaks at 281.7 and 284.1 suggest surface RuO_x ($2 < x < 3$) and RuO_4 , respectively.

3.2.3.3 Ru@Fe nanoparticles for transfer hydrogenation

In order to test the activity of Ru@FeNPs for transfer hydrogenation, 10 mL reaction vessels were sealed (to prevent the solvent from boiling off) after being charged with 5 mL 2-propanol (which served both as the solvent and hydrogen transfer agent), 1 mmol hydrogenation substrate, 15 mol % KOH, 1 mol% Ru@FeNP (with respect to Ruthenium content), and a magnetic stir bar.

Table 3.2.1. Transfer hydrogenation conditions screening.^a

| Entry | Catalyst | Base | Temp (°C) | Yield ^b |
|-------|----------|--------------|-----------|--------------------|
| 1 | Ru@FeNP | KOH (15mol%) | 85 | 30 |
| 2 | FeNP | KOH (15mol%) | 85 | 11 |
| 3 | Ru@FeNP | KOH (15mol%) | 100 | 95 |
| 4 | Ru@FeNP | None | 100 | 12 |
| 5 | FeNP | KOH (15mol%) | 100 | 49 |
| 6 | FeNP | None | 100 | 0 |
| 7 | None | None | 100 | 0 |

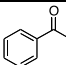
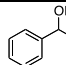
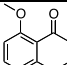
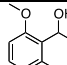
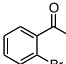
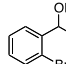
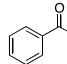
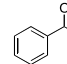
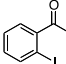
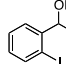
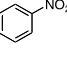
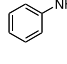
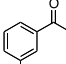
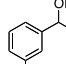
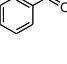
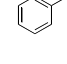
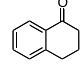
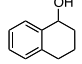
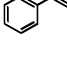
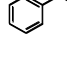
^a reaction conditions: 1 mmol acetophenone, 50 mg catalyst, 5 mL 2-propanol, 24 hours

^b Yield determined by GC-FID with decane as internal standard

With conditions optimized for transfer hydrogenation of acetophenone (Table 3.2.1) in hand, the study probed the reactivity of other substrates (Table 3.2.2). Acetophenone derivatives displayed reactivity proportional to the steric bulk near the carbonyl. For example, 2'-bromoacetophenone reacted slower than acetophenone and the even bulkier 2'-iodoacetophenone reacted slower still. Moving the substituent to the 3'-position (3'-bromoacetophenone) brought the yield more in line with acetophenone. Trifluoro acetophenone displayed good reactivity and the system demonstrated excellent selectivity against both nitro and aldehyde reduction. In order to demonstrate the durability and reuseability of the catalyst, the study magnetically recovered (by allowing the nanoparticles to settle back onto the stir bar at the end of the reaction) and recycled the catalyst for the transfer hydrogenation of acetophenone. The catalyst could be used up to 5 times with no appreciable decrease in yield (Figure 3.2.1). In order to provide evidence for a heterogeneous mechanism, the study probed the reactivity of species in the reaction supernatant. First, Ru@FeNPs were subjected to the regular catalytic conditions, then, while still hot, the supernatant was then filtered through celite and subsequently used for catalysis, which only resulted in trace amounts of product. Second, the standard reaction of acetophenone was allowed to run for 1 hour, and then similarly hot filtered through celite to remove any heterogeneous material, and allowed to complete the 24-hour reaction time. The yield did not appreciably

increase from the pre-filtering value (18%) to the value after reacting for another 23 hours in the absence of heterogeneous material (20%)—a second result suggestive of a heterogeneous mechanism.

Table 3.2.2. Transfer hydrogenation substrate scope.^a

| Substrate | Product | Yield ^b | Substrate | Product | Yield ^b |
|---|---|--------------------|---|--|--------------------|
|  |  | 95 |  |  | 26 |
|  |  | 74 |  |  | 91 |
|  |  | 13 |  |  | 0 |
|  |  | 84 |  |  | 4 |
|  |  | 14 |  |  | 51 |

^a reaction conditions: 1 mmol substrate, 1 mol% Ru@FeNP, 15 mol% KOH, 2-propanol (5 mL).

^b Yield determined by GC-FID with decane as internal standard

Interestingly, the FeNP without Ru displayed moderate yield for the transfer hydrogenation of acetophenone. This semi-positive ‘blank’ experiment highlights an interesting fundamental reactivity of a generally inactive metal: iron. Ongoing research in our lab aims to bring this reactivity of just iron particles in line with the more synthetically useful yields demonstrated with the ruthenium-plated analogue described herein.

Table 3.2.3. Catalyst recycling for acetophenone transfer hydrogenation.^a

| Run | 1 | 2 | 3 | 4 | 5 |
|-----------|----|----|----|----|----|
| Yield (%) | 95 | 99 | 99 | 99 | 94 |

^a Reaction conditions: 1 mmol acetophenone, 1 mol% Ru@FeNP, 15 mol% KOH, 2-propanol (5 mL).

3.2.4 Conclusions

The study demonstrated the synthesis of a novel Ru@FeNP catalyst generated by simple addition of RuCl₃ to a solution of core-shell iron-iron oxide nanoparticles. These magnetically recyclable particles could be used directly for transfer hydrogenation reactions, providing good yields on many acetophenone derivatives and demonstrated a strict selectivity for ketones over aldehydes and nitro groups. These particles pose little difficulty in their synthesis, use, or recycling, making them a potentially attractive option for practical industrial applications.

3.2.5 Acknowledgements

We thank the Natural Science and Engineering Research Council of Canada (NSERC), the Canada Foundation for Innovation (CFI), the Canada Research Chairs (CRC), the Fonds de Recherche sur la Nature et les Technologies (FQRNT), the Centre for Green Chemistry and Catalysis (CGCC), the Green Chemistry - NSERC Collaborative Research and Training Experience (CREATE) Program, and McGill University for financial support. We thank Kevin Wilkinson from Université de Montreal and Josianne Lefebvre from Ecole Polytechnique for ICP and XPS analyses, respectively.

3.2.6 References

1. V. Polshettiwar and R. S. Varma, *Green Chem.*, 2010, 12, 743-754.

2. A. M. Molenbroek, S. Helveg, H. Topsøe and B. S. Clausen, *Top. Catal.*, 2009, 52, 1303-1311.
3. D. Astruc, F. Lu and J. Ruiz Aranzaes, *Angew. Chem., Int. Ed.*, 2005, 44, 7852-7872.
4. V. Polshettiwar, R. Luque, A. Fihri, H. Zhu, M. Bouhrara and J.-M. Bassett, *Chem. Rev.*, 2011, 111, 3036-3075.
5. A. H. Lu, E. L. Salabas and F. Schüth, *Angew. Chem., Int. Ed.*, 2007, 46, 1222-1244.
6. P. D. Stevens, J. Fan, H. M. R. Gardimalla, M. Yen and Y. Gao, *Org. Lett.*, 2005, 7, 2085-2088.
7. T. Zeng, L. Yang, R. Hudson, G. Song, A. R. Moores and C.-J. Li, *Org. Lett.*, 2011, 13, 442-445.
8. G. Lv, W. Mai, R. Jin and L. Gao, *Synlett*, 2008, 19, 1418-1422.
9. B. G. Wang, B. C. Ma, Q. Wang and W. Wang, *Adv. Synth. Catal.*, 2010, 352, 2923-2928.
10. V. Polshettiwar, B. Baruwati and R. S. Varma, *Green Chem.*, 2009, 11, 127-131.
11. V. Polshettiwar and R. S. Varma, *Chem. Euro. J.*, 2009, 15, 1582-1586.
12. V. Polshettiwar and R. S. Varma, *Org. Biomol. Chem.*, 2009, 7, 37-40.
13. V. Polshettiwar, B. Baruwati and R. S. Varma, *Chem. Commun.*, 2009, 0, 1837-1839.
14. O. Gleeson, G.-L. Davies, A. Peschiulli, R. Tekoriute, Y. K. Gun'ko and S. J. Connon, *Org. Biomol. Chem.*, 2011, 9, 7929-7940.
15. B. V. S. Reddy, A. S. Krishna, A. V. Ganesh and G. G. K. S. N. Kumar, *Tetrahedron Lett.*, 2011, 52, 1359-1362.
16. T. Zeng, G. Song, A. Moores and C. Li, *Synlett*, 2010, 13, 2002-2008.
17. T. Q. Zeng, W.-W. Chen, C. M. Cirtiu, A. Moores, G. H. Song and C. J. Li, *Green Chem.*, 2010, 12, 570-573.
18. F. Shi, M. K. Tse, M.-M. Pohl, A. Brückner, S. Zhang and M. Beller, *Angew. Chem. Int. Ed.*, 2007, 46, 8866-8868.
19. K. K. Senapati, C. Borgohain and P. Phukan, *J. Mol. Catal. A: Chem.*, 2011, 339, 24-31.

20. M. L. Kantam, J. Yadav, S. Laha and S. Jha, *Synlett*, 2009, 1791-1794.
21. M. L. Kantam, J. Yadav, S. Laha, P. Srinivas, B. Sreedhar and F. Figueras, *J. Org. Chem.*, 2009, 74, 4608-4611.
22. M. Kooti and M. Afshari, *Scientia Iranica*, 2012, 19.
23. B. Kumar, K. H. V. Reddy, B. Madhav, K. Ramesh and Y. V. D. Nageswar, *Tetrahedron Lett.*, 2012, 53, 4595-4599.
24. L. Menini, M. C. Pereira, L. A. Parreira, J. D. Fabris and E. V. Gusevskaya, *J. Catal.*, 2008, 254, 355-364.
25. N. Panda, A. K. Jena and S. Mohapatra, *Chem. Lett.*, 2011, 40, 956-958.
26. N. Panda, A. K. Jena, S. Mohapatra and S. R. Rout, *Tetrahedron Lett.*, 2011, 52, 1924-1927.
27. C. Rangheard, C. De Julian Fernandez, P. H. Phua, J. Hoorn, L. Lefort and J. G. De Vries, *Dalton Trans.*, 2010, 39, 8464-8471.
28. P. H. Phua, L. Lefort, J. A. F. Boogers, M. Tristany and J. G. de Vries, *Chem. Commun.*, 2009, 3747-3749.
29. R. Hudson, A. Riviere, C. M. Cirtiu, K. L. Luska and A. Moores, *Chem. Commun.*, 2012, 48, 3360-3362.
30. R. Hudson, C. J. Li and A. Moores, *Green Chem.*, 2012, 14, 622-624.
31. S. Zhou, M. Johnson and J. G. C. Veinot, *Chem. Commun.*, 2010, 46, 2411-2413.
32. G. Yan, Y. Jiang, C. Kuang, S. Wang, H. Liu, Y. Zhang and J. Wang, *Chem. Commun.*, 2010, 46, 3170-3172.
33. R. Hudson, *Synlett*, 2013, 1309-1310.
34. R. Hudson, S. Ishikawa, C. J. Li and A. Moores, *Synlett*, 2013, DOI: 10.1055/s-0033-1339278.
35. R. Z. Zhang, J. M. Liu, S. F. Wang, J. Z. Niu, C. G. Xia and W. Sun, *ChemCatChem*, 2011, 3, 146-149.
36. K. Swapna, S. N. Murthy, M. T. Jyothi and Y. V. D. Nageswar, *Org. Biomol. Chem.*, 2011, 9, 5989-5996.
37. K. Swapna, S. N. Murthy and Y. V. D. Nageswar, *Eur. J. Org. Chem.*, 2011, 1940-1946.
38. S. Ishikawa, R. Hudson, A. Moores and C.-J. Li, *Heterocycles*, 2012, 86, 1970.

39. J. E. Tasca, A. Ponzinibbio, G. Diaz, R. D. Bravo, A. Lavat and M. G. Gonzalez, *Top. Catal.*, 2010, 53, 1087-1090.
40. B. Sreedhar, A. S. Kumar and D. Yada, *Tetrahedron Lett.*, 2011, 52, 3565-3569.
41. J. F. Sonnenberg, N. Coombs, P. A. Dube and R. H. Morris, *J. Am. Chem. Soc.* , 2012, 134, 5893-5899.
42. M. Dinç, Ö. Metin and S. Özkar, *Catal. Today*, 2012, 183, 10-16.
43. J.-M. Yan, X.-B. Zhang, S. Han, H. Shioyama and Q. Xu, *Angew. Chem. Int. Ed.* , 2008, 47, 2287-2289.
44. R. B. Bedford, M. Betham, D. W. Bruce, S. A. Davis, R. M. Frost and M. Hird, *Chem. Comm.*, 2006, 1398-1400.
45. T. Almeelbi and A. Bezbaruah, *J. Nanopart. Res.*, 2012, 14.
46. W. X. Zhang, *J. Nanopart. Res.*, 2003, 5, 323-332.
47. Y. F. Xi, M. Mallavarapu and R. Naidu, *Mater. Res. Bull.*, 2010, 45, 1361-1367.
48. Y. Q. Liu, S. A. Majetich, R. D. Tilton, D. S. Sholl and G. V. Lowry, *Environ. Sci. Tech.*, 2005, 39, 1338-1345.
49. R. Hudson, G. Hamasaka, T. Osako, Y. M. A. Yamada, C.-J. Li, Y. Uozumi and A. Moores, *Green Chem.*, 2013.
50. R. B. Nasir Baig and R. S. Varma, *ACS Sustain. Chem. Eng.*, 2013, 1, 805-809.
51. B. Baruwati, V. Polshettiwar and R. S. Varma, *Tetrahedron Lett.*, 2009, 50, 1215-1218.

3.2.7 Appendix

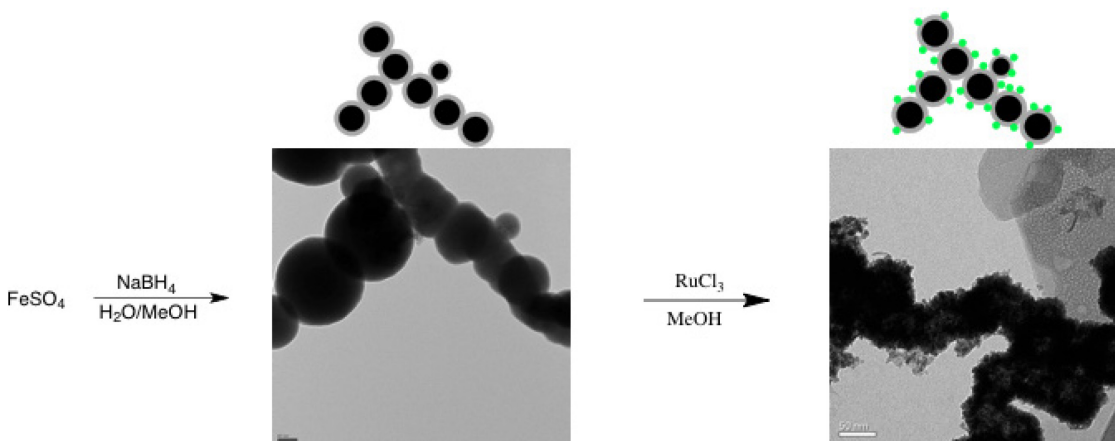


Figure 3.2.1. TEM images of core shell iron-iron oxide nanoparticles and ruthenium plated iron-iron oxide nanoparticles below schematic representations.

3.2.7.1 Experimental details

3.2.7.1.1 Reagents:

Sodium Borohydride (sigma Aldrich, 99%)

$\text{FeSO}_4 \times 6 \text{H}_2\text{O}$ (alfa aesar, 99+%)

MeOH (Fischer Scientific, ACS grade)

RuCl_3 (Sigma Aldrich – Ru content 45-55%)

HNO_3 (ACP, ACS grade)

2-propanol (Fischer Scientific, ACS grade)

KOH (Fischer Scientific, ACS grade)

Acetphenone (Sigma Aldrich, >99.0%)

2'-bromoacetophenone (Sigma Aldrich, 99%)

2'-iodoacetophenone (Sigma Aldrich, 97%)

3'-bromoacetophenone (Sigma Alrich, 99%)

Alphatetralone (Sigma Aldrich, 97%)

2',6'-dimethylacetophenone (Sigma Aldrich)

2,2,2-Trifluoroacetophenone (Sigma Aldrich, 99%)

Nitrobenzene (Sigma Aldrich, 99%)

Benzaldehyde (Sigma Aldrich, 99.5%)

Styrene (Sigma Aldrich, 99.9%)

3.2.7.1.2 Instruments

TEM analysis was performed on a Tecnai F20 operated at 200kV.
Reaction yields were obtained on a GC-FID (Agilent Technologies, 7890A).
XPS analysis was performed on a VG Escalab 3 MKII at 300W (15kV, 20mA) and analyzed at a depth of 50-100 Angstroms.

4 CuFe₂O₄ Nanoparticles for Catalysis

Seeking another strategy for bi-metallic magnetic nanoparticle catalysis, we turned to CuFe₂O₄ nanoparticles. In this system, the iron enables magnetic recovery, while copper expands the catalytic offering. These particles are commercially available, and were used as is for cross-dehydrogenative coupling and the Biginelli condensation.

This chapter is based on three published articles, which are reprinted here with permission from Thieme Chemistry (for the two *Synlett* articles) and International ASET Inc. (for the International Conference on Nanotechnology conference proceedings). All co-authors for these manuscripts likewise gave copyright clearance. It should be noted that the introduction to this chapter is a mini-review article that cites one of the articles, which appears as a later subchapter within this chapter.

Reuben Hudson. Spotlight: Copper Ferrite (CuFe₂O₄) Nanoparticles. *Synlett*. 2013; 24(10): 1309-1310

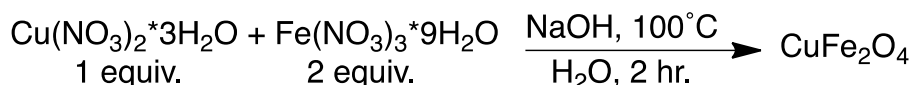
Reuben Hudson, Shingo Ishikawa, Chao-Jun Li and Audrey Moores. Magnetically Recoverable CuFe₂O₄ Nanoparticles as Highly Active Catalysts for Csp³-Csp and Csp³-Csp³ Oxidative Cross-Dehydrogenative Coupling. *Synlett*. 2013; 24(13): 1637-1642

Reuben Hudson, Julian Silverman, Chao-Jun Li and Audrey Moores. Copper ferrite nanoparticle catalyzed Biginelli condensation: proof of concept for a novel class of magnetically recoverable catalyst. *Proceedings of the 3rd International Conference on Nanotechnology*. 7-9 August 2012. Paper No. 318

4.1 General Introduction: Copper Ferrite (CuFe₂O₄) Nanoparticles For Catalysis

4.1.1 Introduction

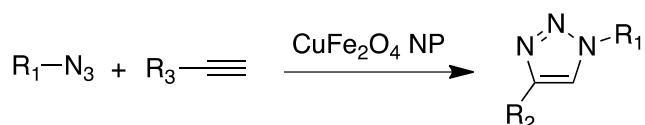
Ferrite (Fe₃O₄) nanoparticles (NPs) present as a black, magnetic powder. They have been used as a catalyst for many organic transformations¹⁻⁷ because their nanoscale size equates to a large surface area-to-volume ratio (meaning many accessible active sites).⁸ Moreover, iron-based magnetic properties enable easy catalyst recovery by the application of an external magnet. The catalytic scope of iron, however, pales in comparison with that of copper. Therefore, by substituting copper within the crystal lattice, the catalytic scope is greatly expanded, while the means of easy magnetic recovery are retained. The resulting copper ferrite nanoparticles (CuFe₂O₄ NPs) contain Cu(II) and Fe(III) species. Such nanoparticles can be obtained by co-precipitation of Cu(II) and Fe(III) salts (scheme 1).⁹ They are also commercially available. Herein the catalytic scope of CuFe₂O₄ NPs is highlighted and reviewed.



Scheme 4.1.1. Synthesis of CuFe₂O₄ NPs by co-precipitation⁹

4.1.1.1 Azide-alkyne ‘click’ reaction

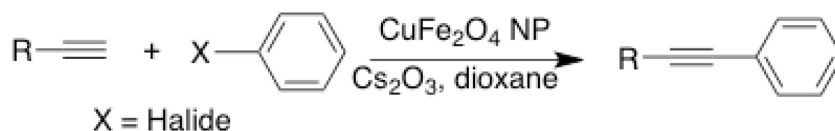
Under homogeneous Cu(I) conditions, the reaction can occur at room temperature in water.^{10,11} Under these heterogeneous conditions, the reaction requires either 70°C temperatures¹² or the addition of a ligand such as 2,2-bipyridine.¹³



Scheme 4.1.2. CuFe₂O₄ catalyzed azide-alkyne ‘click’ reaction.

4.1.1.2 C-C cross coupling

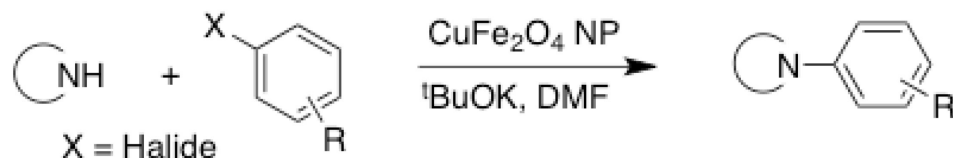
Panda and co-workers¹⁴ demonstrated a synergistic effect between copper and iron within the CuFe₂O₄ lattice to catalyze the coupling of terminal alkynes with arylhalides. Neither CuO NP nor Fe₃O₄ NP alone could catalyze the transformation as effectively.



Scheme 4.1.3. CuFe₂O₄ catalyzed C-C cross coupling.

4.1.1.3 C-N cross coupling

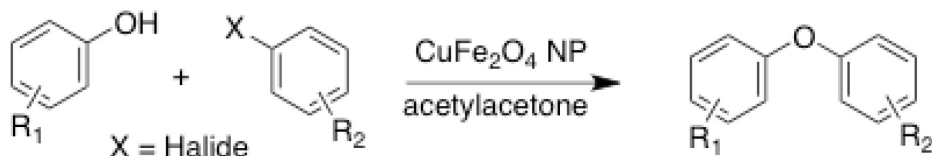
Panda and co-workers¹⁵ again demonstrated a synergistic effect between copper and iron, this time in the CuFe₂O₄ NP catalyzed coupling of N-heterocycles with aryl halides.



Scheme 4.1.4. CuFe₂O₄ catalyzed C-N cross coupling.

4.1.1.4 C-O cross coupling

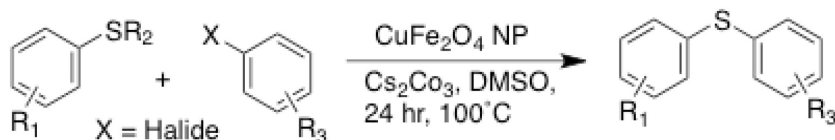
The Sun group¹⁶ effectively coupled aryl halides with phenols to generate the corresponding bi-aryl ethers by catalysis with CuFe_2O_4 nanoparticles.



Scheme 4.1.5. CuFe_2O_4 catalyzed C-O cross coupling.

4.1.1.5 C-S cross coupling

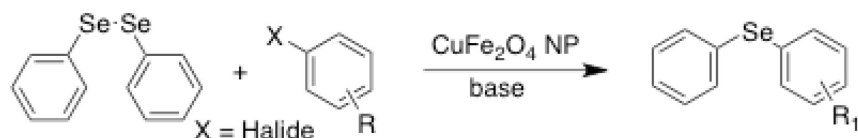
The coupling under basic conditions and elevated temperatures of aryl halides with either aromatic thiols or diaryl sulphides affords the corresponding diaryl sulphide in excellent yields. The catalytic efficiency of various $[\text{M}]\text{Fe}_2\text{O}_4$ nanoparticles were compared and $\text{M}=\text{Cu}$ was found to be the most reactive for this transformation.¹⁷



Scheme 4.1.6. CuFe_2O_4 catalyzed C-S cross coupling.

4.1.1.6 C-Se cross coupling

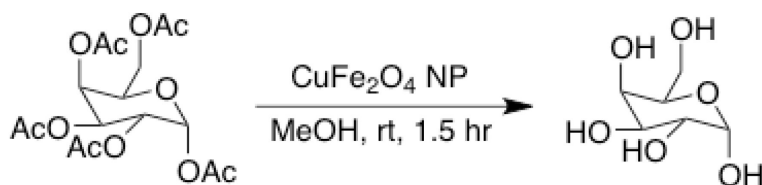
Various diaryl selenides were synthesized by the coupling of aryl halides with diaryl diselenides. The reaction required use of a base and temperatures of 120°C .¹⁸



Scheme 4.1.7. CuFe_2O_4 catalyzed C-Se cross coupling.

4.1.1.7 Sugar deacylation

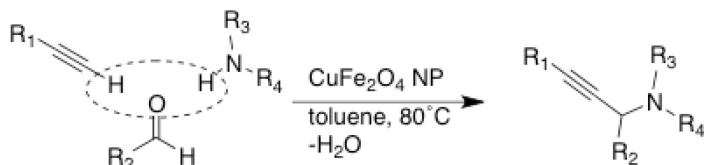
Various protected sugars were deacylated with copper ferrite nanoparticles under mild conditions. By altering the solvent, and reducing the reaction time, selective deacylation at the anomeric position could be achieved.¹⁹



Scheme 4.1.8. CuFe_2O_4 catalyzed sugar deacylation.

4.1.1.8 A³ coupling

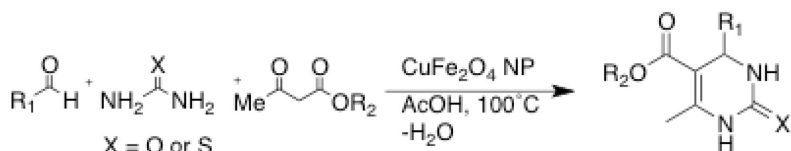
The three-component, one-pot coupling of aldehyde, alkyne and amine was reported. Although A³ coupling has already been achieved for Fe_3O_4 nanoparticles, substituting copper within the lattice effectively enabled the use of milder conditions.²⁰



Scheme 4.1.9. CuFe₂O₄ catalyzed A3 coupling.

4.1.1.9 Biginelli condensation

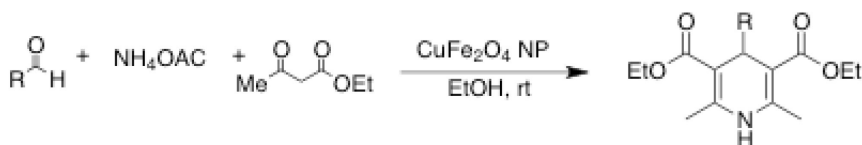
In another demonstration of a three-component one-pot reaction, the Biginelli condensation between an aldehyde, urea or thiourea, and β -ketoesters was achieved with CuFe₂O₄ nanoparticles to afford the corresponding dihydropyrimidinones or dihydropyrimidinethiones.²¹



Scheme 4.1.10. CuFe₂O₄ catalyzed Biginelli condensation.

4.1.1.10 Synthesis of dihydropyridines

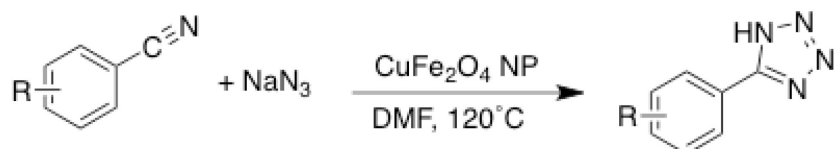
By a similar, Biginelli-related, three-component coupling of an aldehyde, ammonium acetate and a β -ketoester, Viswanath and Murthy²² later achieved the synthesis of various dihydropyridines under CuFe₂O₄ nanoparticle catalysis.



Scheme 4.1.11. CuFe₂O₄ catalyzed synthesis of dihydropyridines.

4.1.1.11 Tetrazole synthesis

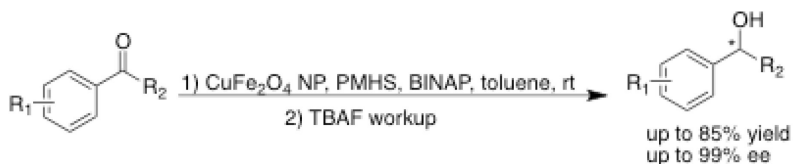
Sreedhar and co-workers²³ achieved the synthesis of 5-aryl 1H tetrazoles by CuFe_2O_4 catalyzed reaction of aryl nitriles with sodium azide in DMF at 120°C.



Scheme 4.1.12. CuFe_2O_4 catalyzed tetrazole synthesis.

4.1.1.12 Asymmetric hydrosilation

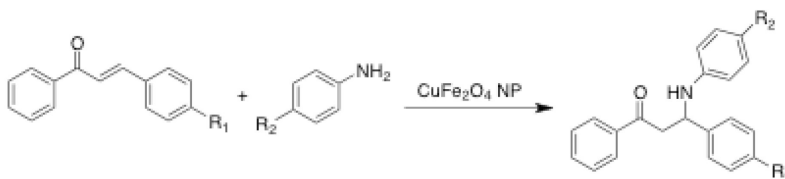
With the aid of a chiral BINAP ligand, CuFe_2O_4 nanoparticles have catalyzed the asymmetric hydrosilation of prochiral ketones, which afford the corresponding alcohol upon TBAF workup.²⁴



Scheme 4.1.13. CuFe_2O_4 catalyzed asymmetric hydrosilation.

4.1.1.13 Aza-Michael addition

Various β -amidoketones were synthesized by CuFe_2O_4 nanoparticle catalyzed aza-Michael addition of aniline derivatives to chalcone derivatives.²⁵



Scheme 4.1.14. CuFe_2O_4 catalyzed aza-Michael addition.

4.1.2 References

1. Shi, F.; Tse, M. K.; Pohl, M.-M.; Brückner, A.; Zhang, S.; Beller, M. *Angew. Chem. Int. Ed.* 2007, 8866.
2. Rajabi, F.; Karimi, N.; Saidi, M. R.; Primo, A.; Varma R. S.; Luque, R. *Adv. Synth. Catal.* 2012, 1707.
3. Zeng, T.; Song, G.; Moores A.; Li, C.J. *Synlett* 2010, 2002.
4. Zeng, T. Q.; Chen, W.-W.; Cirtiu, C. M.; Moores, A.; Song, G. H.; Li, C. J. *Green Chem.* 2010, 570.
5. Sreedhar, B.; Kumar A. S.; Reddy, P. S. *Tetrahedron Lett.*, 2010, 1891.
6. Reddy, B. V. S.; Krishna, A. S.; Ganesh A. V.; Kumar, A. S. *Tetrahedron Lett.*, 2011, 1359.
7. Firouzabadi, H.; Iranpoor, N.; Gholinejad M.; Hoseini, *Adv. Synth. Catal.* 2011, 125.
8. Yan, N.; Xiao, C.; Kou, Y. *Coord. Chem. Rev.* 2010, 1179.
9. Mahmood, N. M. *Desalination* 2011, 332
10. Tornøe, C. W.; Christensen, C.; Meldal, M. *J. Org. Chem.* 2002, 3057.
11. Rostovtsev, V. V.; Green, L. G.; Fokin, V. V.; Sharpless, K. B. *Angew. Chem. Int. Ed.* 2002, 2596.
12. Kumar, B. S. P. A.; Reddy, K. H. V.; Madhav, B.; Ramesh, K.; Nageswar, Y. V. D. *Tetrahedron Lett.*, 2012, 4595.
13. Ishikawa, S.; Hudson, R.; Moores, A.; Li, C.-J. *Heterocycles* 2012, 1023.
14. Panda, N.; Jena, A. K.; Mohapatra, S. *Chem. Lett.*, 2011, 956.
15. Panda, N.; Jena, A. K.; Mohapatra, S.; Rout, S. R. *Tetrahedron Lett.*, 2011, 1924.

16. Zhang, R.; Liu, J.; Wang, S.; Niu, J.; Xia, C.; Sun, W. *ChemCatChem* 2011, 146.
17. Swapna, K.; Murthy, S. N.; Jyothi, M. T.; Nageswar, Y. V. D. *Org. Biomol. Chem.* 2011, 5989.
18. Swapna, K.; Murthy, S. N.; Nageswar, Y. V. D. *Eur. J. Org. Chem.* 2011, 1940.
19. Tasca, J. E.; Ponzinibbio, A.; Diaz, G.; Bravo, R. D.; Lavat, A.; González, M. G. *Top. Catal.* 2010, 1087.
20. Kantam, M. L.; Yadav, J.; Laha, S.; Jha, S. *Synlett* 2009, 1791.
21. Hudson, R.; Silverman, J.; Li, C.-J.; Moores, A. *Proceedings of the 3rd International Conference on Nanotechnology*. Paper No. 318.
22. Viswanath, I. V. K.; Murthy, Y. L. N. *Chem. Sci. Trans.* 2013, 227.
23. Sreedhar, B.; Kumar, A. S.; Yada, D. *Tetrahedron Lett.*, 2011, 3565.
24. Kantam, M. L.; Yadav, J.; Laha, S.; Srinivas, P.; Sreedhar, B.; Figueras, F. *J. Org. Chem.* 2009, 4608.
25. Zohreh, S.; Pourayoubi, M. 12th *Iranian Inorganic Chemistry Conference*. 2010. 2010-09-16.

4.2 Magnetically Recoverable CuFe₂O₄ Nanoparticles as Highly Active Catalysts for Csp³-Csp and Csp³-Csp³ Oxidative Cross-Dehydrogenative-Coupling

4.2.1 Abstract

This study probes the versatility of [metal] ferrite ([M]Fe₂O₄) nanoparticles as an effective catalyst platform for oxidative Cross-Dehydrogenative-Coupling (CDC) by comparing the reactivity of simple magnetite (Fe₃O₄) with that of the copper substituted analogue, copper ferrite (CuFe₂O₄). In either case, the iron within the lattice enables magnetic recovery of the nanoparticles, simplifying the process of catalyst recycling. Both iron and copper effectively catalyze the CDC of two sp³ carbons, while copper provides reactivity that iron cannot: activation of sp hybridized carbons for coupling to sp³ centers.

4.2.2 Introduction

Efforts to both develop more direct chemical syntheses and to use simple, easily recoverable heterogeneous catalysts¹⁻³ to afford the necessary transformations represent two influential thrusts of the sustainable chemistry movement.^{4,5}

Iron-based nanoparticles fit the bill as easily recoverable heterogeneous catalysts because their magnetic nature enables recovery and recycling by simple application of an external magnet.^{6,7} Most schemes for this type of catalyst recovery take advantage of the magnetic particle (Fe, Fe₃O₄, Fe₂O₃, etc...) only as a support for which to anchor another catalytically active metal. Catalyst preparation becomes lengthy and complicated when this second metal^{8,9} or organo catalyst^{10,11} is anchored via a linker to the nanoparticle directly or instead to a protective polymer^{12,13} or silica^{14,15} coating. In an effort to move toward more simple schemes, several groups have developed a series of bare magnetic nanoparticles as purely heterogeneous catalysts for organic transformations (Figure 4.2.1).

Simple iron¹⁶ or iron-iron oxide core-shell nanoparticles can catalyze olefin hydrogenation,¹⁷⁻²⁰ dehydrogenation of ammonia borane^{21,22} for release of stored hydrogen, and the coupling of aryl Grignard reagents with alkyl halides.²³ With the understanding that iron bestows only a limited catalytic scope, a bi-metallic scheme also emerged.^{24,25} Introduction of a metal salt to a dispersion of iron-iron oxide core shell nanoparticles generates by galvanic reduction an iron-based nanoparticle decorated with nanoparticles of a more catalytically relevant metal. Introduction of palladium into such a scheme enables Suzuki-Miyaura coupling,²⁴ while copper facilitates the Huisgen 1-3 dipolar cycloaddition.²⁵

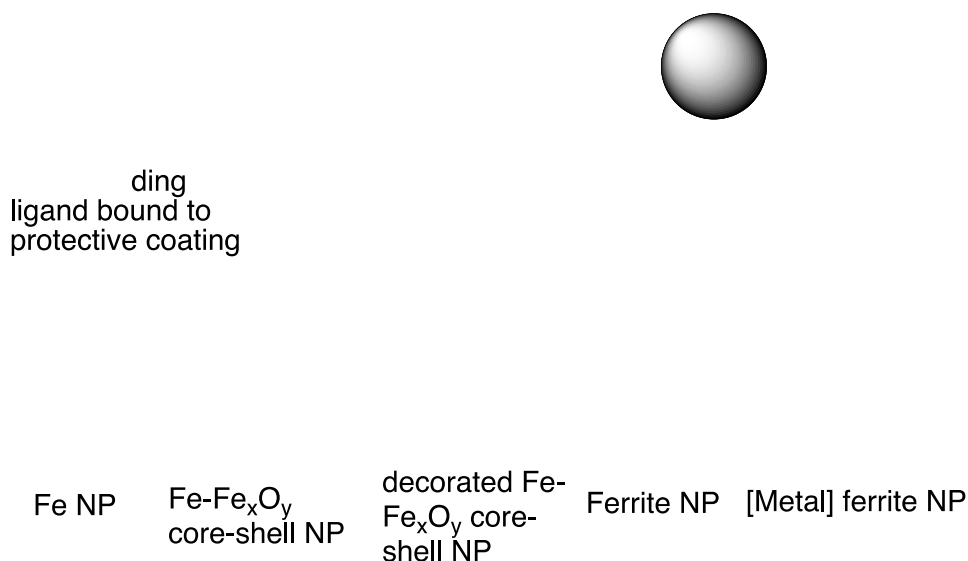
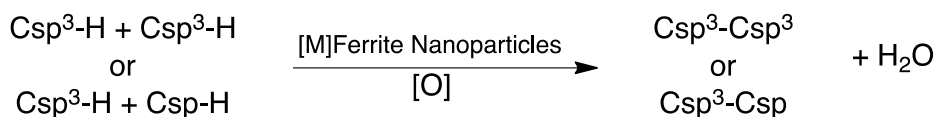


Figure 4.2.1. Various types of magnetically recoverable nanoparticle catalysts.

Catalysts that rely on a reduced iron core will always be susceptible to oxidative degradation over time. To overcome this limitation, the exploration of oxidized ferrite nanoparticles²⁶⁻²⁸ and their metal substituted analogues²⁹⁻⁴⁵ (again to overcome the limited catalytic scope of iron alone) have been explored to facilitate numerous organic transformations. For example, Fe₃O₄ can catalyze the

oxidation of olefins and alcohols,²⁷ as well as A³ coupling²⁸ and similar reactions.²⁶ Introduction of another catalytically active metal into the ferrite lattice can expand the scope of accessible reactions.^{31, 33, 35} Cobalt ferrite nanoparticles can catalyze the Knoevenangel reaction,³⁶ while copper ferrite can catalyze C-O,^{40,43} C-C,⁴⁶ and C-N³⁵ coupling reactions as well as the Biginelli condensation,⁴¹ and azide-alkyne ‘click’ reaction.⁴² This study examines for the first time a comparative analysis of a simple (Fe₃O₄) vs. a substituted (MFe₂O₄) ferrite for the catalysis of one class of reactions—in this case the oxidative CDC of Csp³ carbons with other Csp³ or Csp carbons (scheme 4.2.1).



Scheme 4.2.1 Oxidative CDC with Fe₃O₄ and CuFe₂O₄ nanoparticles.

The oxidative CDC represents a unique synthetic challenge whereby two C-H bonds are coupled to form a new C-C bond.⁴⁷⁻⁵³ Most schemes for C-H bond formation require prefunctionalization. By circumventing functionalization steps, CDC reactions effectively shorten synthetic routes. Such transformations have been carried out with various catalysts including copper⁵⁰ or iron⁵⁴ and a range of oxidants from hydrogen peroxide,⁵⁵ O₂,^{56,57} tert-butylhydroperoxide (TBHP),⁵⁸ 2,3-dichloro-5,6-dicyanobenzoquinone⁵⁹ (DDQ) or even in the absence⁶⁰ of an oxidant. Since both iron and copper represent effective catalysts for CDC reactions, we sought to compare the established reactivity of Fe₃O₄⁴⁶ with that of the copper substituted analogue (CuFe₂O₄) in hopes that the latter would both increase yields and open new catalytic avenues, specifically Csp-Csp³ coupling. The direct and exhaustive comparison of the activity of magnetite (Fe₃O₄) vs. copper ferrite nanoparticles for this reaction is unique to this study.

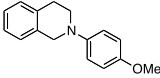
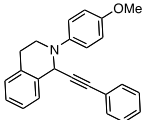
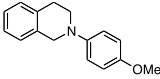
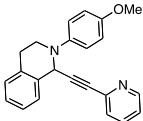
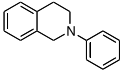
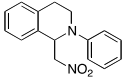
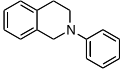
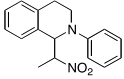
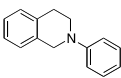
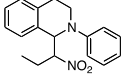
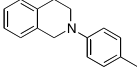
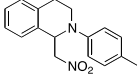
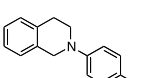
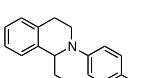
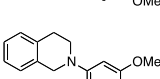
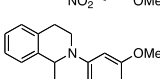
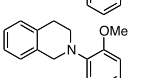
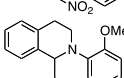
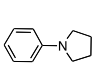
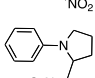
4.2.3 Results and Discussion

To compare the catalytic efficiency of Fe_3O_4 and CuFe_2O_4 nanoparticles for CDC reactivity, N-arylated analogues of tetrahydroisoquinoline (a common natural product substructure) were coupled with various aromatic alkynes or nitroalkanes. Both displayed excellent yields coupling to nitroalkanes, but only copper ferrite afforded the alkynylated product. This second result is not surprising given the ability of copper to activate alkyne species. This disparity in yield between CuFe_2O_4 and Fe_3O_4 toward Csp-Csp³ coupling and marginal yield increase for CuFe_2O_4 nanoparticle catalyzed Csp-Csp coupling validates our approach of comprehensively comparing these two catalyst systems. Different oxidants are used in the two types of coupling reactions because O_2 worked for the Csp³-Csp³ coupling, but not sufficiently for the Csp³-Csp coupling.

Table 4.2.1. Comparison of Csp³-Csp³ and Csp³-Csp CDC reaction catalyzed by Fe_3O_4 and CuFe_2O_4 nanoparticles.^a

| Entry | Substrate | Product | Yield (%) ^b |
|----------------|-----------|---------|---|
| 1 ^c | | | Fe_3O_4 : trace CuFe_2O_4 : 68 |
| 2 ^c | | | Fe_3O_4 : trace CuFe_2O_4 : 71 |
| 3 ^c | | | Fe_3O_4 : trace CuFe_2O_4 : 61 |

Reduced Iron Nanoparticles Decorated with a more Catalytically Active Metal

| | | | |
|-----------------|---|---|---|
| 4 ^c |  |  | Fe ₃ O ₄ : trace CuFe ₂ O ₄ : 69 |
| 5 ^c |  |  | Fe ₃ O ₄ : trace CuFe ₂ O ₄ : 53 |
| 6 ^d |  |  | Fe ₃ O ₄ ^e : 90 CuFe ₂ O ₄ : 92 |
| 7 ^d |  |  | Fe ₃ O ₄ ^e : 69 CuFe ₂ O ₄ : 76 |
| 8 ^d |  |  | Fe ₃ O ₄ ^e : 59 CuFe ₂ O ₄ : 73 |
| 9 ^d |  |  | Fe ₃ O ₄ ^e : 72 CuFe ₂ O ₄ : 87 |
| 10 ^d |  |  | Fe ₃ O ₄ ^e : 91 CuFe ₂ O ₄ : 91 |
| 11 ^d |  |  | Fe ₃ O ₄ ^e : 93 CuFe ₂ O ₄ : 92 |
| 12 ^d |  |  | Fe ₃ O ₄ ^e : 79 CuFe ₂ O ₄ : 88 |
| 13 ^d |  |  | Fe ₃ O ₄ ^e : 32 CuFe ₂ O ₄ : 41 |

^a Tertiary amine (0.2 mmol), [M]ferrite nanoparticles (10 mol%), 100°C, 24 hr.

^b isolated.

^c aromatic alkyne (0.22 mmol), decane (0.5 ml), [O] = DDQ (0.2 mmol).

^d nitroalkane (0.5 mL), [O] = O₂ (1 atm).

^e Csp³-Csp³ for Fe₃O₄ nanoparticle catalyzed CDC reactions were previously reported¹⁵ by our group, verified in this study and reproduced herein for comparison.

In order to establish the reusability of the catalyst and its operation under a heterogeneous mechanism, we performed several additional tests on the model reaction of copper ferrite catalyzed coupling of 2-phenyl-1,2,3,4-tetrahydroisoquinoline with nitromethane. After being subjected to catalytic conditions, the nanoparticles were magnetically recovered, the supernatant decanted and filtered through celite to remove any remaining particulate matter. This process was carried out immediately after removing the reaction vessel from the heat source in order to disfavor any equilibrium shifts that may occur if the

solution were allowed to cool to room temperature. This supernatant was then used for a second round of catalysis, affording only a 40% yield. This value is in accordance with the uncatalyzed yield (41%), suggesting that no leached species are leaving the nanoparticle to conduct homogeneous catalysis. To further corroborate this claim, ICP analysis was performed on the supernatant, indicating that less than 0.39 ppm of dissolved copper was present in solution. These results strongly suggest a heterogeneous mechanism. Furthermore, the nanoparticles could be easily recovered (Figure 4.2.2), washed with ethyl acetate, and recycled up to 10 times with little appreciable decrease in yield (Figure 4.2.3). Additionally, TEM (appendix) images of the nanoparticles indicate no discernable change in size, shape or morphology from before the reaction to after 10 cycles of catalysis. Before catalysis the average particle size was 34 ± 11.6 nm, while after 10 cycles they measured at 31 ± 12.6 nm.

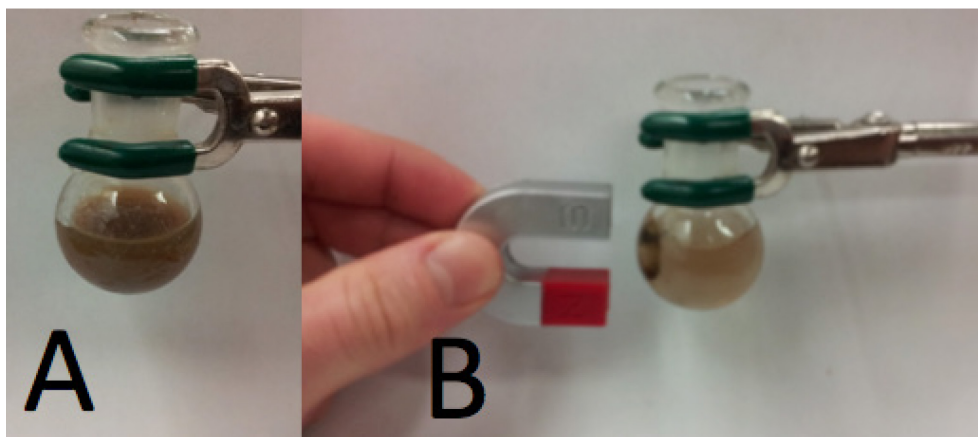


Figure 4.2.2. Photographs of A: reaction mixture with active stirring; B: CuFe_2O_4 nanoparticles adsorbed to the stir bar and attracted to external magnet.

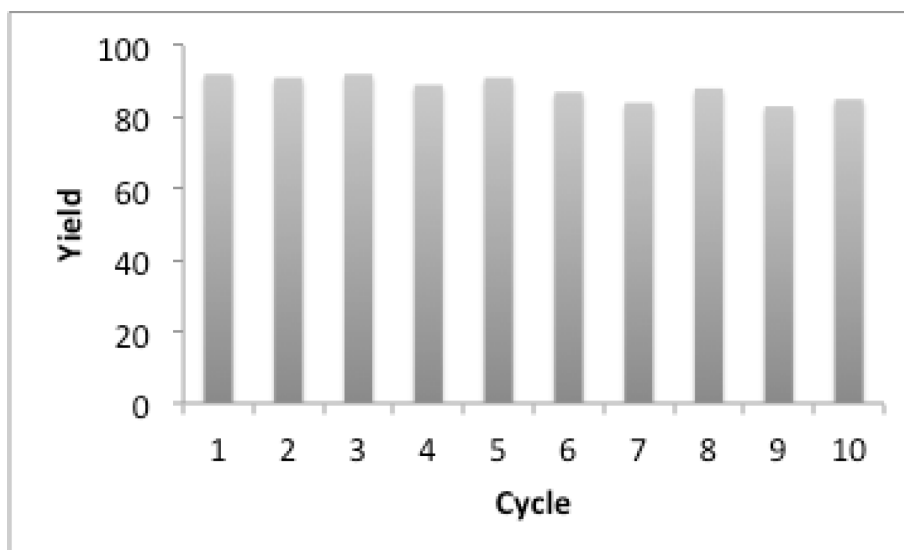
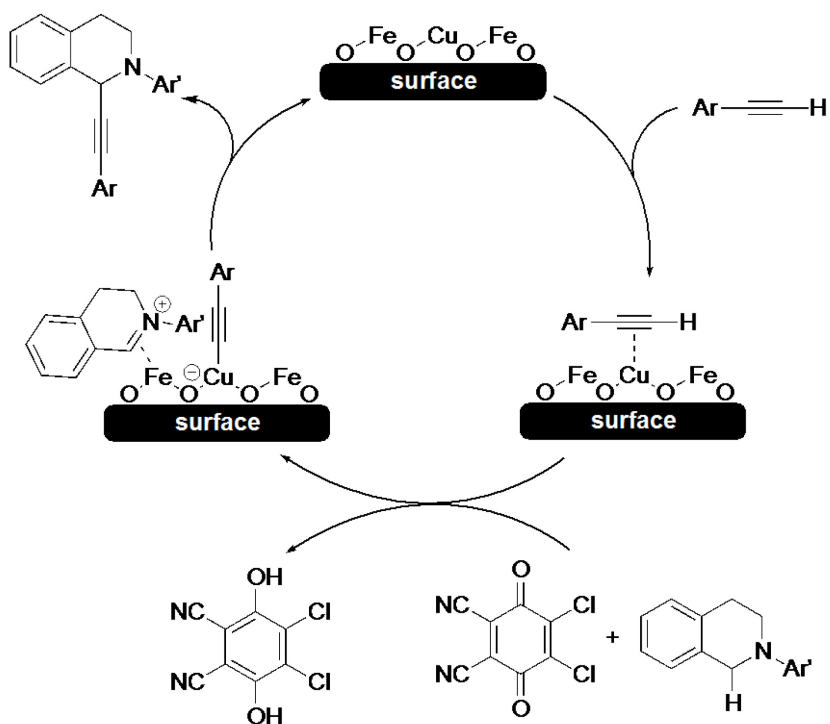


Figure 4.2.3. Recycling of CuFe₂O₄ nanoparticles (0.02 mmol) for the coupling of nitromethane (0.5 mL) with 2-phenyl-1,2,3,4-tetrahydroisoquinoline (0.2 mmol) with 1atm O₂ at 100°C for 24 hours.

A mechanism has already been proposed for the Fe₃O₄ nanoparticle catalyzed CDC reaction of nitroalkanes to tertiary amines.¹⁵ Herein we propose a similar mechanism for CuFe₂O₄ nanoparticle catalyzed coupling of aromatic alkynes to tertiary amines (scheme 2). The notable difference is that we propose that copper must activate the alkyne while the iminium cation generated from the tertiary amine can coordinate to a neighboring Fe or Cu atom within the ferrite lattice, before the two are ultimately coupled. The proposed route of coupling through an sp² hybridized intermediate suggests that this coupling could also be referred to as pseudo sp².



Scheme 4.2.2. Proposed mechanism for CuFe_2O_4 nanoparticle catalyzed Csp^3 - Csp Cross-Dehydrogenative-Coupling.

4.2.4 Conclusions

Both iron and copper are effective catalysts for the Cross-Dehydrogenative-Coupling of two Csp^3 -H bonds. The ability of both CuFe_2O_4 and Fe_3O_4 to catalyze these reactions is therefore not surprising. Copper however, offers the unique benefit of alkyne activation, which means CuFe_2O_4 nanoparticles expand the scope of [metal] ferrite nanoparticles beyond that of simple unsubstituted Fe_3O_4 nanoparticles. This finding then implies that the ferrite lattice is a versatile catalyst platform into which various metals can be substituted to afford different reactivities. No matter the metal substitution, the iron within the lattice imparts a magnetic nature, which offers an easy and environmentally benign means for catalyst recovery and recycling.

4.2.5 Experimental Procedure

CuFe₂O₃ (<50 nm particle size), Fe₂O₄ (<50 nm particle size) and other reagents were purchased from Sigma-Aldrich and used as received. 2-aryl-1,2,3,4-tetrahydroisoquinolines were prepared by a previously reported method. For coupling with nitroalkanes, CuFe₂O₃ nanoparticles (0.02 mmol), nitroalkane (0.5 mL), 2-aryl-1,2,3,4-tetrahydroisoquinolines (0.2 mmol) and a magnetic stir bar were added to a reaction vessel to which a refluxing condenser was connected and a balloon of O₂ sealed the top and reacted at 100°C for 24 hours. For coupling with aromatic alkynes, CuFe₂O₃ nanoparticles (0.02 mmol), aromatic alkyne (0.22 mmol), 2-aryl-1,2,3,4-tetrahydroisoquinolines (0.2 mmol), 2,3-dichloro-5,6-dicyano-1,4-benzoquinone (0.2 mmol), decane (0.5 mL) and a magnetic stir bar were added to a reaction vessel, sealed and reacted at 100°C for 24 hours. The nanoparticles were magnetically recovered, washed with ethyl acetate, air-dried, reused without further modification (only for the recycling tests). The reaction supernatant was filtered through Celite, and any volatile compounds removed under vacuum. The residue was purified by flash column chromatography on silica gel (eluent = hexane:ethyl acetate 5:1).

4.2.6 Acknowledgements

We thank the National Science and Engineering Council of Canada (NSERC), the Canada Foundation for Innovation (CFI), the Canada Research Chairs (CRC), the Fonds de Recherche sur la Nature et les Technologies (FQRNT), the Center for Green Chemistry and Catalysis (CCGC), and the Green Chemistry - NSERC Collaborative Research and Training Experience (CREATE) Program, for their financial support.

4.2.7 References

1. Astruc, D.; Lu, F.; Ruiz Aranzaes, J. *Angew. Chem., Int. Ed.* 2005, 44, 7852

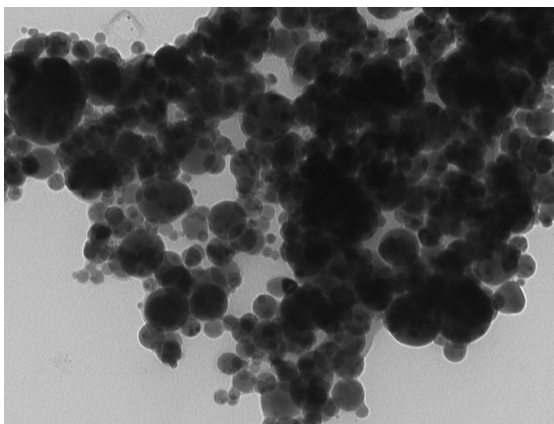
2. Molenbroek, A. M.; Helveg, S.; Topsoe, H.; Clausen, B. S. *Top. Catal.* 2009, 52, 1303
3. Polshettiwar, V.; Varma, R. S. *Green Chem.* 2010, 12, 743.
4. Anastas, P. T.; Bartlett, L. B.; Kirchhoff, M. M.; Williamson, T. C. *Catal. Today* 2000, 55, 11
5. Anastas, P. T.; Kirchhoff, M. M. *Acc. Chem. Res.* 2002, 35, 686.
6. Lu, A. H.; Salabas, E. L.; Schüth, F. *Angew. Chem., Int. Ed.* 2007, 46, 1222
7. Polshettiwar, V.; Luque, R.; Fihri, A.; Zhu, H.; Bouhrara, M.; Bassett, J.-M. *Chem. Rev.* 2011, 111, 3036.
8. Polshettiwar, V.; Varma, R. S. *Chem. Euro. J.* 2009, 15, 1582
9. Polshettiwar, V.; Varma, R. S. *Org. Biomol. Chem.* 2009, 7, 37.
10. Polshettiwar, V.; Baruwati, B.; Varma, R. S. *Chem. Commun.* 2009, 1837
11. Gleeson, O.; Davies, G.-L.; Peschiulli, A.; Tekoriute, R.; Gun'ko, Y. K.; Connon, S. *J. Org. Biomol. Chem.* 2011, 9, 7929.
12. Stevens, P. D.; Fan, J.; Gardimalla, H. M. R.; Yen, M.; Gao, Y. *Org. Lett.* 2005, 7, 2085
13. Zeng, T.; Yang, L.; Hudson, R.; Song, G.; Moores, A. R.; Li, C.-J. *Org. Lett.* 2011, 13, 422.
14. Lv, G.; Mai, W.; Jin, R.; Gao, L. *Synlett* 2008, 1418
15. Wang, B. G.; Ma, B. C.; Wang, Q.; Wang, W. *Adv. Synth. Catal.* 2010, 352, 2923.
16. Huber, D. L. *Small* 2005, 1, 482.
17. Hudson, R.; Riviere, A.; Cirtiu, C. M.; Luska, K. L.; Moores, A. *Chem. Commun.* 2012, 3360
18. Phua, P. H.; Lefort, L.; Boogers, J. A. F.; Tristany, M.; de Vries, J. G. *Chem. Commun.* 2009, 3747
19. Rangheard, C.; De Julian Fernandez, C.; Phua, P. H.; Hoorn, J.; Lefort, L.; De Vries, J. G. *Dalton Trans.* 2010, 39, 8464
20. Stein, M.; Wieland, J.; Steurer, P.; Toelle, F.; Muelhaupt, R.; Breit, B. *Adv. Synth. Catal.* 2011, 353, 523.
21. Yan, J.-M.; Zhang, X.-B.; Han, S.; Shioyama, H.; Xu, Q. *Angew. Chem., Int. Ed.* 2008, 47, 2287

22. Dinç, M.; Metin, Ö.; Özkar, S. *Catal. Today* 2012, 183, 10.
23. Bedford, R. B.; Betham, M.; Bruce, D. W.; Davis, S. A.; Frost, R. M.; Hird, M. *Chem. Comm.* 2006, 1398.
24. Zhou, S.; Johnson, M.; Veinot, J. G. C. *Chem. Commun.* 2010, 2411
25. Hudson, R.; Li, C. J.; Moores, A. *Green Chem.* 2012, 14, 622.
26. Reddy, B. V. S.; Krishna, A. S.; Ganesh, A. V.; Kumar, G. G. K. S. N. *Tetrahedron Lett.* 2011, 52, 1359
27. Shi, F.; Tse, M. K.; Pohl, M.-M.; Brückner, A.; Zhang, S.; Beller, M. *Angew. Chem. Int. Ed.* 2007, 46, 8866
28. Zeng, T. Q.; Chen, W.-W.; Cirtiu, C. M.; Moores, A.; Song, G. H.; Li, C.-J. *Green Chem.* 2010, 12, 570.
29. Kantam, M. L.; Yadav, J.; Laha, S.; Jha, S. *Synlett* 2009, 1791
30. Kantam, M. L.; Yadav, J.; Laha, S.; Srinivas, P.; Sreedhar, B.; Figueras, F. J. *Org. Chem.* 2009, 74, 4608
31. Kooti, M.; Afshari, M. *Scientia Iranica* 2012, 19, 1991
32. Kumar, B.; Reddy, K. H. V.; Madhav, B.; Ramesh, K.; Nageswar, Y. V. D. *Tetrahedron Lett.* 2012, 53, 4595
33. Menini, L.; Pereira, M. C.; Parreira, L. A.; Fabris, J. D.; Gusevskaya, E. V. *J. Catal.* 2008, 254, 355
34. Panda, N.; Jena, A. K.; Mohapatra, S. *Chem. Lett.* 2011, 40, 956
35. Panda, N.; Jena, A. K.; Mohapatra, S.; Rout, S. R. *Tetrahedron Lett.* 2011, 52, 1924
36. Senapati, K. K.; Borgohain, C.; Phukan, P. *J. Mol. Catal. A: Chem.* 2011, 339, 24
37. Sreedhar, B.; Kumar, A. S.; Yada, D. *Tetrahedron Lett.* 2011, 52, 3565
38. Swapna, K.; Murthy, S. N.; Jyothi, M. T.; Nageswar, Y. V. D. *Org. Biomol. Chem.* 2011, 9, 5989
39. Swapna, K.; Murthy, S. N.; Nageswar, Y. V. D. *Eur. J. Org. Chem.* 2011, 1940
40. Zhang, R. Z.; Liu, J. M.; Wang, S. F.; Niu, J. Z.; Xia, C. G.; Sun, W. *ChemCatChem* 2011, 3, 146.
41. Hudson, R.; Silverman, J.; Li, C.-J.; Moores, A. *Proceedings of the Third International Conference on Nanotechnology*. 7-9 August 2012. Paper No. 318.

42. Ishikawa, S.; Hudson, R.; Moores, A.; Li, C.-J. *Heterocycles*. 2012, 86, 1023.
43. Yang, S.; Wu, C.; Zhou, H.; Yang, Y.; Zhao, Y.; Wang, C.; Yang, W.; Xu, J. *Adv. Synth. Catal.* 2013, 355, 53.
44. Hudson, R. *Synlett*. DOI: 10.1055/s-0033-1338949
45. Yang, S.; Xie, W.; Zhou, H.; Wu, C.; Yang, Y.; Niu, J.; Yang, W.; Xu, J. *Tetrahedron*, 2013, 69, 16, 3415.
46. Zeng, T.; Song, G.; Moores, A.; Li, C.-J. *Synlett* 2010, 2002.
47. Li, C.-J. *Acc. Chem. Res.* 2008, 42, 335
48. Zhao, L.; Baslé, O.; Li, C.-J. *Proc. Natl. Acad. Sci.* 2009, 106, 4106
49. Li, Z.; Li, C.-J. *J. Am. Chem. Soc.* 2005, 127, 3672
50. Li, Z.; Li, C.-J. *J. Am. Chem. Soc.* 2005, 127, 6968
51. Zhang, Y.; Li, C. J. *Angew. Chem.* 2006, 118, 1883
52. Scheuermann, C. J. *Chem. Asian J.* 2010, 5, 436
53. Correia, C. A.; Li, C.-J. *Adv. Synth. Catal.* 2010, 352, 1446.
54. Li, Y. Z.; Li, B. J.; Lu, X. Y.; Lin, S.; Shi, Z. J. *Angew. Chem., Int. Ed.* 2009, 48, 3817.
55. Yoo, W.-J.; Li, C.-J. *CH Activation* 2010, 281.
56. Alagiri, K.; Kumara, G. S. R.; Prabhu, K. R. *Chem. Commun.* 2011, 11787
57. Murarka, S.; Studer, A. *Org. Lett.* 2011, 13, 2746.
58. Li, Z.; Bohle, D. S.; Li, C.-J. *Proc. Natl. Acad. Sci.* 2006, 103, 8928.
59. Zhang, Y.; Li, C.-J. *J. Am. Chem. Soc.* 2006, 128, 4242.
60. Shu, X.-Z.; Yang, Y.-F.; Xia, X.-F.; Ji, K.-G.; Liu, X.-Y.; Liang, Y.-M. *Org. Biomol. Chem.* 2010, 8, 4077.

4.2.8 Appendix

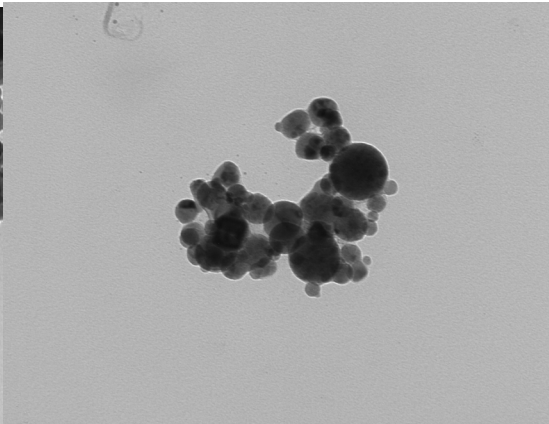
Before Catalysis:



E51.tif
Print Mag: 165000x @ 7.0 in
9:18:35 a 03/08/13

100 nm
HV=120.0kV
Direct Mag: 49000x
F20R

After 10 cycles of catalysis:



E55.tif
Print Mag: 165000x @ 7.0 in
9:26:20 a 03/08/13

100 nm
HV=120.0kV
Direct Mag: 49000x
F20R

Figure 4.2.4. TEM images of CuFe_2O_4 nanoparticles before catalysis and after 10 cycles

Average particle size before catalysis: 34 +/- 11.6 nm

Average particle size after catalysis: 31 +/- 12.6 nm

4.3 Copper-Iron-Oxide Nanoparticles as Magnetically Recoverable Catalysts for the Biginelli Condensation

4.3.1 Abstract

Unprotected, commercial and magnetic CuFe_2O_4 nanoparticles are active catalysts for the Biginelli condensation to access 3,4-dihydropyrimidine-2-ones (DHPMs). In this system, iron offers a means for magnetic recoverability, while copper brings catalytic activity. The heterogeneous nature of the catalytic reactivity was assessed and the recyclability of the catalyst tested. Reasonable to good yields were obtained over a wide scope of reagents.

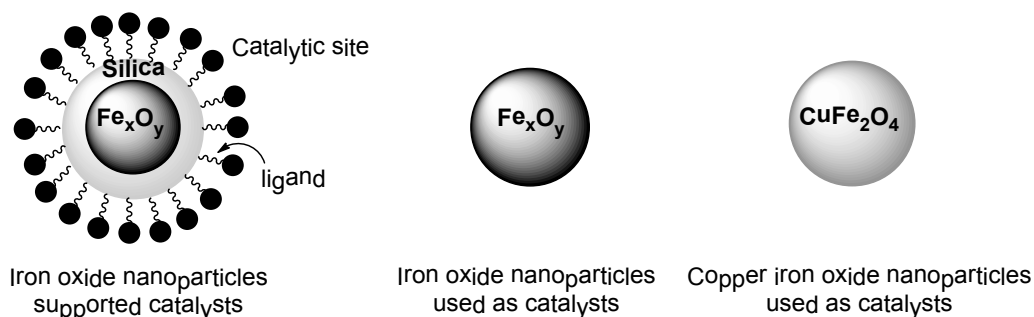
4.3.2 Introduction

Recently, many approaches have been developed to bridge the so-called gap between homogeneous and heterogeneous catalysis.¹⁻³ Successful systems managed to combine the activity and selectivity of the former with the recoverability and ease of use of the latter. Such examples include the grafting of homogeneous catalysts onto solid, porous materials, polymers or dendrimers.^{4, 5} Similarly, catalysis using colloidal metal nanoparticles has also demonstrated a great potential to achieve high selectivity, tunability and recoverability.^{2, 6-8}

Magnetic nanoparticles—separable from products and reaction media by application of an external magnet or internal stirbar—have also been used as easily separable catalyst supports.⁹ Several recent reviews summarize this effort.¹⁰⁻¹² Most of these systems are based on the following synthetic scheme. A magnetic core is typically coated with a small molecule¹³⁻¹⁸ or a polymer¹⁹ able to complex a metal center or catalytically active nanoparticles.²⁰ In other strategies, the iron core is coated with a shell of silica^{21, 22} prior to further functionalization (Scheme 1). Reported systems usually exhibit high activity and offer the potential for easy, economical, and environmentally benign processes.²³ Their fabrication, however, is inherently multi-step and atom intensive — with silica coating, ligand anchoring,

Reduced Iron Nanoparticles Decorated with a more Catalytically Active Metal

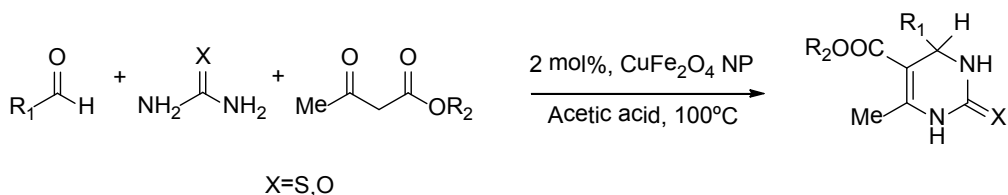
and metal complexation — which limits their applicability and relegates the magnetic particles to a mere role of support (scheme 4.3.1).



Scheme 4.3.1 Examples of magnetically recoverable nanoparticles catalysts.

Recently, some successes have been achieved with the use of simple, non-functionalized nanoparticles. Commercial, bare iron oxide (Fe_2O_3 and Fe_3O_4) nanoparticles have proven to be powerful, robust and recyclable catalysts (Scheme 1) for oxidation of olefins and alcohols,²⁴ the three component couplings of aldehyde, amine and cyanide²⁵ or alkyne,²⁶ and oxidative cross dehydrogenative $\text{Csp}^3\text{-Csp}^3$ coupling.²⁷

In addition to these examples, reduced, zero-valent iron nanoparticles have also been demonstrated as effective hydrogenation²⁸ and coupling²⁹ catalysts under remarkably mild conditions. The mechanism of stabilization of these particles is still unclear. These particles are also susceptible to oxidation and thus deactivation under aerobic conditions. Several groups also reported the successful use in catalysis of alloy or core shell magnetic nanoparticles composed of zero-valent iron and other transition metals. These materials perform well for reactions typically catalyzed by metal zero centers, such as hydrogenation reactions or couplings.^{30, 31}



Scheme 4.3.2. 3,4-dihydropyrimidine-2-ones (DHPMs) synthesis by Biginelli Condensation

In expanding the scope of reactions that can be catalyzed by magnetically recoverable nanoparticles, the use of mixed iron oxides (in which other metal centers are incorporated into the lattice), have not been much investigated (Scheme 1). In mixed iron oxides, of general formula MFe_2O_4 , iron (III) provides a means for magnetic recoverability while M (II) offers new catalytic avenues. These nanoparticles have several advantages besides being magnetic: they are air and colloidally stable without functionalization, commercially available, and robust to many reaction conditions. One such example was released during the course of this manuscript preparation; Senapati et al.³² reported the effectiveness of cobalt ferrite ($CoFe_2O_4$) for catalysis of the Knoevenagel reaction.

Liu et al.³³ recently demonstrated that the three component (aldehyde, β -ketoester and (thio)urea), one pot Biginelli condensation (scheme 2) could be catalyzed by soluble copper (II) sulfamate. It is important to note that under the reaction conditions this reaction can proceed in absence of a catalyst but only partial conversions are then obtained. In 2009, Prodius et al. suggested that $Cu(II)/Fe(III)$ oxide clusters were also active for the Biginelli reaction.³⁴ However, the clusters used were too small to be magnetically recoverable. Many products of the Biginelli condensation, 3,4-dihydropyrimidine-2-ones (DHPMs) and thiones, have biological significance, demonstrating antibacterial, antiviral, antitumor, and anti-inflammatory properties.³³ Additionally, several DHPMs serve as synthetic precursors to important calcium channel blockers.³⁵

Herein, we report the use of commercial copper ferrite ($CuFe_2O_4$) nanoparticles as readily recyclable magnetic nanoparticle catalysts, expanding the

catalytic scope of bare, unprotected, magnetic nanoparticles, by demonstrating the activity for the Biginelli condensation. For this model system, we verified catalysis was heterogeneous in nature, characterized the nanoparticles before and after catalysis to ensure their stability, reused the catalyst 12 times, and explored the scope of this reaction.

4.3.3 Results and Discussion

4.3.3.1 Catalytic Tests

In a first series of tests, we performed the classic Biginelli condensation between benzaldehyde, urea and ethylacetoacetate in the presence of CuFe_2O_4 NP at 2 mol% (based on copper content assuming perfect CuFe_2O_4 stoichiometry). The reaction was run in acetic acid at 100°C for 18 hours, in accordance with previously reported conditions.³³ A conversion of 76% was measured, which is more than twice the result obtained in absence of catalyst (table 4.3.1).

Table 4.3.1 Catalytic Tests

| Catalyst | Isolated Yield (%) |
|--------------------------------------|--------------------|
| CuFe_2O_4 | 76 |
| None | 34 |
| CuFe_2O_4 | 35 |
| Supernatant ^a | |
| Cu(II) acetate ^b | 35 |
| Fe_3O_4 | 24 |

Reaction conditions: all reactions were carried out with benzaldehyde (2mmol), urea (3mmol), ethylacetoacetate (2 mmol) and catalyst (2 mol%) with 5 mL AcOH and heated to 100°C for 18 hr. ^a Supernatant was obtained by filtering the reaction solution through celite after 1 catalytic cycle. ^b $5\ \mu\text{M} = 0.0025\text{mol}\%$.

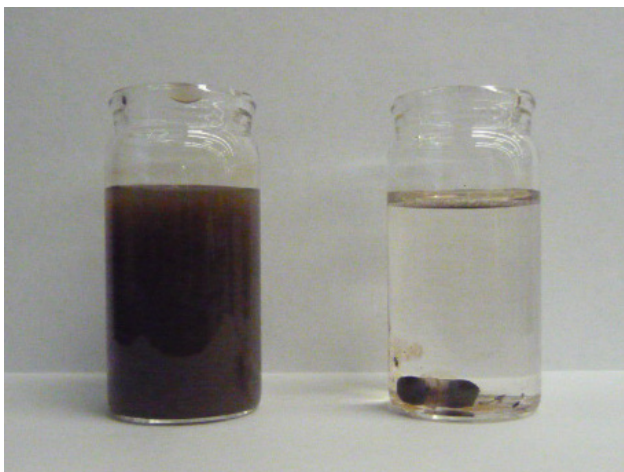


Figure 4.3.1. CuFe₂O₄ NP dispersed in solution (left) and adsorbed to a magnetic stir bar (right).

Copper ferrite nanoparticles are dispersible in acetic acid. While magnetic stirring is active, the solution presents as a dark homogeneous suspension of nanoparticles, because the dispersive forces are sufficient to counteract magnetic attraction between the nanoparticles and the stir bar. Conversely, the stoppage of stirring enables the nanoparticles to stick to the stir bar (Figure 4.3.1), leaving a clear slightly yellow solution. After the reaction the catalyst was separated magnetically by simply removing the stir bar. The product could be isolated in analytically pure form by recrystallization. Only the recrystallization product was analyzed, so the side products were left uncharacterized.

4.3.3.2 Evaluation of the Heterogeneous Nature of the Reaction

The conversion we measured is on par with the results obtained with the copper homogeneously catalyzed reaction.³³ Hence, it was necessary to understand if the process was catalyzed heterogeneously by the copper ferrite nanoparticles, or if it was dissolved copper (II) salts.³⁶ In order to discriminate between these two hypotheses, we filtered the reaction supernatant to remove any nanoparticles and exposed this solution to fresh reagents. We did not observe any more activity than

in the uncatalyzed system (Table 4.3.1), suggesting that no catalytically active homogeneous species had leached from the nanoparticle during the course of the reaction. Indeed, ICP analysis of the supernatant revealed only 4.57 μM of dissolved copper in the supernatant. To further refute potential contributions of solubilized copper, 5 μM of copper (II) acetate was loaded as the catalyst and demonstrated no appreciable increase in activity over the uncatalyzed system. Likewise, catalysis via iron oxides was rebutted by a lack of catalytic activity of Fe_3O_4 nanoparticles. According to XPS (appendix) analysis of the CuFe_2O_4 nanoparticles, Cu(II) atoms are present within the surface shell of the particles.³⁷ XRD analyses were also performed. Sharp peaks at $2\theta = 30.24^\circ, 35.52^\circ, 43.16^\circ, 53.52^\circ, 57.08^\circ, 62.72^\circ$ are characteristic of cubic phase of copper ferrite (JCPDS 34-0425).³⁸ Given the robust nature of the catalyst, the ineffectiveness of homogeneous copper (II) acetate and heterogeneous Fe_3O_4 NPs, we propose a heterogeneous mechanism involving Cu(II)oxide surface atoms.

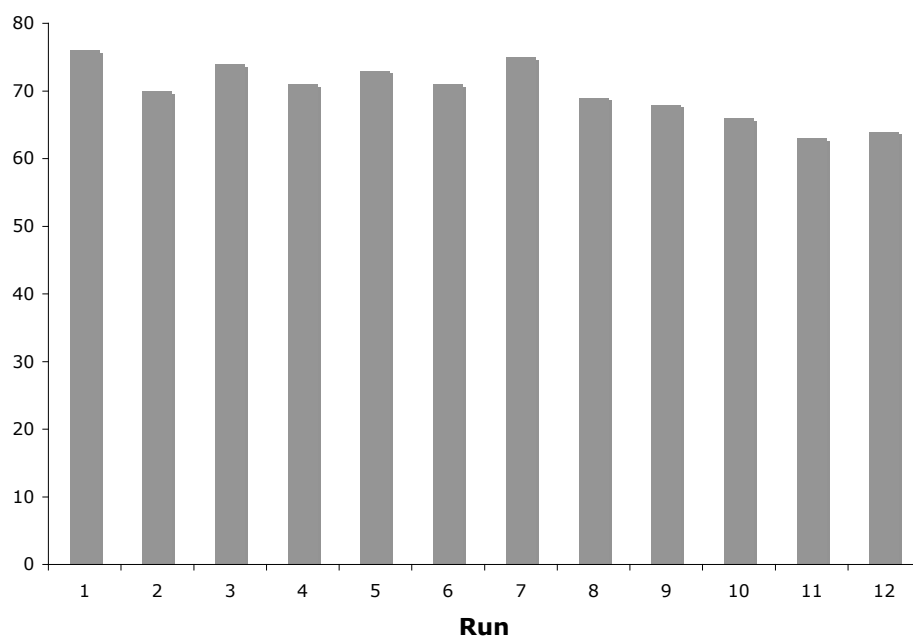


Figure 4.3.2 Recycling tests of CuFe_2O_4 NPs for the Biginelli Condensation

In support of a heterogeneous mechanism, the nanoparticles could be recycled up to 7 times with no appreciable loss in activity, and maintained >85% of their original activity after 12 cycles (figure 4.3.2). Similarly demonstrating the robust nature of the catalyst, TEM imaging indicated no visible degradation of size and shape alteration after 7 reaction cycles (figure 4.3.3). Before reaction, we measured an average size of 31 ± 11 nm. This figure was hardly altered after reaction with an average diameter of 29 ± 8 nm.

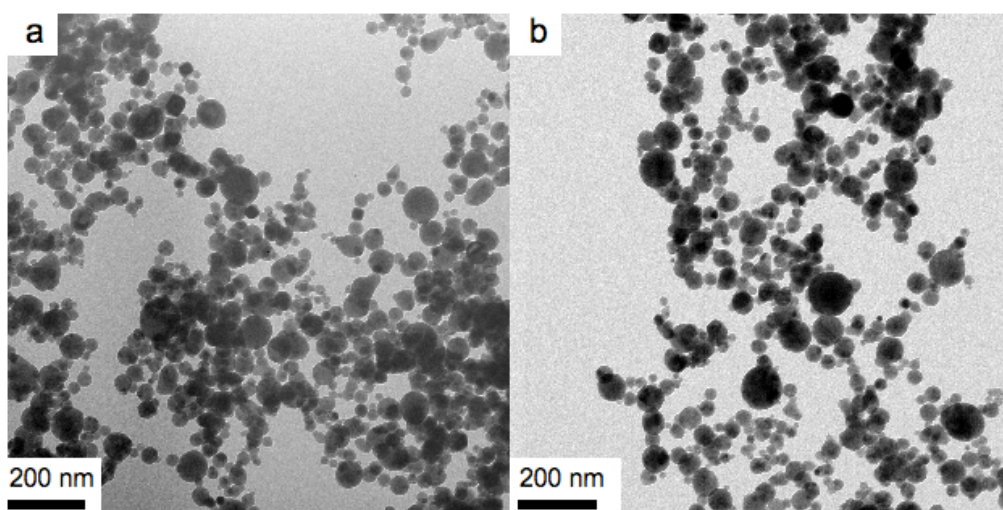
4.3.3.3 Reaction Scope

Table 4.3.2 presents the scope of the Biginelli condensation achieved with CuFe_2O_4 nanoparticles as catalysts. Compared to the model Biginelli reaction (entries 1 and 9, 76% and 73%, respectively), the introduction of the electron withdrawing nitro group in the meta position (entry 2, 64%) deactivates the aldehyde. The introduction of the same group in the para position (entry 6, 82%) has the opposite effect. The introduction of a fluorine or an alcohol on the para position (entries 3 and 8, 83% and 81%, respectively) affords high yields, while other halogenides or methoxy groups on the meta and para positions deactivate the aldehydes (entries 4, 5 and 7). The replacement of urea by thiourea led to a lesser overall reactivity (entries 10 to 12).

Table 4.3.2. Biginelli condensation reaction scope

| Entry | R ₁ | X | R ₂ | Yield ^b (%) | MP (°C) | Lit MP (°C) |
|-------|--|---|----------------|------------------------|---------|-----------------------|
| 1 | C ₆ H ₅ | O | Et | 76 | 202-204 | 201-204 ³³ |
| 2 | 3-NO ₂ -C ₆ H ₄ | O | Et | 64 | 220-230 | 224-226 ³³ |
| 3 | 4-F-C ₆ H ₄ | O | Et | 83 | 180-184 | 183-185 ³³ |
| 4 | 3-Br-C ₆ H ₄ | O | Et | 70 | 189-191 | 190-192 ³³ |
| 5 | 4-Cl-C ₆ H ₄ | O | Et | 66 | 213-215 | 212-214 ³³ |
| 6 | 4-NO ₂ -C ₆ H ₄ | O | Et | 82 | 208-210 | 211-212 ³⁹ |
| 7 | 4-OMe-C ₆ H ₄ | O | Et | 71 | 196-199 | 202-204 ³⁹ |
| 8 | 4-OH-C ₆ H ₄ | O | Me | 81 | 230-235 | 231-233 ³³ |
| 9 | C ₆ H ₅ | O | Me | 73 | 201-208 | 212-214 ³³ |
| 10 | C ₆ H ₅ | S | Et | 54 | 207-210 | 207-209 ³³ |
| 11 | 3-NO ₂ -C ₆ H ₄ | S | Et | 51 | 205-210 | 210-212 ³³ |
| 12 | 3-Br-C ₆ H ₄ | S | Et | 58 | 184-187 | 182-184 ³³ |

^a Reaction conditions: aldehyde (2mmol), (thio)urea (3mmol), β -ketoester (2 mmol) and CuFe₂O₄ NPs (2 mol%) were combined with 5 mL AcOH and heated to 100°C for 18 hr. ^b Isolated yield

**Fig. 4.3.3. CuFe₂O₄ NPs (a) before catalysis and (b) after 7 cycles**

4.3.4 Experimental Section

4.3.4.1 Materials and Equipments

CuFe_2O_4 , Fe_3O_4 (<50 nm particle size (TEM), 98%), and all reagents were purchased from Sigma-Aldrich, with the exception of acetic acid from ACP Chemicals. The TEM images were obtained on an FEI Technai 12 operated at 120 kV. For size analysis, 100 nanoparticles were counted. The XRD analysis was performed on a Phillips PW1710 operated at 200 kV. The ICP analysis was performed at Vassar College with a Spectro Genesis 76004549. The XPS analysis was performed at Ecole Polytechnique Montreal on a VG ESCLAB 3 MKII with a power of 206 W. A surface of 2x3 mm was analyzed at a depth of 50-100 Å.

4.3.4.2 Biginelli Condensation Catalytic Tests

To a 10 mL round bottom charged with magnetic stir bar and CuFe_2O_4 nanoparticles (2 mol %) in air, aldehyde (2 mmol), (thio)urea (3 mmol), β -ketoester (2 mmol) and 5 mL AcOH were added. The reaction mixture was stirred at 100°C for 18 hr. The nanoparticles adsorbed on to the stir bar when stirring was stopped. The reaction solution was filtered through celite in a pipette eluting with ethyl acetate. The liquid was removed in vacuo and the crude solid recrystallized in ethanol to afford the purified product, which was characterized by melting point and some by NMR on a Mercury 300. The nanoparticles were washed with acetic acid, air-dried and used directly for the next round of reactions without further purification. In our ICP analysis about twice the quantity of iron was detected compared to the quantity of copper, in the supernatant, which is consistent with the stoichiometry of the CuFe_2O_4 nanoparticles.

4.3.5 Conclusions

This study demonstrated that copper ferrite nanoparticles serve as an effective heterogeneous catalyst for the Biginelli condensation. A diverse range of DHPMs were obtained in moderate to high yield under mild conditions in air. Moreover, the impact of this research is not limited to the Biginelli condensation. Instead, the use of such fully-oxidized bi-metallic nanoparticles opens new catalytic avenues and is a proof of concept for expanding the scope of reactions that can be catalyzed by simple, bare, magnetically recoverable nanoparticles.

4.3.6 Acknowledgements

We thank the Natural Science and Engineering Research Council of Canada (NSERC), the Canada Foundation for Innovation (CFI), the Canada Research Chairs (CRC), the Fonds de Recherche sur la Nature et les Technologies (FQRNT), the Center for Green Chemistry and Catalysis (CGCC) and McGill University for their financial support. We are grateful to the Vassar Chemistry Department and Ecole Polytechnique Montreal for ICP and XPS analyses, respectively.

4.3.7 References

1. D. J. Cole-Hamilton, *Science*. 2003, 299, 1702-1706.
2. D. Astruc, F. Lu and J. Ruiz Aranzaes, *Angew. Chem., Int. Ed.*, 2005, 44, 7852-7872.
3. M. Lombardo, A. Quintavalla, M. Chiarucci and C. Trombini, *Synlett*, 2010, 1746-1765.
4. K. Ding and Y. Uozumi, *Handbook of Asymmetric Heterogeneous Catalysis*, Wiley-VCH, Weinheim, 2008.
5. G. Rothenberg, *Catalysis: Concepts and Green Applications*, Wiley-VCH, Weinheim, 2008.
6. D. Astruc, *Nanoparticles and Catalysis*, Wiley-VCH, Weinheim, 2008.

7. A. M. Molenbroek, S. Helveg, H. Topsoe and B. S. Clausen, *Top. Catal.*, 2009, 52, 1303-1311.
8. V. Polshettiwar and R. S. Varma, *Green Chem.*, 2010, 12, 743-754.
9. T.-J. Yoon, W. Lee, Y.-S. Oh and J.-K. Lee, *New J. Chem.*, 2003, 27, 227-229.
10. A. H. Lu, E. L. Salabas and F. Schüth, *Angew. Chem., Int. Ed.*, 2007, 46, 1222-1244.
11. A. H. Latham and M. E. Williams, *Acc. Chem. Res.*, 2008, 41, 411-420.
12. S. Shylesh, V. Schünemann and W. R. Thiel, *Angew. Chem., Int. Ed.*, 2010, 49, 3428-3459.
13. Z. Wang, B. Shen, Z. Aihua and N. He, *Chem. Eng. J.*, 2005, 113, 27-34.
14. D. Guin, B. Baruwati and S. V. Manorama, *Org. Lett.*, 2007, 9, 1419-1421.
15. B. Baruwati, D. Guin and S. V. Manorama, *Org. Lett.*, 2007, 9, 5377-5380.
16. S. Luo, X. Zheng, H. Xu, X. Mi, L. Zhang and J.-P. Cheng, *Adv. Synth. Catal.*, 2007, 349, 2431-2434.
17. V. Polshettiwar, B. Baruwati and R. S. Varma, *Green Chem.*, 2009, 11, 127-131.
18. V. Polshettiwar, B. Baruwati and R. S. Varma, *Chem. Comm.*, 2009, 1837-1839.
19. P. D. Stevens, J. Fan, H. M. R. Gardimalla, M. Yen and Y. Gao, *Org. Lett.*, 2005, 7, 2085-2088.
20. J. Liu, X. Peng, W. Sun, Y. Zhao and C. Xia, *Org. Lett.*, 2008, 10, 3933-3936.
21. L. M. Rossi, F. P. Silva, L. L. R. Vono, P. K. Kiyohara, E. L. Duarte, R. Itri, R. Landers and G. Machado, *Green Chem.*, 2007, 9, 379-385.
22. T. Zeng, L. Yang, R. Hudson, G. Song, A. Moores and C.-J. Li, *Org. Lett.*, 2010, 13, 442-445.
23. A. H. Lu, E. L. Salabas and F. Schüth, 2007, 46, 1222-1244.
24. F. Shi, M. K. Tse, M. M. Pohl, A. Brückner, S. Zhang and M. Beller, *Angew. Chem., Int. Ed.*, 2007, 46, 8866-8868.
25. B. V. S. Reddy, A. S. Krishna, A. V. Ganesh and G. G. K. S. N. Kumar, *Tetrahedron Lett.*, 2011, 52, 1359-1362.

26. T. Q. Zeng, W.-W. Chen, C. M. Cirtiu, A. Moores, G. H. Song and C. J. Li, *Green Chem.*, 2010, 12, 570-573.
27. T. Zeng, G. Song, A. Moores and C.-J. Li, *Synlett*, 2010, 13, 2002-2008.
28. C. Rangheard, C. De Julian Fernandez, P. H. Phua, J. Hoorn, L. Lefort and J. G. De Vries, *Dalton Trans.*, 2010, 39, 8464-8471.
29. R. B. Bedford, M. Betham, D. W. Bruce, S. A. Davis, R. M. Frost and M. Hird, *Chem. Comm.*, 2006, 1398-1400.
30. J. Kim, Y. Lee and S. H. Sun, *J. Am. Chem. Soc.*, 2010, 132, 4996-+.
31. S. C. Tsang, V. Caps, I. Paraskevas, D. Chadwick and D. Thompsett, *Angew. Chem., Int. Ed.*, 2004, 43, 5645-5649.
32. K. K. Senapati, C. Borgohain and P. Phukan, *J. Mol. Catal. A: Chem.*, 2011, 339, 24-31.
33. C. J. Liu and J. D. Wang, *Molecules*, 2009, 14, 763-770.
34. D. Prodius, F. Macaev, V. Mereacre, S. Shova, Y. Lutsenco, E. Styngach, P. Ruiz, D. Muraviev, J. Lipkowski, Y. A. Simonov and C. Turta, *Inorg. Chem. Comm.*, 2009, 12, 642-645.
35. K. S. Atwal and S. Moreland, *Bioorg. Med. Chem. Lett.*, 1991, 1, 291-294.
36. I. W. Davies, L. Matty, D. L. Hughes and P. J. Reider, *J. Am. Chem. Soc.*, 2001, 123, 10139-10140.
37. N. S. McIntyre and M. G. Cook, *Anal. Chem.*, 1975, 47, 2208-2213.
38. Y. M. Z. Ahmed, M. M. Hessien, M. M. Rashad and I. A. Ibrahim, *J. Magn. Magn. Mater.*, 2009, 321, 181-187.
39. R. Ghosh, S. Maiti and A. Chakraborty, *J. Mol. Catal. A: Chem.*, 2004, 217, 47-50.

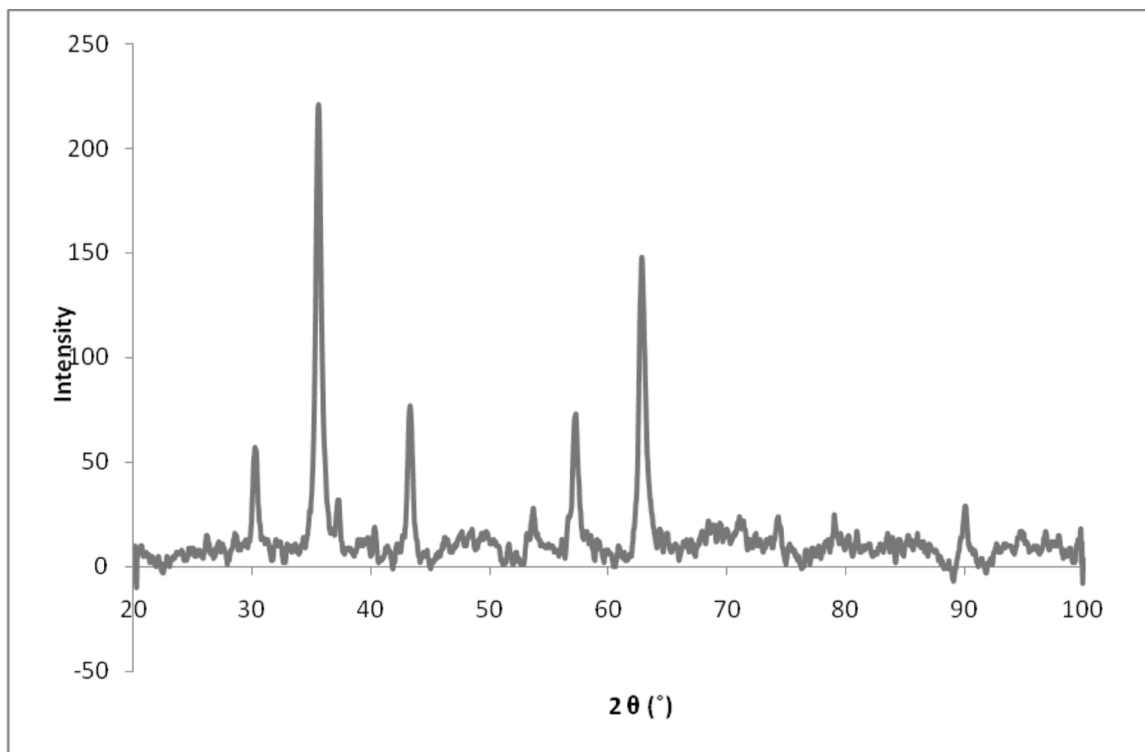
4.3.8 Appendix

Figure 4.3.4. XRD Analysis of a commercial sample of CuFe_2O_4 nanoparticles.

Sharp peaks at $2\theta = 30.24^\circ, 35.52^\circ, 43.16^\circ, 53.52^\circ, 57.08^\circ, 62.72^\circ$ are characteristic of cubic phase of copper ferrite.¹

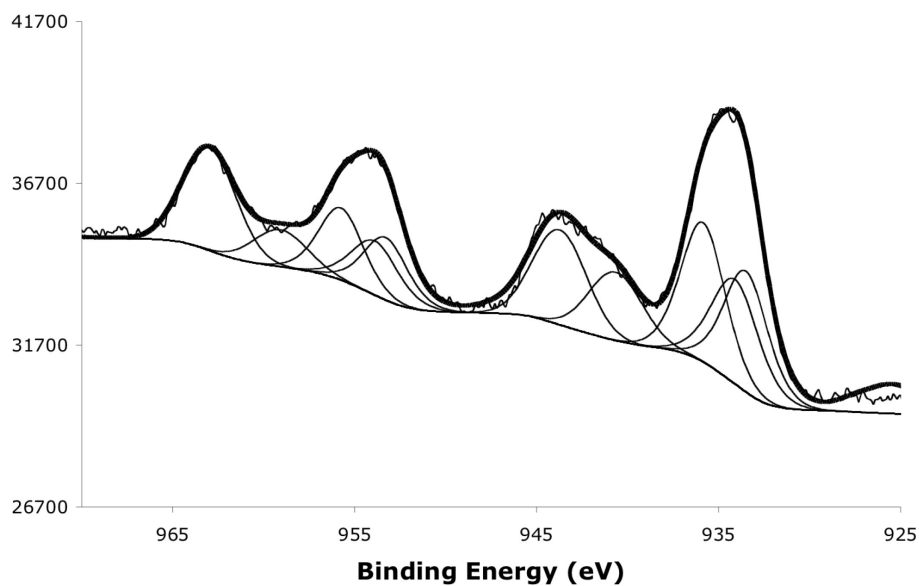


Figure 4.3.5. XPS analysis of a commercial sample of CuFe_2O_4 nanoparticles.

4.3.8.1 Appendix References

- [1] Y. M. Z. Ahmed, M. M. Hessien, M. M. Rashad, I. A. Ibrahim, J. Magn. Magn. Mater. 2009, 321, 181-187.

5 Conclusions and Future Work

5.1 Conclusions

The field of nanoparticle catalysis has been expanding rapidly over the last 10 years because it effectively bridges the gaps between homogeneous and heterogeneous catalysis.¹⁻³ Specifically, the subfield of magnetic nanoparticle catalysis has also proliferated over the past 5 years because it further simplifies the recovery process.^{4, 5} Most systems under the magnetic nanoparticle umbrella use the magnetic particle only as a vehicle for magnetic recovery rather than the actual surface for catalysis. In hopes of further simplifying the system, the work in this thesis focuses on the use of bare magnetic nanoparticles as both the means for magnetic recovery and the catalyst itself for various organic transformations.

The use of core-shell iron-iron oxide nanoparticles to catalyze hydrogenation reactions provided a means to protect the reduced iron core from further oxidation. Previous examples of hydrogenation with oxide-free reduced iron nanoparticles proved extremely sensitive to oxidative catalyst deactivation.⁶⁻⁸ The system described herein was robust to oxidation and easily recoverable and recyclable for up to ten rounds of catalysis. This system could also be adapted to a flow system by synthesizing the particles in a polymer support—obviating the need for magnetic recovery, but opening new doors for industrially relevant processes catalyzed by simple iron particles. The amphiphilic polymer also helped to limit the damages of catalyst oxidation.

In hopes of expanding the catalytic offering of these mono-metallic reduced iron nanoparticles, further work in this thesis detailed the use of the same particles decorated with either ruthenium or copper for transfer hydrogenation and the azide-alkyne ‘click’ reaction, respectively. This technique addressed the issue of the limited catalytic scope of iron, but not entirely the issue of oxidative catalyst deactivation over time.

In an effort to lessen worries about oxidation, while at the same time expanding the catalytic offering of mono-metallic iron particles, the study embraced oxidation by using oxidized copper-iron oxide nanoparticles: CuFe_2O_4 . In this system, the iron allowed for magnetic recovery while copper enabled reactions impossible to the same extent with iron alone: the Biginelli condensation and cross-dehydrogenative coupling.

With strategies ranging from mono-metallic reduced or oxidized iron particles, reduced iron particles decorated with a more catalytically active metal, and the use of mixed metal oxide particles, the field of simple magnetic nanoparticle catalysis is poised to make significant gains. The impetus behind the magnetic nanoparticle catalysis movement has been to simplify the separation process. The work outlined in this thesis represents efforts to further simplify the process of catalyst preparation and use.

5.2 Future Work

The demonstration of iron nanoparticles catalyzing hydrogenation reactions in flow conditions generated considerable industrial interest, and therefore spawned a follow-up visit of another graduate student to the facilities at Institute for Molecular Science in Okazaki. While in Japan, she will probe the mechanism by which the amphiphillic polymer helps to protect the nanoparticle against oxidation. This study will vary the relative proportion, presence and absence of the various polymer components (polystyrene bead, polyethylene glycol linker and terminal amine functionality). Other polymers will also be tested, such as chitosan, as well as further testing with particles generated via the black tea reduction method, and altering the iron loading in both the reduction and thermal decomposition methods. The study will also seek to benchmark the activity of this catalyst against common industrial hydrogenation catalysts, such as platinum on carbon. To further probe the industrial relevance of this system, other solvents will also be tested. Last, in an effort to demonstrate a mechanism involving hydrogenation via H_2 rather than

transfer hydrogenation from EtOH, the study will attempt a deuteration experiment with D₂ pressure and check for deuterated vs. hydrogenated product.

In the study of transfer hydrogenation reactions with ruthenium decorated core-shell iron-iron oxide nanoparticles, several of the 'blank' experiments indicated that the monometallic iron particles are active for acetophenone transfer hydrogenation, albeit much less so than their ruthenium decorated analogues. Nonetheless, this modest reactivity demonstrated by iron is still impressive and warrants further investigation. Follow-up experiments could force the conditions from 100°C to 150°C. Since this far surpasses the boiling point of 2-propanol (the solvent and hydrogen transfer agent), the solvent could be switched to the higher boiling, but chemically similar 3-pentanol.

One of the emerging applications for iron nanoparticles is the dehydrogenation of ammonia-borane for release of stored H₂. Coupling this reactivity with the reactivity we already demonstrated for hydrogenation reactions could represent another system for transfer hydrogenation. In one pot, ammonia borane could be dehydrogenated with iron nanoparticles followed by the hydrogenation of unsaturated compounds.

Ongoing research in the lab focuses on the use of ligand modified CuFe₂O₄ nanoparticles for the azide-alkyne 'click' reaction as well as to catalyze the coupling of aryl halides with phosphorous nucleophiles. Additionally, high resolution TEM, XPS and XRD analysis of these particles before and after ligand modification will help to determine the nature of this modification.

Likewise, a full materials characterization of the copper decorated core-shell iron-iron oxide nanoparticles is under way as well. These particles are also being examined for the catalysis of dye tagged hormones via the azide-alkyne 'click' reaction in hopes that the easy mode of catalyst recovery will reduce the amount of copper leached into these biologically relevant molecules.

5.3 References

1. V. Polshettiwar and R. S. Varma, *Green Chem.*, 2010, **12**, 743-754.
2. A. M. Molenbroek, S. Helveg, H. Topsoe and B. S. Clausen, *Top. Catal.*, 2009, **52**, 1303-1311.
3. D. Astruc, F. Lu and J. Ruiz Aranzaes, *Angew. Chem., Int. Ed.*, 2005, **44**, 7852-7872.
4. V. Polshettiwar, R. Luque, A. Fihri, H. Zhu, M. Bouhrara and J.-M. Bassett, *Chem. Rev.*, 2011, **111**, 3036-3075.
5. A. H. Lu, E. L. Salabas and F. Schüth, *Angew. Chem., Int. Ed.*, 2007, **46**, 1222-1244.
6. C. Rangheard, C. De Julian Fernandez, P. H. Phua, J. Hoorn, L. Lefort and J. G. De Vries, *Dalton Trans.*, 2010, **39**, 8464-8471.
7. P. H. Phua, L. Lefort, J. A. F. Boogers, M. Tristany and J. G. de Vries, *Chem. Commun.*, 2009, 3747-3749.
8. M. Stein, J. Wieland, P. Steurer, F. Toelle, R. Muelhaupt and B. Breit, *Adv. Synth. Catal.*, 2011, **353**, 523-527.